The interactions of complex structures with the immune system

Johan Jacob Frederik Verhoef

The interactions of complex structures with the immune system
Johan Jacob Frederik Verhoef

Department of Pharmaceutics, Utrecht Institute for Pharmaceutical Sciences (UIPS), Faculty of Science, Utrecht University, the Netherlands

ISBN: 978-90-393-6746-9

Cover
Bryce Canyon, Utah, USA. This photo was obtained from The Independent

Lay-out
Johan Jacob Frederik Verhoef

Printed by
Proefschriftmaken.nl || Uitgeverij Boxpress

The research leading to this thesis has received support from Vifor Pharma AG, Glattbrugg, Switzerland

The printing of this thesis was financially supported by the Utrecht Institute for Pharmaceutical Sciences (UIPS), Utrecht, the Netherlands

The interactions of complex structures with the immune system

De interacties van complexe structuren met het immuunsysteem
(met een samenvatting in het Nederlands)

Proefschrift

ter verkrijging van de graad van doctor aan de Universiteit Utrecht op gezag van de rector magnificus, prof. dr. G.J. van der Zwaan, ingevolge het besluit van het college voor promoties in het openbaar te verdedigen op vrijdag 10 maart 2017 des middags te 12.45 uur

door

Johan Jacob Frederik Verhoef

geboren op 21 december 1988
te Bunnik

Promotor:
Prof. dr. H. Schellekens

Copromotor:
Dr. C. Maas

"Problems that remain persistently insoluble should always be suspected as questions asked in the wrong way."

Alan Watts

Table of contents

Chapter | 1

General introduction

Nanomedicines

An ideal pharmaceutical product, either a chemical entity or therapeutic protein, needs to be effective and safe by having high specificity and affinity to its biological target (pharmacodynamics) as well as be able to reach it at sufficient concentrations (pharmacokinetics). Only then it will induce a biological effect and little toxicity as a result of binding to tissues or cells other than the intended target. Unfortunately, most chemical entities and a selection of therapeutic proteins show an unfavorable systemic distribution upon intravenous administration [1]. These agents are rapidly cleared from the circulation, allowing only a fraction of the administered dose to bind its target. In the case of tumor treatment only a fraction of cytotoxic agents is able to reach the tumor, only a fraction of antibiotic the sight of infection, and in gene therapy the genetic therapeutic to be effectively taken up by the cells of interest.

Ensuring favorable pharmacokinetics is thus essential for clinical success. The development of pharmaceutical formulations allowing prolonged systemic distribution of therapeutics as well as the ability to 'deliver' these more effectively to the tissue or cells of interest, has attracted much interest [2,3]. In the last decades, both industry and academia have applied nanotechnology to encapsulate therapeutic compounds into colloidal drug delivery systems [3]. These formulations are referred to as nanomedicines. Another, advantage of formulating drugs into nanomedicine formulation is that therapeutic compounds are only exposed to the systemic environment when released from the formulation. Because many therapeutic products, especially chemical entities, induce unwanted side-effects due to interactions with targets other than those developed for, releasing these compounds only in the diseased tissue or cells can diminish systemic exposure resulting in less toxicity.

The application of Nanotechnology in pharmaceutical development is a multidisciplinary activity which combines among others chemistry, biology, engineering and medicine [2]. A widely used definition of nanomedicines is the "the use of nanoscale or nanostructured materials in medicine that according to their structure have unique medical effects" [3]. The formulation of therapeutic molecules into nanosized delivery systems allows for numerous advantageous to traditional therapeutics [4]. It involves the combination of a therapeutic molecule encapsulated into a formulation consisting out of biomaterials such as lipids, polymers, or other chemical nanostructures that are biocompatible [3]. The formulation of therapeutic molecules into these nanosized formulations offer additional advantages: (1) improving the solubility of hydrophobic compounds otherwise unsuitable for administration, (2) targeting of specific cells or tissues, and (3) controlled-release of the encapsulated therapeutic molecule [6-7]. At the moment, different types of nanomedicines are used or investigated in clinical practice, such as liposomal formulations, polymeric micelles, iron carbohydrate colloids, conjugates of a therapeutic molecule with either a water-soluble polymer or monoclonal antibody, dendrimers and inorganic nanoparticles [2,7,8]. All these different formulations have been used for different indications, such as accumulation of anti-inflammatory agents in inflamed tissue or cytotoxic agents in tumor tissue, inorganic particulates that can kill cancerous cells by the production of heat upon light irradiation, or formulations that contain a contrast agent in order to visualize (metastatic-)tumors [9]. Its promising properties have allowed for the development of a wide range of different applications including therapeutics, diagnostic imaging agents and medical devices with cancer and chronic inflammation as major disease areas [2,10].

Despite its clear benefits, the development of nanomedicines remains challenging. Nanomedicines consist of a multitude of closely related structures forming the active pharmaceutical ingredient rather than a homo-molecular structure [7,10]. Because of their complexity, these structures cannot be fully characterized by current physico-chemical analytical tools impeding full determination of their size-(distribution), composition, purity, surface chemistry and stability making it often difficult to determine what the therapeutic performances are of these different structures [7,10].

Ironically, the major obstacles for the successful development of nanomedicines are unfavorable pharmacokinetic properties and a relative high risk for hypersensitivity-like reactions [11]. The first is due to exposure of nanomedicines to both physical and biological barriers, such as shear forces, aggregation, protein adsorption and phagocytosis which influence their distribution and clearance through and from the body [9,11]. Hypersensitivity-like reactions are often due to interactions with proteins and cells from the innate immune system, such as complement factors [12–15]. As such, the immune system plays an important role in which interactions with both serum proteins and cells from the immune system have an effect on both pharmacokinetics and hypersensitivity-like reactions [17]. Interactions of nanomedicines with the innate immune system remains a major challenge for the wider introduction of these therapeutics into the clinic.

Mononuclear Phagocyte System

Cells from the mononuclear phagocyte system (MPS) are part of the innate immune system involved in ensuring first line defense by phagocytosis of pathogens. The MPS consists out of macrophages, dendritic cells, and monocytes residing within blood, lungs, liver, spleen and lymph nodes [18]. Phagocytosis by cells from the MPS is supported by serum proteins and lipids that have the ability to adhere to pathogens and other material to be removed from the circulation, a process referred to as opsonization. These opsonins interact with so-called pattern recognition receptors expressed on cellular membranes of cells from the immune system resulting in rapid internalization, sequestration and removal from the circulation [18]. This thesis will focus on the ability of complex structures (nanomedicines) to interact with these opsonins like complement- and coagulation factors, and their recognition by pattern recognition receptors such as Toll-like receptors.

As nanomedicines are complex structures composed by nonself materials, they have the ability to attract opsonins and become susceptible to phagocytic cell-mediated clearance. The MPS remains a major hurdle in the delivery of therapeutic molecules at an effective dose to tissues and cells. Interactions with the MPS can result in the release of anaphylatoxins, cytokines, interleukins, interferons, and tumor necrosis factor leading to inflammation [18]. Both size and surface chemistry of nanomedicines play a dominant role in recognition by the MPS. When designing a nanomedicine, it is essential to minimize interaction with cells and or plasma proteins other than its intended target.

Complement system

The complement system is composed of a group of proteins which are linked in biochemical cascade with the purpose of removing pathogens from the body [17]. Activation of the complement system can result in the destruction of a pathogen directly or indirectly by inducing phagocytosis. Several nanomedicines, and especially liposomes, are known to induce

complement activation resulting in rapid-clearance from the circulation and the formation of anaphylatoxins C3a and C5a [16]. These anaphylatoxins can cause cardiovascular toxicity and other symptoms of anaphylaxis [16]. Unlike many other receptors involved in the immune system, pattern recognition by the complement system is not solely based on recognition of a specific ligand with a biochemical structure different than that of the host. Rather, complement activation can occur on those surfaces with multiple binding domains for complement factors [19]. It is this polyvalent binding which is the underlying mechanism of pattern recognition.

Toll-like receptors

Toll-like receptors (TLR) are highly conserved transmembrane receptors functioning as signaling receptors. TLR are part of the innate immune system involved in pattern recognition. TLR function by binding to pathogenic structures, although they can also bind structures derived from the host, such as unfolded proteins and cellular debris [18,22]. Among others, ligands recognized by TLR are single-stranded DNA, flagellins and lipopolysaccharides. TLR are expressed on multiple cells such as monocytes, macrophages, natural killer cells, dendritic cells, B-lymphocytes and mast cells [24]. Although TLR only bind biological ligands, several biomaterials are known to induce TLR activation [25,26]. How biomaterials can activate TLR remains unknown, but biomaterials and nanomedicines can adsorb plasma proteins which are known activators of TLR, such as plasmin, fibrinogen and fibronectin [27]. This has resulted in the hypothesis in this thesis that nanomedicines by means of opsonization are able of activating TLR.

Thrombogenicity

Nanomedicines can also activate blood platelets at their surface which may result in the formation of a fibrin clot [17]. This process includes multiple plasma coagulation factors as wells as various cell types such as, platelets, leukocytes, endothelial cells and even some cancer cells [20]. Not every biomaterial is an activator of blood platelets, however, as nanomedicines are developed for prolonged circulation, they are exposed extensively to these coagulation factors and cells which increases their ability to activate the coagulation cascade [16,19]. The formation of a fibrin clot can be initiated by two distinct pathways. The extrinsic pathway is triggered by exposure of blood to damaged blood vessel tissue, and the extrinsic pathway by blood-borne factors [21]. Nanomedicine are believed to induce the formation of thrombus by means of the extrinsic pathway. The extrinsic pathway, also referred to as contact system activation, is able to induce thrombin formation starting by the auto-activation of coagulation factor XII (FXII) when in contact with negatively charged surfaces [20-21]. Auto-activation of FXII then induces a biochemical reaction involving activation of FXI and prekallikrein resulting in thrombin generation, fibrin formation and subsequently the production of a fibrin clot [20-21].

Strategies to prevent interactions with the immune system

Strategies to overcome opsonization have been thoroughly investigated and include coating of nanomedicines by hydrophilic polymers such as zwitterionic ligands and poly(ethyleneglycol) (PEG). These polymers cover the core of the nanomedicine and by the attraction of water molecules shield against adsorption of plasma proteins and cellular recognition resulting in diminished uptake by the MPS [27,28,31]. Although these polymers, and especially PEG, were initially considered biological inert, it is now clear that these polymers do adsorb plasma proteins [30]. Another downside of the attachment of hydrophilic

polymers to nanomedicines is that recognition by the target cells is diminished as well as the potential to induce anti-polymer antibodies which can result in accelerated clearance and hypersensitivity reactions [29,31].

Another promising approach is surface modification by carbohydrates. In contrast to polymers, carbohydrates represent more native-like structures. Several carbohydrates are considered biocompatible and biodegradable and thereby more suitable for nanomedicine modification [33]. Iron carbohydrate colloids used to treat iron deficiency and iron deficiency anemia are a class of nanomedicines which have been modified with different types carbohydrates.

Iron nanomedicines

Iron based nanomedicines are widely used and have been on the market since the 1940's [34]. They can be considered as the first nanomedicines [35]. Over time, different iron nanomedicines have been introduced. Although considered as different products they are comparable in their physico-chemical characteristics as all commercial intravenous iron formulations contain a polynuclear Fe(III)-oxyhydroxide/oxide core surrounded by carbohydrates [36]. These carbohydrates function as a stabilizer preventing direct release of bioactive iron and particle aggregation and can consist out of sucrose, gluconate, dextran, isomaltoside 1,000 or carboxymaltose [33,35]. Besides its stabilizing properties, these carbohydrates also shield the iron core from direct recognition by the MPS [37].

Iron nanomedicines are administered to patients with iron deficiency for whom oral iron supplementation is not sufficient or possible [38]. Although these iron nanomedicines have been administered safely to many patients, these products are associated with (acute) adverse drug reactions, such as bronchospasm and circulatory collapse [39]. Because of the growing use of intravenous iron and the introduction of newer agents onto the market, it is likely that there will be an increased number of patients who will experience adverse drug reactions. The European Medicine Agency (EMA) warned in 2013 stating that physicians should take precaution when administering these products [40]. Currently, the mechanisms behind these hypersensitivity-like reactions remain unknown. Possible factors explaining these reactions are the release of high concentrations of unbound iron into the circulation, recognition of carbohydrates by the immune system and or destabilization of the formulation by dissociation of the carbohydrates covering the iron cores [40–42]. A relation between carbohydrate stability and hypersensitivity-like reactions seems to exist as less stable formulations are more prone to induce hypersensitivity-like reactions and can only be given at lower doses compared to the newer, more stable formulations [39]. In this thesis iron nanomedicines were investigated for their interaction with the immune system. They are a good model to investigate the interactions of nanomedicines with the innate immune system as there are multiple iron nanomedicines on the market which are comparable in their core chemistry, size and charge, but differ in the type and stability of its carbohydrate surface coating [35,43–45].

Accelerated Blood Clearance due to PEGylation

PEG is widely used to extend circulation times of nanomedicines and therapeutic proteins believed to occur through its repulsive nature on opsonins believed to occur through

the binding of water molecules to the PEG chains. In addition, PEGylation neutralizes the surface charge of particles diminishing the attraction of plasma proteins. Several studies have reported that PEGylation does indeed increase circulation times but does not reduce the binding of total plasma proteins [32]. In fact, several studies even reported that the amount of plasma proteins bound to nanomedicines actually increased, suggesting that it is actually specific plasma proteins which inhibit recognition of the nanomedicine by the MSP or prevent the binding of opsonins.

Although the general assumption is that PEG is not immunogenic, in the last decade several papers reported that an intravenous injection of PEGylated nanomedicines causes a second dose to be cleared rapidly from the body [46,47]. This process is referred to as the accelerated blood clearance (ABC) and is observed with both proteins, liposomes and micelles. It is believed that PEG is able to induce an immune response by the induction of anti-PEG IgG or IgM antibodies and subsequently activates the complement system. The incidence of anti-PEG antibodies in healthy population is believed to vary between 0-30% due to the exposure to PEG in food and cosmetics [27,48,49].

Aims and outline of thesis

The first part of this thesis discusses the incidence of hypersensitivity-like reactions by nanomedicines, its possible mechanisms, as well as a novel oral formulation consisting out of thermosensitive block-co-polymers to deliver high quantities of iron through the oral route of administration. In **chapter 2** the incidence of hypersensitivity-like reactions by different types of iron nanomedicnes are described. Here, pharmacovigilance data from the WHO safety database was analyzed and subsequently normalized to the total amount of administered iron per product by country. **Chapter 3** describes an in depth investigation on the biological interactions of iron nanomedicines with the innate immune system. This chapter describes the immunological potential of these therapeutics and may be an explanation for the hypersensitivity-like reactions described in chapter 2. It links physico-chemical characterizations to their potential to activate Toll-like receptors, complement system and the production of cytokines. Because of the need for a more safe formulation which can also be orally administered, **chapter 4** describes a novel oral iron formulation that can deliver higher quantities of iron to the systemic circulation than conventional oral iron formulations.

The second part of this thesis consists of an analysis on the potential immunological effect of poly(ethyleneglycol). In **chapter 5** a literature review is presented summarizing immunological responses to PEGylated therapeutics. It looks at the problems with assays claiming to identify anti-PEG antibodies and proposes a mechanisms how the immune system may react to PEG. **Chapter 6** describes an anti-PEG analysis on patient serum treated with PEG-asparaginase who experienced either rapid clearance of the therapeutic or hypersensitivity reactions following treatment.

The third part of this thesis describes the existence of nature's own nanoparticles. In **chapter 7** we identify that blood platelets possess high concentrations of polyphosphates complexed with calcium in their dense granules. Upon activation these complexed polyphosphate nanoparticles are presented on the surface of platelets with the purpose to coagulation by means of FXII contact system activation. FXII activation and its induction

on thrombus formation is a major challenge when designing nanomedicines. This newly discovered mechanism how the coagulation system has evolved to induce platelet activation towards polyphosphate nanoparticles can provide better understanding why nanomedicines induce unwanted coagulation. Understanding this process is essential for the development of long circulating nanomedicines in the future.

This final part of this thesis, **chapter 8**, describes the perspectives for the different parts this thesis.

References

[1] T. Lammers, W. E. Hennink, and G. Storm, "Tumour-targeted nanomedicines: principles and practice," Br. J. Cancer, vol. 99, no. 3, pp. 392–397, Aug. 2008.

[2] Y. Min, J. M. Caster, M. J. Eblan, and A. Z. Wang, "Clinical Translation of Nanomedicine," Chem. Rev., vol. 115, no. 19, pp. 11147–11190, Oct. 2015.

[3] V. Wagner, A. Dullaart, A.-K. Bock, and A. Zweck, "The emerging nanomedicine landscape," Nat. Biotechnol., vol. 24, no. 10, pp. 1211–1217, Oct. 2006.

[4] R. Duncan and R. Gaspar, "Nanomedicine(s) under the microscope," Mol. Pharm., vol. 8, no. 6, pp. 2101–2141, Dec. 2011.

[5] D. Neuman and J. N. Chandhok, "Patent Watch: Nanomedicine patents highlight importance of production methods," Nat. Rev. Drug Discov., vol. 15, no. 7, pp. 448–449, Jun. 2016.

[6] O. C. Farokhzad and R. Langer, "Impact of Nanotechnology on Drug Delivery," ACS Nano, vol. 3, no1, pp. 16–20, Jan. 2009.

[7] H. Schellekens et al., "How to regulate nonbiological complex drugs (NBCD) and their follow-on versions: points to consider," AAPS J., vol. 16, no. 1, pp. 15–21, Jan. 2014.

[8] D. J. A. Crommelin et al., "The similarity question for biologicals and non-biological complex drugs," Eur. J. Pharm. Sci., vol. 76, pp. 10–17, Aug. 2015.

[9] S. Wilhelm et al., "Analysis of nanoparticle delivery to tumours," Nat. Rev. Mater., vol. 1, p. 16014, Apr. 2016.

[10] L. Y. Rizzo, B. Theek, G. Storm, F. Kiessling, and T. Lammers, "Recent progress in nanomedicine: therapeutic, diagnostic and theranostic applications," Curr. Opin. Biotechnol., vol. 24, no. 6, pp. 1159–1166, Dec. 2013.

[11] C. D. Walkey, J. B. Olsen, H. Guo, A. Emili, and W. C. W. Chan, "Nanoparticle Size and Surface Chemistry Determine Serum Protein Adsorption and Macrophage Uptake," J. Am. Chem. Soc., vol. 134, no. 4, pp. 2139–2147, Feb. 2012.

[12] C. M. Dawidczyk et al., "State-of-the-art in design rules for drug delivery platforms: lessons learned from FDA-approved nanomedicines," J. Control. Release Off. J. Control. Release Soc., vol. 187, pp. 133–144, Aug. 2014.

[13] M. Herklotz et al., "Biomaterials trigger endothelial cell activation when co-incubated with human whole blood," Biomaterials, vol. 104, pp. 258–268, Oct. 2016.

[14] O. M. Merkel et al., "In vitro and in vivo complement activation and related anaphylactic effects associated with polyethylenimine and polyethylenimine-graft-poly(ethylene glycol)block copolymers," Biomaterials, vol. 32, no. 21, pp. 4936–4942, Jul. 2011.

[15] J. Szebeni and G. Storm, "Complement activation as a bioequivalence issue relevant to the development of generic liposomes and other nanoparticulate drugs," Biochem. Biophys. Res. Commun., vol. 468, no. 3, pp. 490–497, Dec. 2015.

[16] J. Szebeni, "Complement activation-related pseudoallergy: A stress reaction in blood triggered by nanomedicines and biologicals," Mol. Immunol., vol. 61, no. 2, pp. 163–173, Oct. 2014.

[17] M. A. Dobrovolskaia, P. Aggarwal, J. B. Hall, and S. E. McNeil, "Preclinical Studies To Understand Nanoparticle Interaction with the Immune System and Its Potential Effects on Nanoparticle Biodistribution," Mol. Pharm., vol. 5, no. 4, pp. 487–495, Aug. 2008.

[18] C. von Roemeling, W. Jiang, C. K. Chan, I. L. Weissman, and B. Y. S. Kim, "Breaking Down the Barriers to Precision Cancer Nanomedicine," Trends Biotechnol., Aug. 2016.

[19] T. Vorup-Jensen, "On the roles of polyvalent binding in immune recognition: Perspectives in the nanoscience of immunology and the immune response to nanomedicines," Adv. Drug Deliv. Rev., vol. 64, no. 15, pp. 1759–1781, Dec. 2012.

[20] M. A. Dobrovolskaia and S. E. McNeil, "Understanding the correlation between in vitro and in vivo immunotoxicity tests for nanomedicines," J. Controlled Release, vol. 172, no. 2, pp. 456–466, Dec. 2013.

[21] T. Renné, A. H. Schmaier, K. F. Nickel, M. Blombäck, and C. Maas, "In vivo roles of factor XII," Blood, vol. 120, no. 22, pp. 4296–4303, Nov. 2012.

[22] A. T. Long, E. Kenne, R. Jung, T. A. Fuchs, and T. Renné, "Contact system revisited: an interface between inflammation, coagulation, and innate immunity," J. Thromb. Haemost. JTH, vol. 14, no. 3, pp. 427–437, Mar. 2016.

[23] T. Kawai and S. Akira, "The role of pattern-recognition receptors in innate immunity: update on Toll-like receptors," Nat. Immunol., vol. 11, no. 5, pp. 373–384, May 2010.

[24] M. Muzio et al., "Differential Expression and Regulation of Toll-Like Receptors (TLR) in Human Leukocytes: Selective Expression of TLR3 in Dendritic Cells," J. Immunol., vol. 164, no. 11, pp. 5998–6004, Jun. 2000.

[25] J. I. Pearl et al., "Role of the Toll-like receptor pathway in the recognition of orthopedic implant wear-debris particles," Biomaterials, vol. 32, no. 24, pp. 5535–5542, Aug. 2011.

[26] F. A. Sharp et al., "Uptake of particulate vaccine adjuvants by dendritic cells activates the NALP3 inflammasome," Proc. Natl. Acad. Sci. U. S. A., vol. 106, no. 3, pp. 870–875, Jan. 2009.

[27] T. H. Rogers and J. E. Babensee, "Altered adherent leukocyte profile on biomaterials in Toll-like receptor 4 deficient mice," Biomaterials, vol. 31, no. 4, pp. 594–601, Feb. 2010.

[28] S. Chen, L. Li, C. Zhao, and J. Zheng, "Surface hydration: Principles and applications toward low fouing/nonfouling biomaterials," Polymer, vol. 51, no. 23, pp. 5283–5293, Oct. 2010.

[29] K. S. Soppimath, T. M. Aminabhavi, A. R. Kulkarni, and W. E. Rudzinski, "Biodegradable polymeric nanoparticles as drug delivery devices," J. Controlled Release, vol. 70, no. 1–2, pp. 1–20, Jan. 2001.

[30] J. J. F. Verhoef and T. J. Anchordoquy, "Questioning the Use of PEGylation for Drug Delivery," Drug Deliv. Transl. Res., vol. 3, no. 6, pp. 499–503, Dec. 2013.

[31] F. M. Veronese and G. Pasut, "PEGylation, successful approach to drug delivery," Drug Discov. Today, vol. 10, no. 21, pp. 1451–1458, Nov. 2005.

[32] J. J. F. Verhoef, J. F. Carpenter, T. J. Anchordoquy, and H. Schellekens, "Potential induction of anti-PEG antibodies and complement activation toward PEGylated therapeutics," Drug Discov. Today, vol. 19, no. 12, pp. 1945–1952, Dec. 2014.

[33] C. Lemarchand, R. Gref, and P. Couvreur, "Polysaccharide-decorated nanoparticles," Eur. J. Pharm. Biopharm., vol. 58, no. 2, pp. 327–341, Sep. 2004.

[34] M. Auerbach and H. Ballard, "Clinical use of intravenous iron: administration, efficacy, and safety," Hematol. Educ. Program Am. Soc. Hematol. Am. Soc. Hematol. Educ. Program, vol. 2010, pp. 338–347, 2010.

[35] J. Nissim, "INTRAVENOUS ADMINISTRATION OF IRON," The Lancet, vol. 250, no. 6463, pp. 49–51, Jul. 1947.

[36] P. Geisser and S. Burckhardt, "The pharmacokinetics and pharmacodynamics of iron preparations," Pharmaceutics, vol. 3, no. 1, pp. 12–33, 2011.

[37] B. G. Danielson, "Structure, chemistry, and pharmacokinetics of intravenous iron agents," J. Am. Soc. Nephrol. JASN, vol. 15 Suppl 2, pp. S93-98, Dec. 2004.

[38] J. Umbreit, "Iron deficiency: a concise review," Am. J. Hematol., vol. 78, no. 3, pp. 225–231, Mar. 2005.

[39] G. R. Bailie and J.-J. Verhoef, "Differences in the reporting rates of serious allergic adverse events from intravenous iron by country and population," Clin. Adv. Hematol. Oncol. HO, vol. 10, no. 2, pp. 101–108, Feb. 2012.

[40] "New recommendations to manage risk of allergic reactions with intravenous iron-containing medicines - WC500144874.pdf." .

[41] R. D. Cançado and M. Muñoz, "Intravenous iron therapy: how far have we come?," Rev. Bras. Hematol. E. Hemoter., vol. 33, no. 6, pp. 461–469, 2011.

[42] A. J. Bircher and M. Auerbach, "Hypersensitivity from intravenous iron products," Immunol. Allergy Clin. North Am., vol. 34, no. 3, pp. 707–723, x–xi, Aug. 2014.

[43] H. S. Novey, M. Pahl, I. Haydik, and N. D. Vaziri, "Immunologic studies of anaphylaxis to iron dextran in patients on renal dialysis," Ann. Allergy, vol. 72, no. 3, pp. 224–228, Mar. 1994.

[44] A. B. Pai, T. Conner, C. R. McQuade, J. Olp, and P. Hicks, "Non-transferrin bound iron, cytokine activation and intracellular reactive oxygen species generation in hemodialysis patients receiving intravenous iron dextran or iron sucrose," Biometals Int. J. Role Met. Ions Biol. Biochem. Med., vol. 24, no. 4, pp. 603–613, Aug. 2011.

[45] C. Wang et al., "Comparative Risk of Anaphylactic Reactions Associated With Intravenous Iron Products," JAMA, vol. 314, no. 19, pp. 2062–2068, Nov. 2015.

[46] J. Szebeni et al., "Hypersensitivity to intravenous iron: classification, terminology, mechanisms and management," Br. J. Pharmacol., vol. 172, no. 21, pp. 5025–5036, Nov. 2015.

[47] K. Shiraishi et al., "Exploring the relationship between anti-PEG IgM behaviors and PEGylated nanoparticles and its significance for accelerated blood clearance," J. Control. Release Off. J. Control. Release Soc., vol. 234, pp. 59–67, Jul. 2016.

[48] T. Shimizu et al., "Anti-PEG IgM and complement system are required for the association of second doses of PEGylated liposomes with splenic marginal zone B cells," Immunobiology, vol. 220, no. 10, pp. 1151–1160, Oct. 2015.

[49] R. P. Garay, R. El-Gewely, J. K. Armstrong, G. Garratty, and P. Richette, "Antibodies against polyethylene glycol in healthy subjects and in patients treated with PEG-conjugated agents," Expert Opin. Drug Deliv., vol. 9, no. 11, pp. 1319–1323, Nov. 2012.

[50] H. Schellekens, W. E. Hennink, and V. Brinks, "The immunogenicity of polyethylene glycol: facts and fiction," Pharm. Res., vol. 30, no. 7, pp. 1729–1734, Jul. 2013.

Chapter | 2

Differences in serious allergic adverse events reporting rates from intravenous iron by country and population

Bailie GR, Verhoef JJF.

Article published in:
Clinical Advances in Hematology & Oncology.
2012 Feb;2:101-108.

Abstract

Background Previous studies compared rates of adverse events (AE) between intravenous (IV) iron preparations. There has been no comparison of AE rates by country and population. Objectives To compare rates of AE to IV iron products by country and population. Methods All AE reported from 18 countries, from 01-01-03 to 06-30-09, were obtained for iron dextran (ID), iron sucrose (IS), IS similars (ISS) and sodium ferric gluconate (FG). Rates of all AE and serious AE (anaphylaxis plus other serious allergic reactions) were calculated as number of events/gram of iron sold (gFe)/million inhabitants (mil) x 10^{-3}. Odds ratios (OR) were calculated for the risks of AE between products. Results Iron use ranged from 1 (Poland) to 48,674 gFe/mil (Italy). Rates of all AE (reports/gFe/mil x 10^{-3}) ranged: for IS, from 0 (Poland, Austria, Czech Republic) to 1,222 (Ireland); FG, from 3.3 (Czech Republic) to 183.6 (US); ID, from 0.9 (Turkey) to 46,875 (Switzerland); ISS, no reports. In a subset of countries that used >2 iron products and had >1 serious AE, rates (reports/gFe/mil x 10^{-3}) of all AE and serious AE were smallest for IS (39.8 and 1.7), intermediate for FG (54.8 and 4.5) and greatest for ID (337.7 and 20.5). IS had lower risks for all AE (OR = 0.63, P<0.0001) and serious AE (OR = 0.31, P = 0.001) vs. FG and for all AE (OR = 0.13, P<0.0001) and serious AE (OR = 0.07, P <0.0001) vs. ID. FG had lower risks for all AE (OR = 0.20, P <0.0001) and serious AE (OR = 0.24, P <0.0001) vs. ID. Conclusions Considerable international variation existed in the extent and choice of iron product and AE reporting, suggesting under-reporting in some instances. Clinicians should appreciate the differential risks between available products and critically review local reporting practices.

1. Introduction

There has been increasing use of intravenous (IV) iron over the last decade, probably as a result of increased understanding of the appropriate management of moderate to severe anemia that is associated with numerous conditions, such as chronic kidney disease, pregnancy and the post-partum period, heavy uterine bleeding, inflammatory bowel diseases, bariatric surgery, chronic heart failure, oncology and chemotherapy-induced anemia and elective surgery [1-9]. It has become increasingly clear that judicious use of IV iron can optimize anemia management, reduce the need for erythropoiesis stimulating agents and red cell transfusions, and reduce costs [10-13].

IV iron has the potential to cause allergic reactions, but the relative risks of these adverse events differs by agent [14-17]. Recent papers have indicated that, of the IV iron products studied, the highest risk for spontaneous reports of anaphylaxis and other serious allergic reactions (e.g. bronchospasm, circulatory collapse, loss of consciousness) occurs with iron dextran (both high molecular weight and low molecular weight) products [14-17]. Further, there appears to be a difference in the rates of these adverse events between countries in Europe and North America [17]. Because of world-wide growing use of IV iron preparations, administration to an ever-broadening scope of patient populations, and the introduction of newer agents, generics and similars onto the market, it is likely that the rates of reported adverse events will continue to increase.

Previous studies have compared reports of serious adverse events within a country between products based on rates of reported events. There has never been a comparison of relative rates for serious adverse events by country and by population at risk of receiving an IV iron product. Such an evaluation should be able to further identify trends in adverse events and reporting practices by country and might identify possible issues of either over- or under-reporting. We hypothesize that there will be large differences in the rates of adverse events including serious allergic adverse events by product when standardized to population.

2. Methods

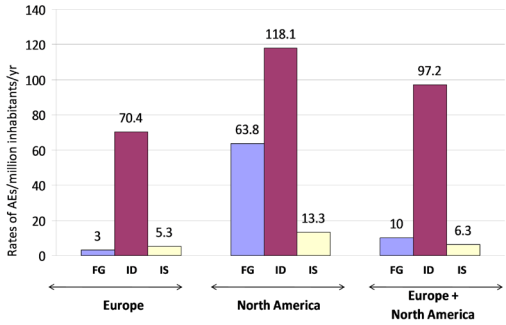

Figure 1. Rates of serious allergic adverse events (anaphylaxis and other serious allergic reactions) per gram of iron per million inhabitants per year in 2003–2009, by IV iron product and continent.

FG=sodium ferric gluconate; ID=iron dextran*; IS=iron sucrose.
*Note: in Europe, only low-molecular-weight iron dextran is available; in North America, data are combined for both high-molecular-weight and low-molecular-weight iron dextran products.

We used data that had been collected and published in an earlier analysis [17]. Briefly, all IV iron related adverse events that had been reported to the World Health Organization (WHO) from 16 European countries (Austria, Czech Republic, Denmark, Estonia, Finland, France, Germany, Ireland, Italy, Norway, Poland, Spain, Sweden, Switzerland, Turkey and United Kingdom) and North America (United States and Canada) from the first quarter 2003 through the second quarter 2009 were obtained from the Uppsala Monitoring Centre, Sweden. For the current analysis, we examined data for iron dextran, iron sucrose, iron sucrose similars (i.e. "generic" iron sucrose products other than the originator product) and sodium ferric gluconate. Ferumoxytol, ferric carboxymaltose and generic sodium ferric gluconate were not included in this study because they were either unavailable during the study period or had very recently been brought to the market. In North America, both high- and low-molecular weight iron dextran were available and reports for these, and when unspecified, were combined. Only low molecular weight iron dextran was used in Europe, and comparisons were made with the combined iron dextrans in North America. For each iron product, data were obtained for all adverse events and for serious allergic adverse events. All adverse events were defined as the total number of adverse events associated with the products. Serious allergic adverse events were defined as anaphylaxis plus other serious allergic reactions. Anaphylaxis was defined using the WHO's Adverse Reaction Terminology standardized coding system. Other serious allergic reactions were classified as any other events where the reports included any terms or codes for systemic allergy (i.e. bronchospasm, circulatory collapse, dyspnoea, hypotension or decreased blood pressure, laryngeal or laryngotracheal edema, loss of consciousness, oropharyngeal swelling, pharyngeal edema,stridor, syncope or tongue edema) combined with any term or code with cutaneous evidence of bradykinin or histamine release (i.e. angioedema, urticaria, idiopathic urticaria, injection site urticaria, papular urticaria or urticaria vesiculosa).

IV iron sales were purchased from IMS Health (Hergiswil, Switzerland), and the quantities converted into 100 mg dose equivalents (DEq) of iron. Iron use for each country was calculated as the total number of grams of iron sold per million inhabitants over the entire 6.5 year period (gFe/mil). Country populations were determined from census reports from the Population Reference Bureau (www.prb.org) from 2006 data (midpoint of study period). Rates of all adverse events and serious adverse events were reported as the number of events in each country per gFe/mil.

Additionally, data from a subset of specific countries were analyzed separately to determine relative risks for adverse events to individual IV iron products, if they had both of the following criteria present. They had to have at least two different iron products in use and reported more than one serious allergic adverse event within the study period. Using the composite data for these specific countries, mean values were determined for each product for amount of iron use (gFe/mil), numbers of all adverse events and serious allergic adverse events, and rates of all adverse events and serious allergic adverse events (gFe/mil). Odds ratios (OR) for the risks of all adverse events or serious allergic adverse events from one product compared to another were calculated in a 2 x 2 table using the numbers of all adverse events or serious allergic adverse events and the amount of iron used per million of population. OR were reported with 95% confidence intervals and statistical significance was tested using a Chi-square. $P < 0.05$ was considered statistically significant.

3. Results

The populations of countries ranged from 1.3 million for Estonia to 299.1 million for the United States, with total populations of 476.5 million for all 16 European countries, 331.7 million for North America and 808.2 million for all countries combined.

Table 1 indicates the numbers of all adverse events for each product by year. There was a trend towards increasing numbers of annual reports of adverse events, from 154 in 2003 to 560 in 2008. Data from the first six months of 2009 (316) suggest continued increases in reports. Changes to the software in the WHO data base, however, resulted in some of the 2007 reports being recorded in 2008 and thereby potentially skewing the 2007 downwards and the 2008 data upwards. The total numbers of adverse events for each product were similar (ranging from 466 to 606 reports) despite large differences in the amount of each iron used (previously reported) [17]. There were no reports of adverse events for iron sucrose similars.

Table 1: Number of all reported adverse events by year

IV iron product	Year							
	2003	2004	2005	2006	2007*	2008	2009**	Total 2003-2009
Iron dextran (combined)	81	74	94	67	7	152	107	582
Sodium ferric gluconate	39	44	63	47	6	159	108	466
Iron sucrose+	34	50	49	112	11	249	101	606
Total	154	168	206	226	24	560	316	1654

Note: The table includes data for all 16 European countries and North America
*Due to software changes in WHO, most 2007 reports were entered into the system in 2008
**2009 only covers the period January through June
+There were no separate reports for iron sucrose similars

Total IV iron use was 228,427 gFe/mil, although was highly impacted by just two countries, Switzerland and Italy, which together generated 36% of total use. Iron sucrose was used in all countries, sodium ferric gluconate in eight countries, iron dextran in 12, iron sucrose similars in three (Table 2). For countries that did use a particular product, inter-country use of the product varied considerably: use of iron sucrose ranged from 7 (Ireland) to 34,769 gFe/mil (Switzerland); use of sodium ferric gluconate ranged from 1 (Poland) to 48,674 gFe/mil (Italy, where an undefined proportion of sodium ferric gluconate use is oral); use of iron dextran ranged from 1 (Switzerland) to 4,581 gFe/mil (United States); use of iron sucrose similars ranged from 239 (France) to 2,173 gFe/mil (Spain) over the 6.5 year period.

Many countries had low or no reports of adverse events despite substantial iron use. Thus, rates of all adverse events and serious allergic adverse events reported for each product varied considerably by country (Table 2). For example, rates of all and serious allergic adverse events for iron sucrose ranged from 0 (Poland, Austria and Czech Republic) to 1,222 x 10^{-3} (Ireland) reports/gFe/mil and from 0.2 x 10^{-3} (Finland) to 2.7 x 10^{-3} (Germany) reports/gFe/mil, respectively; rates of all and serious allergic adverse events for sodium ferric gluconate ranged from 3.3 x 10^{-3} (Czech Republic) to 183.6 x 10^{-3} (United States) reports/gFe/mil and from 1 x 10^{-3} (Austria, Czech Republic) to 90 x 10^{-3} (United States) reports/gFe/mil, respectively; and rates of all and serious allergic adverse events for iron dextran ranged from 0.9 x 10^{-3} (Turkey) to 46,875 x 10^{-3} (Switzerland) reports/gFe/mil and from 0.9 x 10^{-3} (Turkey)

Table 3: Total iron use and numbers and rates of all adverse events and serious allergic adverse events by country over the period of January 2003 through June 2009 for sodium ferric gluconate and iron dextran

Country	Population (millions)	Sodium ferric gluconate					Iron dextran					Total iron use
		Iron use	# all AE	AE rate	# SAE	SAE rate	Iron use	# all AE	AE rate	# SAE	SAE rate	
Europe												
Austria	8.3		8	N/A	1	N/A	108	4	37.2	1	9.3	3,839
Czech Republic	10.3	10,764	36	3.3	1	0.1						10,881
Denmark	5.4							4	N/A			5,703
Estonia	1.3	250										2,708
Finland	5.3							5	N/A			5,073
France	61.2											12,394
Germany	82.4	12,933	111	8.6	6	0.5	771	259	335.9	26	33.7	15,206
Ireland	4.2						1,667	15	9	2	1.2	1,674
Italy	59.0	48,674	243	5.0	26	0.5						48,808
Norway	4.7						888	34	38.3	3	3.4	5,892
Poland	38.1	1					781	30	38.4	1	1.3	3,888
Spain	45.5	20					256	3	11.7			14,640
Sweden	9.1						330	9	27.2	3	9.1	11,712
Switzerland	7.5		3	N/A			1	25	46,875			34,769
Turkey	73.7						1,136	1	0.9	1	0.9	12,362
United Kingdom	60.5						511	201	393.3	24	47.0	6,549
North America												
United States	299.1	8,534	1,567	183.6	90	10.5	4,581	1,264	275.9	108	23.6	28,397
Canada	32.6	843	115	136.4	2	2.4	2,630	292	111	23	8.7	4,747

Iron use is in grams of iron per million inhabitants
AE rate=number of all adverse events per grams of iron used per million inhabitants ($\times 10^{-3}$)
SAE rate=number of serious allergic adverse events per grams of iron used per million inhabitants ($\times 10^{-3}$)

to 47 x 10^{-3} (United Kingdom) reports/gFe/mil, respectively. There were no reports that differentiated iron sucrose similars from iron sucrose and therefore no separation of adverse events could be provided for iron sucrose similars.

Table 2: Numbers and rates of all adverse events and serious allergic adverse events by country over the period of January 2003 through June 2009 for iron sucrose and iron sucrose similars

Country	Population (millions)	Iron sucrose					Iron sucrose similars*
		Iron use	# all AE	AE rate	# SAE	SAE rate	Iron use
Europe							
Austria	8.3	3,731					
Czech Republic	10.3	118					
Denmark	5.4	5,703	2	0.4			
Estonia	1.3	2,458	6	2.4	1	0.4	
Finland	5.3	5,073	6	1.2	1	0.2	
France	61.2	12,155	184	15.1	9	0.7	239
Germany	82.4	1,503	45	29.9	4	2.7	
Ireland	4.2	7	8	1,221.8			
Italy	59.0	134	4	29.8			
Norway	4.7	5,004	3	0.6			
Poland	38.1	3,106		0.0			
Spain	45.5	12,190	8	0.7			2,173
Sweden	9.1	11,382	45	4.0	3	0.3	
Switzerland	7.5	34,769	669	19.2	53	1.5	
Turkey	73.7	10,219	36	3.5	9	0.9	1,008
United Kingdom	60.5	6,038	224	37.1	12	2.0	
North America							
United States	299.1	15,282	654	42.8	31	2.0	
Canada	32.6	1,273	155	121.7	3	2.4	

Iron use is in grams of iron per million inhabitants
AE rate=number of all adverse events per grams of iron used per million inhabitants ($\times 10^{-3}$)
SAE rate=number of serious allergic adverse events per grams of iron used per million inhabitants ($\times 10^{-3}$)
*Iron sucrose similars have been available in France since 2009, in Spain since 2005, and in Turkey since 2006, but no reports on adverse events or serious adverse events have been sent to the WHO Monitoring Centre in Uppsala.

There was little consistency between countries for the rates of reported adverse events for any one IV iron product: some countries have very low rates of reports of adverse events even though others may have large rates for the same product. For example, Turkey had a reported total adverse event rate of less than 1.0 x 10^{-3} reports/gFe/mil for iron dextran, while Switzerland's rate for the same product exceeded 46,000 x 10^{-3} reports/gFe/mil. Rates of reports for different products also varied considerably within a specific country. For example, in Germany, there were 8.6 x 10^{-3} total reports/gFe/mil for sodium ferric gluconate, about 30 x 10^{-3} for iron sucrose and 336 x 10^{-3} for iron dextran. Alternatively, the United States had the highest rate for iron dextran (276 x 10^{-3} reports/gFe/mil), intermediate for sodium ferric gluconate (183 x 10^{-3} reports/gFe/mil) and lowest for iron sucrose (43 x 10^{-3} reports/gFe/mil).

Six countries (Germany, Sweden, Turkey, United Kingdom, Canada and United States) each used at least two different iron products in the study period and reported serious adverse events. Table 3 indicates the mean values of iron use for each product, numbers and rates of all adverse events and serious allergic adverse events. The rates of all adverse events were smallest for iron sucrose (39.8 x 10^{-3} reports/gFe/mil), intermediate for sodium ferric gluconate

(54.8 x 10^{-3} reports/gFe/mil) and greatest for iron dextran (337.7 x 10^{-3} reports/gFe/mil). Rates of serious allergic adverse events were also lowest for iron sucrose (1.7 x 10^{-3} reports/gFe/mil), intermediate for sodium ferric gluconate (4.5 x 10^{-3} reports/gFe/mil) and highest for iron dextran (20.5 x 10^{-3} reports/gFe/mil).

Table 4: Total iron use and correlating adverse events and serious allergic adverse events January 2003–June 2009 for countries that used more than one iron product

IV iron product	Iron use	# all AE	All AE rate	# SAE	SAE rate
Iron sucrose	7,616.1	193.2	39.8	10.33	1.7
Sodium ferric gluconate	7,436.5	298.8	54.8	32.67	4.5
Iron dextran	1,659.8	337.7	190.7	30.83	20.5

Iron use=grams of iron per million inhabitants
AE rate=number of all adverse events per grams of iron used per million inhabitants (× 10^{-3}).
SAE rate=number of serious allergic adverse events per grams of iron used per million inhabitants (× 10^{-3}).
*Germany, Sweden, Turkey, the United Kingdom, Canada, and the United States were the 6 countries that used more than 1 iron product.

Odds ratios (OR) and statistical comparisons of risks for all adverse events and serious allergic adverse events are shown in Table 4. Iron sucrose had a significantly lower risk for all adverse events (OR = 0.63, P<0.0001) or serious allergic adverse events (OR = 0.31, P = 0.001) compared to sodium ferric gluconate. Iron sucrose also had a significantly lower risk for all adverse events (OR = 0.13, P<0.0001) or serious allergic adverse events (OR = 0.07, P <0.0001) compared to iron dextran. Sodium ferric gluconate had lower risks for all adverse events (OR = 0.20, P <0.0001) and serious allergic adverse events (OR = 0.24, P <0.0001) compared to iron dextran.

4. Discussion

To our knowledge, this paper represents the first comparison of adverse event rates of IV iron products in different countries, including an analysis by population at risk. Previous studies have demonstrated that changing trends in iron prescribing practices are associated with changes in rates of reported adverse events [14-17] However, such studies have been unable to examine IV iron use by country or show the relative use of iron products within and between countries. This current study sheds light upon the relative use of IV iron within populations, and shows interesting and extensive differences in practices.

Table 5: Odds ratios for comparison of all adverse events and serious allergic adverse events by intravenous iron product

Comparison	OR (95% CI) [P]	
	All AE	SAE
Iron sucrose *vs.* sodium ferric gluconate	0.63 (0.52-0.76) [<0.0001]	0.31 (0.14-0.65) [0.001]
Iron sucrose *vs.* iron dextran	0.13 (0.10-0.15) [<0.0001]	0.07 (0.03-0.15) [<0.0001]
Sodium ferric gluconate *vs.* iron dextran	0.20 (0.17-0.23) [<0.0001]	0.24 (0.14-0.40) [<0.0001]

AE=adverse events; CI=confidence intervals; SAE=serious allergic adverse events.

There is considerable variation in the choice of iron product used by country, with some countries demonstrating substantial preferences for one particular product over others (e.g. iron sucrose is predominantly chosen by Austria, Denmark, Finland, France, Norway, Poland, Spain, Sweden, Switzerland, Turkey and the United Kingdom; sodium ferric gluconate has most use in the Czech Republic, Germany and Italy; iron dextran is the most common choice in Ireland and Canada). The reasons for this are unclear, but may be influenced by national formularies, local practices and regional commercial agreements and marketing strategies. Additionally, geographic differences may be influenced by cultural expectations of care, prescribers' adherence to international and regional clinical practice guidelines, and perhaps different mixes of patient types that might receive IV iron.

There is also a sizeable variation in the amount of iron that is used from country to country, as standardized by grams of iron sold per million of the population (ranging from 1,674 gFe/mil in Ireland to 48,808 gFe/mil in Italy). The reasons for this are also unclear.

Interestingly, some countries have reported adverse events to products that they apparently do not purchase (e.g. Austria and Switzerland to sodium ferric gluconate and Denmark and Finland to iron dextran). It is possible that these countries may have imported the products from other countries, or that some of these products may be sold directly to hospitals without recording these sales at IMS (e.g. tender business). There were no reports of any adverse events for iron sucrose similars. There are several potential explanations, including the possibility that there were indeed no such adverse events. This explanation seems implausible given animal data demonstrating that iron sucrose similars have an increased risk of causing biochemical, histological and functional adverse events compared to the originator [18,19]. It is more credible that any adverse events observed by clinicians associated with iron sucrose similars were reported only as iron sucrose. Thus, the importance of inclusion of brand names within an adverse event report must be emphasized in order to be able to differentiate any signals arising from these types of product, as recently suggested [16]

Interesting insight was obtained when we compared those six countries each using at least two different products and reporting at least one severe adverse event (Germany, Sweden, Turkey, the United Kingdom, Canada and the United States). These countries had a combined population of 557.4 million inhabitants (69% of the total for all countries) and used a total of 78,973 gFe/mil (34.6% of 228,427 gFe/mil total iron use). Table 3 indicates a similar trend for all adverse events and serious allergic adverse events, where the lowest rates were for iron sucrose, intermediate rates were associated with sodium ferric gluconate and iron dextran had the highest rates. Odds ratios demonstrate a 37% reduced risk of all adverse events and 69% reduced risk of serious allergic adverse events with iron sucrose compared to sodium ferric gluconate, and 87% and 93% reduced risks, respectively, compared to iron dextran. Sodium ferric gluconate also had significant reductions in risks for both adverse events compared to iron dextran.

Limitations are inherent in studies such as this. Databases are only as accurate and complete as the reports that are delivered to them. There are substantial risks for under-reporting, and the risks of the Weber effect and clinician bias towards over-reporting are also well recognized [20-22]. The inability of databases to differentiate reports relating to iron sucrose similars from the originator product is worrisome as it minimize detection of

a potential signal. This might become problematic in the United States too since the recent introduction of generic/similar sodium ferric gluconate. Further, sales figures may not necessarily accurately reflect actual administrations of each product – some products might regularly be administered as small doses (e.g. 62.5 mg for sodium ferric gluconate), while iron dextran might be administered at doses of 1,000 mg or more. Labelling, too, for any product might vary from country-to-country (e.g. sodium ferric gluconate is approved for doses of 62.5 mg in Europe and 125 mg in United States; iron sucrose is approved to be given at doses of 200 mg in United States and as 500 mg doses in Germany). Moreover, we have combined data for low- and high molecular weight iron dextran from the United States and compared this to the low molecular weight iron dextran data from Europe. The exact effect of this approach is unclear, particularly since previous reports have suggested that high molecular weight products pose a higher risk of adverse events.15,23 Further, the type of facility and the type of patient might well influence the results. For example, reports could have originated from clinics, hospitals or other institutions and the exact method of administration of agents in those sites might differ. Over the course of the study period, more non-nephrology specialists are likely to have started using IV iron and it is plausible that different patient disease characteristics and demographics could also impact their responses to IV iron. Thus, caution should be exercised in generalized interpretation of the results. Nevertheless, pharmacovigilance and the use of spontaneous reporting databases are legitimate means of assessing epidemiologic adverse event data, and can be used to compare rare signals of events.

Our analysis of risks accounting for population is a novel approach. This method has provided insight into magnitude of iron use by country, and invokes challenging questions about differences in clinical practices between countries. Further, it suggests that there is significant under reporting of serious allergic adverse events in some countries. Assuming that the real risk for a serious adverse event remains constant from individual to individual, then all countries should demonstrate similar rates of events for any particular product. Exact reasons for these discrepancies should be investigated, but may be due to national reporting procedures and regulations.

5. Conclusions

There was considerable international variation in both iron use and of choice of product, and in rates of all adverse events and serious allergic adverse events reported for each product. For those countries that used at least two different iron products in the study period and reported serious allergic adverse events, the rates of all adverse events were smallest for iron sucrose, intermediate for sodium ferric gluconate and greatest for iron dextran. Rates of serious allergic adverse events were also lowest for iron sucrose, intermediate for sodium ferric gluconate and highest for iron dextran. Iron sucrose had a significantly lower risk for all adverse events or serious allergic adverse events compared to sodium ferric gluconate and also had a significantly lower risk for all adverse events or serious allergic adverse events compared to iron dextran. Sodium ferric gluconate had lower risks for both all adverse events and serious allergic adverse events than iron dextran. Because of our suspicions regarding differential adverse event rates with similar versus originators, we urge clinicians to also report adverse events by trade name.

Acknowledgement

The authors thank Anders Viklund, UMC, and Robert Geldof, Vifor Pharma, Ltd., who provided substantial input into assisting interpretation of the data. Some of these data were presented at the American Society of Nephrology annual meeting, Denver, Colorado, USA, November 2010.

Conflicts of interest

This study was supported by a grant from Vifor Pharma, Ltd. Vifor Pharma Ltd. provided input into the design, interpretation of data and review of the manuscript. Final decision regarding study design, data interpretation and manuscript development and submission were performed solely by the authors. George Bailie has been or is currently a consultant for Vifor Pharma, Luitpold Pharmaceuticals, Fresenius Medical Care-North America, Genzyme, Mitsubishi. Johan (Jan-Jaap) Verhoef has completed an internship at Vifor Pharma, Ltd.

Disclaimer

The WHO indicates that the information contained in this manuscript does not necessarily represent the opinion of the WHO.

References

[1] Van Wyck DB, Roppolo M, Martinez CO, et al. A randomized controlled trial comparing IV iron sucrose to oral iron in anemic patients with nondialysis-dependent CKD. *Kidney Int.* 2005;68:2846-2856.

[2] Bager P, Dahlerup JF. The health care cost of intravenous iron treatment in IBD patients depends on the economic evaluation perspective. J Crohns Colitis. 2010;4:427-430.

[3] Krafft A, Breymann C. Iron sucrose with and without recombinant erythropoietin for the treatment of severe postpartum anemia: a prospective, randomized, open-label study. J Obstet Gynaecol Res 2011;37:119-24.

[4] Khalafallah A, Dennis A, Bates J, et al. A prospective, randomized, controlled trial of intravenous versus oral iron for moderate iron deficiency of pregnancy. J Intern Med. 2010;268:286-295.

[5] Van Wyck DB, Mangione A, Morrison J, et al. Large-dose intravenous ferric carboxymaltose injection for iron deficiency anemia in heavy uterine bleeding: a randomized, controlled trial. Transfusion. 2009;49:2719-2728.

[6] Nomura RM, Dias MC, Igai AM, et al. Anemia during pregnancy after silastic ring Roux-en-Y gastric bypass: influence of time to conception. Obes Surg. 2011;21:479-484.

[7] Anker SD, Comin Colet J, Filippatos G, et al. Ferric carboxymaltose in patients with heart failure and iron deficiency. N Engl J Med. 2009;361:2436-2448.

[8] Bastit A, Vandebroek A, Altintas S, et al. Randomized, multicenter, controlled trial comparing the efficacy and safety of darbepoetin alfa administered every 3 weeks with or without intravenous iron in patients with chemotherapy-induced anemia. J Clin Oncol. 2008;26:1611-1618.

[9] Dangsuwan P, Manchana T. Blood transfusion reduction with intravenous iron in gynecologic cancer patients receiving chemotherapy. Gynecol Oncol. 2010;116:522-525.

[10] Pizzi LT, Bunz TJ, Coyne DW, et al. Ferric gluconate treatment provides cost savings in patients with high ferritin and low transferrin saturation. Kidney Int. 2008;74:1588-1595.

[11] Mircescu G, Garneata L, Capusa C, Ursea N. Intravenous iron supplementation for the treatment of anaemia in pre-dialyzed chronic renal failure patients. Nephrol Dial Transplant. 2006;21:120-124

[12] Serrano-Trenas J, Uqalde P, Cabello LM, et al. Role of perioperative intravenous iron therapy in elderly hip fracture patients: a single-center randomized controlled trial. Transfusion. 2011;51:97-104.

[13] Knight TG, Ryan K, Schaefer P, et al. Clinical and economic outcomes in Medicare beneficiaries with stage 3 or stage 4 chronic kidney disease and anemia: the role of intravenous iron therapy. J Manag Care Pharm. 2010;16:605-615.

[14] Bailie GR, Clark JA, Lane CE, Lane PL. Hypersensitivity reactions and deaths associated with intravenous iron preparations. Nephrol Dial Transplant. 2005;20:1443-1449.

[15] Chertow GM, Mason PD, Vaage-Nilsen O, Ahlmen J. Update on adverse drug events associated with parenteral iron. Nephrol Dial Transplant. 2006;21:378-382.

[16] Wysowski DK, Swartz L, Borders-Hemphill BV, et al. Use of parenteral iron products and serious anaphylactic-type reactions. Am J Hematol. 2010;85:650-654.

[17] Bailie GR, Horl WH, Verhoef JJ. Differences in spontaneously reported hypersensitivity and serious adverse events for intravenous iron preparations: comparison of Europe and North America. Arzneimittelforsch. 2011;61:267-275.

[18] Toblli GE, Cao G, Oliveri L, Angerosa M. Differences between original intravenous iron sucrose and iron sucrose similar preparations. Arzneimittelforsch. 2009;59:176-190.

[18] Toblli GE, Cao G, Oliveri L, Angerosa M. Differences between the original iron sucrose complex Venofer and the iron sucrose similar Generis and potential implications. Port J Nephrol Hypert. 2009;23:53-63.

[20] Weber JCP. Epidemiology of adverse reactions to nonsteroidal anti-inflammatory drugs. In: Rainslord KD, Velo EP, eds. Advances in Inflammation Research. New York, NY: Raven Press; 1984:1-7.

[21] Weiss-Smith S, Deshpande G, Chung S, et al. The FDA dug safety surveillance program: adverse event reporting trends. Arch Intern Med. 2011;171:591-593.

[22] Horwitz RI, Feinstein AR. The problem of protopathic bias in case-control studies. Am J Med. 1980;68:255-258.

[23] Bailie GR. Comparison of serious adverse events from intravenous iron products in the United States. Am J Health-Syst Pharm. 2011 (in press).

Chapter | 3

Iron nanomedicines induce Toll-like receptor activation, cytokine production and complement activation

Verhoef JJF, de Groot AM, van Moorsel M, Ritsema J, Beztsinna N, Maas C, Schellekens H

Article published in:
Biomaterials.
2017 Mar;119:68-77.
doi: 10.1016/j.biomaterials.2016

Abstract

Approximately a dozen of intravenous iron nanomedicines gained marketing authorization in the last two decades. These products are generally considered as safe, but have been associated with an increased risk for hypersensitivity-like reactions of which the underlying mechanisms are unknown. We hypothesized that iron nanomedicines can trigger the innate immune system. We hereto investigated the physico-chemical properties of ferric gluconate, iron sucrose, ferric carboxymaltose and iron isomaltoside 1000 and comparatively studied their interaction with Toll-like receptors, the complement system and peripheral blood mononuclear cells. Two out of four formulations appeared as aggregates by Scanning Transmission Electron Microscopy analysis and were actively taken up by HEK293T- and peripheral blood mononuclear cells in a cholesterol-dependent manner. These formulations triggered in vitro activation of intracellular Toll-like receptors 3, -7 and -9 in a dose- and serum-dependent manner. In parallel experiments, we determined that these compounds activated the complement system. Finally, we found that uptake of aggregation-prone iron nanomedicines by peripheral blood mononuclear cells in whole blood induced production of the pro-inflammatory cytokine IL-1β, but not IL-6.

1. Introduction

Iron deficiency anemia is a nutritional disorder affecting almost 30% of the world's population [1]. Besides relative low uptake from diet, iron deficiency anemia is seen during pregnancy, hemorrhage and diseases, such as inflammatory bowel disease and chronic kidney failure [2]. Although iron deficiency can be treated with oral iron, patients may require such amounts that are unable to be restored by this route [3]. All commercial intravenous iron formulations consist of a polynuclear Fe(III)-oxyhydroxide/oxide core surrounded by carbohydrates [4]. This carbohydrate shell functions as a stabilizer preventing direct release of bioactive iron and particle aggregation [5]. As such, these products have a diameter between 10 – 30 nm and are considered to be nanomedicines [6]. Examples of carbohydrates used in commercial iron nanomedicines include: sucrose, gluconate, dextran, isomaltoside 1,000 and carboxymaltose.

The number of different intravenous iron nanomedicines on the market was limited until the 1990's, but an ever increasing number of products have since entered the clinic [5]. Although iron nanomedicines are considered safe, they are associated with a product dependent risk for (acute) hypersensitivity-like reactions, such as wheezing, bronchospasm, periorbital edema and circulatory collapse; both of which can result in death [7,8]. Although iron dextran is associated with the greatest risk of hypersensitivity-like events, newer developed non-dextran iron nanomedicines are also linked to these reactions, however less frequent [7,9–11]. As such, the European Medicine Agency send out a warning for all commercially available intravenous iron products in 2013 stating that physicians should take precautions when administering these products [12].

Whereas high molecular weight iron dextran formulations have been associated with anti-dextran antibodies, the mechanisms how non-dextran formulations can induce these hypersensitivity-like reactions remain inconclusive [10,13,14]. As such, high molecular weight iron formulations are no longer available [13]. Possible factors triggering these reactions are the release of high concentrations of unbound iron into the circulation, recognition of carbohydrates by the immune system and or destabilization of the formulation by dissociation of these carbohydrates [4,9,11,15].

In this study, we investigated the physico-chemical characteristics of four different intravenous iron nanomedicines and their interaction with the innate immune system. We found differences in aggregation behavior among the various formulations investigated which associated with higher cellular uptake and activation of Toll-like receptors, the complement system and specific cytokine release.

2. Materials and Methods

2.1. Materials

4-(2-hydroxyethyl)-1-piperazineethanesulfonic acid (HEPES), adenosine triphosphate (ATP), ammonium iron (III) citrate, propidium iodide, chlorpromazine, methyl-beta-cyclodextrin, transferrin, Dulbecco's Phosphate Buffered Saline (PBS) without calcium chloride and magnesium chloride, PBS with calcium chloride and magnesium chloride, fetal bovine serum (FBS), trypsin, ethylenediaminetetraacetic acid (EDTA), RPMI-1640

containing both 20 mM HEPES, L-glutamine and sodium bicarbonate, Dulbecco's Modified Essential Medium containing 4.5 g/L glucose and L-glutamine, and antibiotic–antimycotic solution containing penicillin–streptomycin and antimycotics were all obtained from Sigma-Aldrich (Zwijndrecht, the Netherlands). Ficoll-Paque Plus was obtained from Fisher Scientific (Landsmeer, the Netherlands). Normocin, blasticidin, zeocin, HEK-Blue Selection, PAM3SCK, Poly(I:C) LPS-EK, CL264, ODN2006, and QUANTI-Blue were obtained from Invivogen (Toulouse, France). Ferric gluconate, iron sucrose, ferric carboxymaltose and iron isomaltoside 1,000 were kindly provided by Vifor Pharma (Glattbrug, Switzerland) and freshly used before the expiration date. All iron nanomedicines were endotoxin free, determined by the Pyrogene Recombinant Factor C assay (Lonza Benelux bv, Breda, the Netherlands).

2.2. Physico-chemical characterization

Iron nanomedicines were characterized by their mean hydrodynamic particle size and polydispersity index measured by dynamic light scattering (DLS), using a Malvern ALV CGS-3 multi-angle goniometer equipped with a He–Ne laser source (λ = 632.8 nm, 22 mW output power) under an angle of 90° (Malvern Instruments, Malvern, UK). Hydrodynamic size and polydispersity were recorded with an optical fiber-based detector and a digital LV/LSE-5003 correlator with a temperature controller set at 25 °C. Samples were diluted in PBS to 1 – 2.5 mg iron/mL to realize the highest count rate. Zeta-potential of iron nanomedicines was measured with laser Doppler electrophoresis on a Zetasizer Nano-Z (Malvern Instruments, Malvern, UK) following the diffusion barrier method. A sample of 50 µL was dispersed in 10 mM HEPES buffer pH 7.4 at the bottom of the cell and measured at 150.9 V for 100 runs.

Scanning Transmission Electron Microscopy (STEM) was performed on a Philips 200 kV Tecnai 20F transmission electron microscope (FEI Company, Eindhoven, the Netherlands) equipped with a Field Emission Gun and a Twin objective lens. Images were recorded with a Fischione High Angle Annular Dark Field (HAADF) detector. Energy-dispersive X-ray spectroscopy (EDS) was performed to study chemical composition of the sample. The instrument consisted of a VG Escalab 200 R spectrometer with a MgKα X-ray source (hν = 1253.6 eV). Iron formulations were diluted to 200 µg iron/mL in dH_2O and 3 µL samples were left to dry on carbon coated copper grids.

2.3. Cell culture

HEK-Blue hTLR cells were cultured in DMEM 4.5 g/L glucose to which 10% FBS, 50 U/mL penicillin, 50 mg/mL streptomycin, 100 µg/mL Normocin and 2 mM L-glutamine was added. HEK-Blue hTLR3 culture medium was supplemented with 30 µg/mL blasticidin and 100 µg/mL zeocin, HEK-Blue hTLR7 and -9 culture medium was supplemented with 10 µg/mL blasticidin and 100 µg/mL zeocin and HEK-Blue hTLR4 culture medium with HEk-Blue Selection. HEK293T cells were cultured in DMEM with 4,5 g/L glucose supplemented with 10% FBS and an antibiotic–antimycotic solution.

2.4. Toll-like receptor activation reporter assay

Activation of hTLR2, -3, -4, -7 and -9 was investigated using the HEK-Blue hTLR reporter cell-lines (Invivogen, Toulouse, France). HEK-Blue hTLR cells express both a specific hTLR gene and a NF-κB-inducible secreted embryonic alkaline phosphatase (SEAP) reporter

gene. HEK-Blue hTLR cells were seeded at assay-dependent amounts (details in Table 1) and incubated overnight with the various iron nanomedicines or positive controls in culture medium.

Table 1: Experimental design of the Toll-like receptor activation study using the HEK-Blue hTLR reporter cell-lines.

Cell line	Cells seeded (cells/cm^2)	Positive control
hTLR2	156,250	10 ng/mL PAM3CSK4
hTLR3	156,250	500 ng/mL Poly I:C
hTLR4	78,125	1 ng/mL LPS-EK
hTLR7	250,000	500 ng/mL CL264
hTLR9	250,000	1 μg/mL ODN2006

The next day, SEAP was quantitatively determined by the addition of 20 μL cell supernatant to 180 μL of QUANTI-Blue and incubated for 1 hour at 37°C with 5% CO_2 and subsequently measured at 650 nm using a Biorad Model 550 Microplate Reader (Biorad, Hercules, United States). hTLR activation was expressed by relative alkaline phosphatase levels, defined as sample level divided by PBS control level. Subsequently, synergy between the iron nanomedicines and hTLR agonists was studied by simultaneous incubation of the cells with their specific hTLR agonists and one of the four iron nanomedicines.

hTLR activation without the presence of serum was investigated with HEK-Blue Detection Medium which enables real-time monitoring of SEAP expression without the need for serum. Here, 20 μL sample was added to 180 μL of HEK-Blue Detection Medium and incubated overnight after which absorbance was recorded at 655 nm. SEAP expression was corrected for the absorbance of iron nanomedicines in HEK-Blue Detection Medium.

2.5. Complement activation

Complement activation was investigated by measuring the amount of SC5b-9, a soluble terminal factor released upon activation of either the classical, lectin or alternative pathway. Activation of the alternative pathway was investigated by SC5b-9 analysis in the presence of EGTA/Mg^{2+} and by the detection of the alternative pathway marker Bb. Ferric gluconate, iron sucrose, ferric carboxymaltose and iron isomaltoside 1,000 were incubated in 1:4 diluted serum obtained from healthy donors at 500 μg iron/mL. The incubated serum samples were vigorously shaken for 30 minutes at 37°C. Negative and positive controls included respectively the incubation with PBS and 200 μg/mL zymosan. SC5b-9 and Bb release were measured by either the MicroVue SC5b-9 Plus or Bb Enzyme Immunoassay (Quidel Corp., San-Diego, United States). The samples were diluted 50 fold in the provided reagent diluent supplemented with 25 mM EDTA. The assays were performed according to the manufacturer's protocol.

2.6. Isolation of peripheral blood mononuclear cells

Peripheral blood mononuclear cells (PBMC) were isolated from healthy donors obtained from the mini donor service (MDS) at the University Medical Hospital Utrecht, the Netherlands. Blood was collected in heparinized vacutainers and PBMC were subsequently

isolated using a Ficoll-Paque Plus gradient. Briefly, heparinized blood was diluted 1:1 with PBS and subsequently 35 mL of diluted blood was placed on top of 15 mL Ficoll-Paque Plus before centrifugation at 1,260 x g for 18 min. The PBMC layers were removed, washed in PBS and resuspended in RPMI-1620 supplemented with 10% FBS and an antibiotic-antimycotic solution.

2.7. Cellular uptake of iron NP

Cellular uptake of the iron nanomedicines was investigated in HEK293T cells and PBMC by means of the calcein-AM quenching method, enabling the detection of intracellular ferrous and ferric iron [16,17]. HEK293T cells and PBMC were seeded at respectively 125.000 and 1.562.500 cells/cm^2 in a 96-well plate and incubated at 37°C under 5% CO_2. The next day, ferric gluconate, iron sucrose, ferric carboxymaltose and iron isomaltoside 1,000 were added at concentrations varying between 3.2 – 1,000 µg iron/mL. Samples were incubated for 1-7 hours at 37°C with 5% CO_2 and subsequently washed and resuspended in PBS containing Ca^{2+} and Mg^{2+}. Cells were then incubated with 200 µL 12.5 nM calcein-AM in culture medium for 30 minutes at 37°C with 5% CO_2. The cells were washed twice with PBS and finally resuspended in PBS before analysis by flow cytometry, using the FACS Canto II (BD Biosciences, San Jose, United States) with a 488 nm solid state laser. Fluorescence intensity was recorded in the green fluorescence channel with 530/30 nm filters. As calcein is quenched by iron, relative uptake of iron nanomedicines was determined as the percentage decrease in calcein fluorescence to the cells treated with PBS. Distinction between quenching in monocytes and lymphocytes was made by means of gating in the FSC/SSC scatter plot.

Endocytic pathway analysis was investigated by pre-incubation of HEK293T cells with 100 µL of either 150-75 µM chlorpromazine, 10 µM methyl-beta-cyclodextrin or 40-10 µM transferrin diluted in culture medium for 30 minutes. Subsequently, an equal volume of the iron formulations were added and incubated for 1 hour. Subsequent calcein-AM staining and analysis was performed as described above.

Cell viability was assessed by staining cells with 2 µg/mL propidium iodide (PI) and subsequent detection by flow cytometry using the FACS Canto II and a 488 nm solid state laser with filters set at 695/40 nm. Viability was expressed as the percentage of gated cells being negative for PI staining.

2.8. Cytokine production in human whole blood

Secretion of IL-1β and IL-6 was studied in blood from 9 healthy donors obtained from the MDS. Blood was collected in heparinized vacutainer tubes and diluted 1:1 in RPMI-1640 supplemented with antibiotics. Diluted whole blood (90 µL) was plated in a 96-well plate and incubated with 10 µL of 3.3 – 1.000 µg iron/mL ferric gluconate, iron sucrose, ferric carboxymaltose or iron isomaltoside 1,000. Controls included PBS and ATP + LPS. Samples were incubated for either 3, 24 or 48 hours at 37°C with 5% CO_2 and centrifuged at 1.500 x g for 15 minutes. Secreted IL-1β and IL-6 were quantified using the human IL-1 beta/IL-1F2 DuoSet and the IL-6 DuoSet (R&D Systems, Abingdon, United Kingdom) according to the manufacturer's protocol.

3. Results

3.1. Physico-chemical characterization of iron nanomedicines

The marketed intravenous iron nanomedicines ferric gluconate, iron sucrose, ferric carboxymaltose and iron isomaltoside 1,000 were selected based on their market share, different carbohydrate shielding and stability [4]. As shown in table 2, neutral zeta-potentials between 0 and -1 mV were measured for all iron nanomedicines in 10 mM HEPES. DLS revealed that z-average, indicating the hydrodynamic diameter, differed among the formulations and ranged between 10 – 25 nm.

Table 2: Physico-chemical characterization of four iron nanomedicines.

Sample	Zeta potential (mV)	Z-average (nm)
Ferric gluconate	-0.82 ± 0.05	16.7 ± 0.3
Iron sucrose	-0.86 ± 0.19	12.2 ± 0.5
Ferric carboxymaltose	-0.29 ± 0.08	24.3 ± 0.5
Iron isomaltoside 1,000	-0.53 ± 0.24	15.4 ± 0.2
10 mM HEPES	-10.13 ± 0.53	-

STEM analysis revealed that the iron cores of ferric gluconate, iron sucrose and iron isomaltoside 1,000 was spherical when dried onto a copper grid (Fig. 1A, B and D), while the core of ferric carboxymaltose was rod-shaped (Fig. 1C). Both ferric gluconate and iron sucrose appeared as aggregates, while ferric carboxymaltose and iron isomaltoside 1,000 appeared as single particles. STEM revealed core sizes of 9, 6 and 18 nm for ferric gluconate,

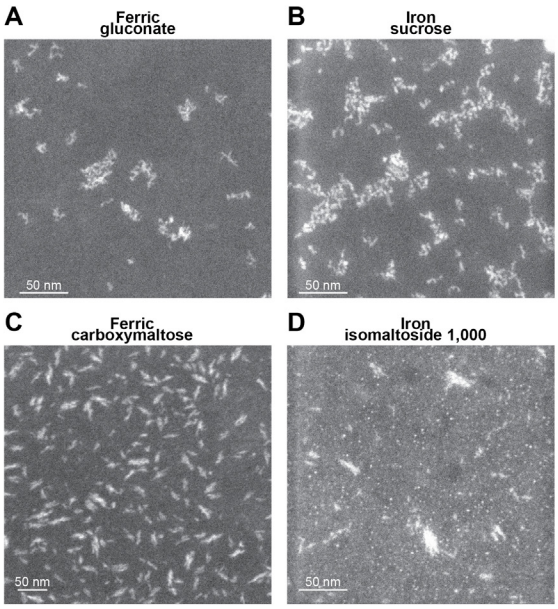

Fig. 1. Imaging of iron oxide cores by Scanning Transmission Electron Microscopy (STEM). Ferric gluconate (A), iron sucrose (B), ferric carboxymaltose (C) and iron isomaltoside 1,000 (D) were diluted to 200 µg iron/mL in dH_2O and dried on carbon coated copper grids before analysis.

iron sucrose and ferric carboxymaltose, respectively. Except iron isomaltoside 1,000, all formulations consisted out of monodisperse particles. Here, two populations were identified with an average core size of 3 and 11 nm respectively.

3.2. Toll-like receptor activation by iron NP

Iron nanomedicine therapy is linked to acute hypersensitivity-like reactions which cannot be explained by IgG- or IgE-antibodies [10,14]. We hypothesized that iron nanomedicines can be recognized by means of pattern recognition, an important feature of the innate immune system involved in early inflammatory responses [18]. In our first series of experiments, we investigated the capacity of iron nanomedicines to activate hTLRs in HEK-Blue reporter cell lines.

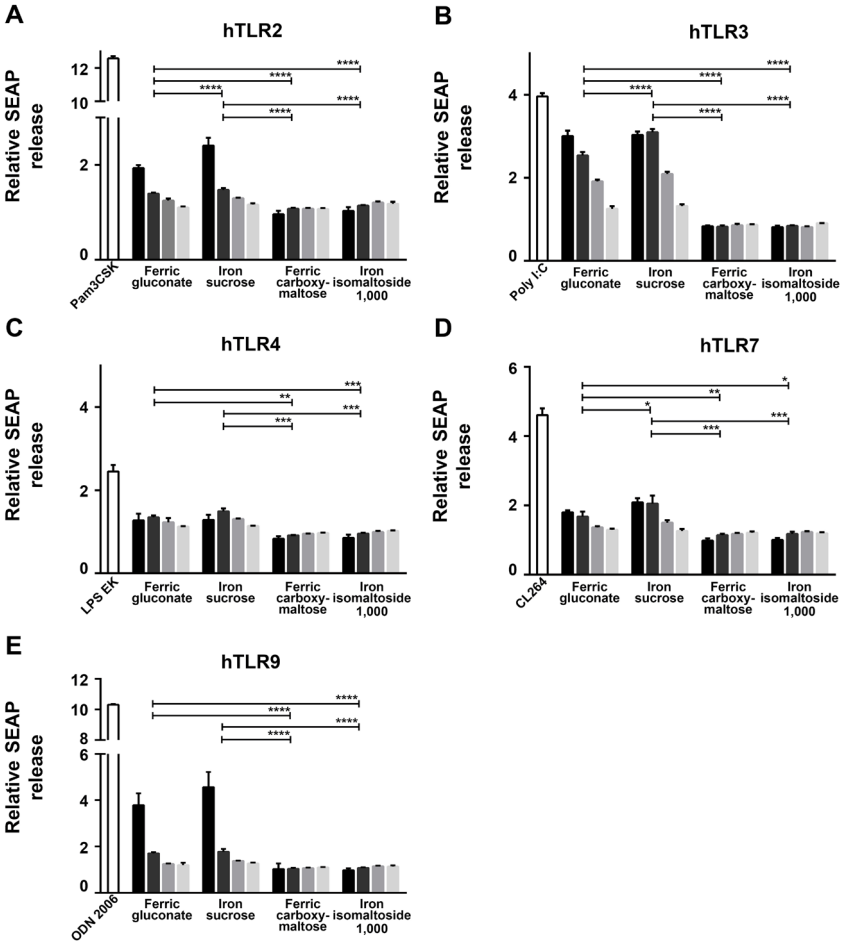

Fig. 2. Activation of Toll-like receptors by iron nanomedicines. hTLR reporter cell-lines were incubated with concentration ranges of ferric gluconate, iron sucrose, ferric carboxymaltose, iron isomaltoside 1,000 or positive controls agonists (A– E; black = 1.000 µg/mL, dark grey = 750 µg/mL, middle grey = 500 µg/mL, light grey 250 µg/mL). Data is normalized to PBS-treated cells. Statistical analysis by one-way ANOVA is shown for iron concentrations of 750 µg/mL.

We found that ferric gluconate and iron sucrose, but not ferric carboxymaltose and iron isomaltoside 1,000, activated hTLR3 and to a lesser extend hTLR2, -7 and -9 in a dose-dependent manner (Fig. 2A–2E). In these experiments, optical behavior between products was comparable (supporting information S1A), cell viability remained unchanged (supporting information S1B) and activation of hTLR3 and -9 was not observed when cells were incubated with ferric iron only (supporting information S2A, -S2B). No hTLR3 activation was observed when iron nanomedicines were incubated in serum-free medium (supporting information S3), suggesting that a serum co-factor is required for iron nanomedicines to bind hTLRs.

We next studied the interaction between the iron nanomedicines and specific positive control hTLR agonists. We found that ferric gluconate and iron sucrose significantly inhibited the activation of hTLR9 by ODN2006 and to a lesser extent hTLR3 by Poly I:C (Fig. 3A–E).

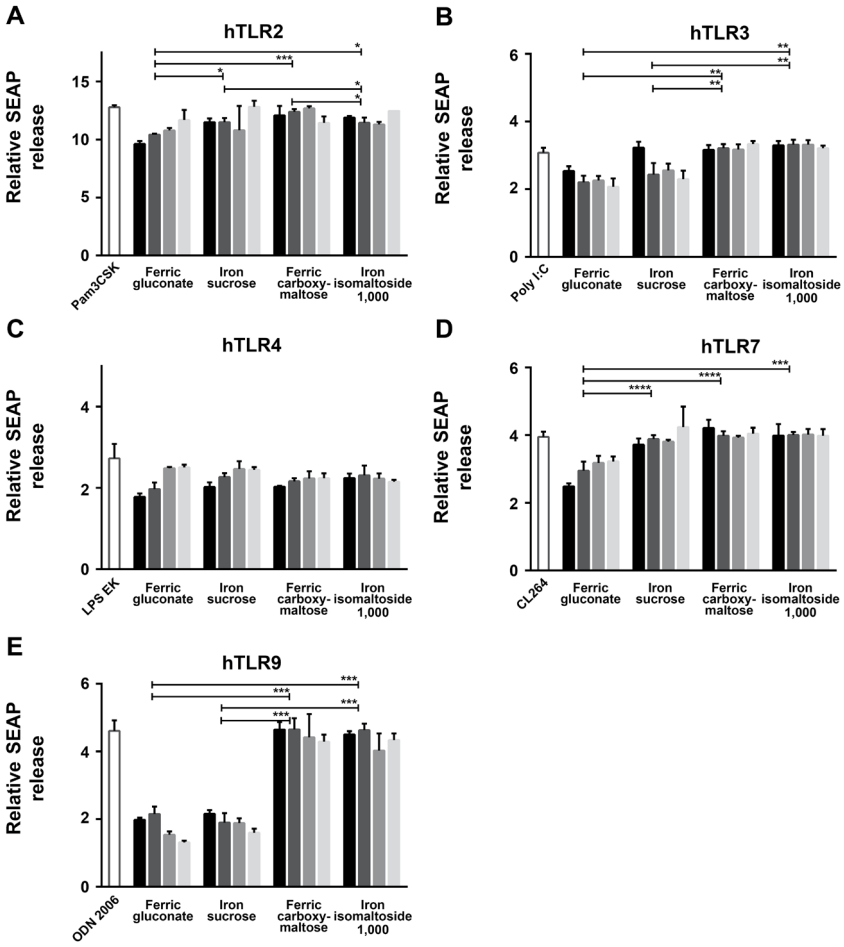

Fig. 3. Interaction between iron nanomedicines and specific positive control agonists during Toll-like receptor activation. hTLR reporter cell-lines were incubated with concentration ranges of ferric gluconate, iron sucrose, ferric carboxymaltose, iron isomaltoside 1,000 in the presence of a fixed concentration of a positive control hTLR agonist (A– E; black = 1 mg/mL, dark grey = 750 µg/mL, middle grey = 500 µg/mL, light grey 250 µg/mL). Statistical analysis by one-way ANOVA is shown for iron concentrations of 750 µg/mL.

3.3. Complement activation

Our hTLR data implies that iron nanomedicines are able to adsorb serum proteins necessary for hTLR recognition. Complement factors are part of the innate immune system and play a key role in binding pathogens and damaged cells with the purpose to enhance their recognition and clearance from the circulation by phagocytic cells [19,20]. As such, we investigated if iron nanomedicines can activate the complement system.

Complement activation was assessed in serum obtained from 5 healthy donors. We investigated the appearance of the soluble SC5b-9 and Bb complexes. SC5b-9 is an activation marker of both the classical, lectin and alternative pathway, as it is generated by the assembly of C5 through C9. Bb is an activation fragment of Factor B which only appears upon activation of the alternative pathway. Complement activation through the alternative pathway was also assessed by measurement of SC5b-9 in calcium chelated serum by EGTA/Mg^{2+}. The classical-, and mannose-binding lectin pathway are calcium dependent whereas the alternative pathway can also be activated in the presence of magnesium [21,22].

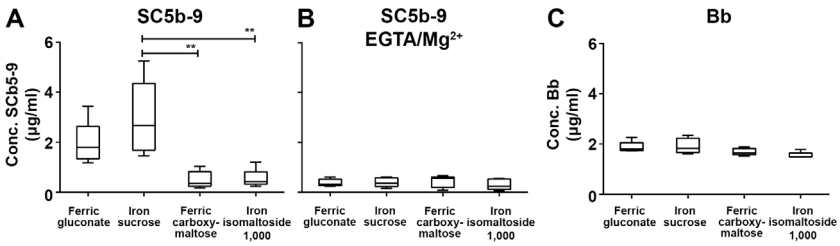

Fig. 4. Complement activation by SC5b-9 and Bb analysis. General complement activation was assessed by measurement of SC5b-9 levels in serum from 5 healthy donors (A). Classical pathway analysis was performed by chelation of Mg^{2+} (B) and measurement of the specific alternative pathway marker Bb (C).

Sera were incubated with the four different formulations at 500 µg iron/mL. In the donors tested iron sucrose induced significant activation of the complement system determined by SC5b-9 levels compared to ferric carboxymaltose and iron isomaltoside 1,000 (Fig. 4A). No SC5b-9 levels were detected in sera incubated with PBS only (data not shown). Ferric gluconate also induced elevated levels of SC5b-9 compared to ferric carboxymaltose and iron isomaltoside 1,000, but were not significantly different ($p < 0.05$). Addition of EGTA/Mg^{2+} diminished SC5b-9 (Fig. 4B), implying that iron nanomedicines induce complement activation in a calcium dependent mechanism which does not rely on the presence of magnesium. This implies that complement activation does not occur through the alternative pathway which was confirmed by the absence of elevated Bb levels above baseline (Fig. 4C).

3.4. Cellular uptake by iron nanomedicines

So far we established that two out of the four iron nanomedicines investigated could activate hTLRs, interfere with specific hTLR positive control agonists and induce complement activation. In human cells, TLR3, -7 and -9 are only expressed intracellular on endosomal membranes. Hence, physiological activation of hTLRs should only occur when agonists are first taken up by cells.

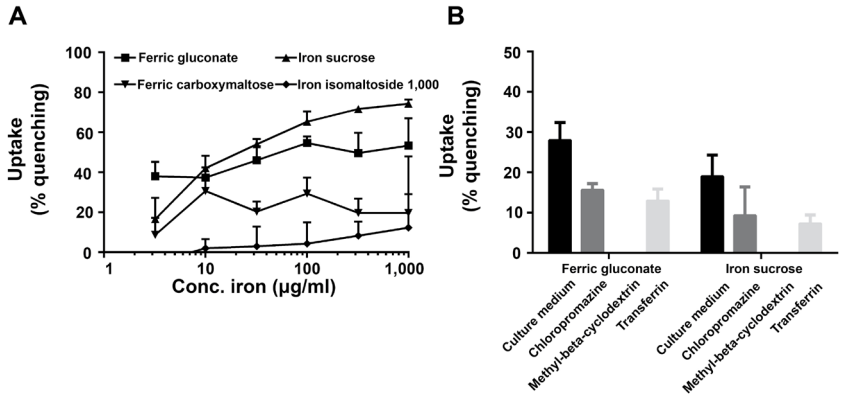

Fig. 5. Iron uptake in HEK293T cells. Uptake was determined by calcein quenching upon 3 hours incubation of the various iron nanomedicines (A). Endocytic pathway analysis was performed by use of the endocytic pathway blockers chlorpromazine, methyl-beta-cyclodextrin and transferrin, respectively known to inhibit clathrin- cholesterol- and transferrin-mediated uptake, on iron uptake (B).

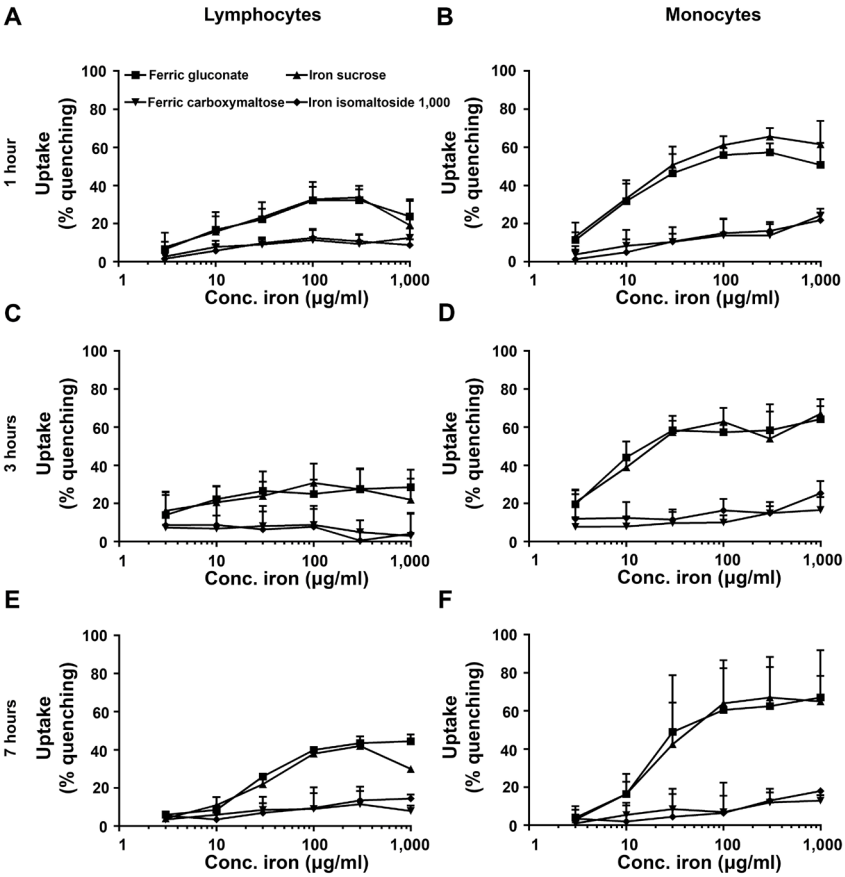

Fig. 6. Iron uptake in PBMC. Uptake was determined by calcein quenching upon 1 (A,B), 3 (C,D) and 7 (E,F) hours incubation of the various iron nanomedicines in lymphocytes (A,C,E) and in monocytes (B,D,F).

As such, we investigated intracellular iron in HEK293T cells after 3 hours of incubation with the various iron nanomedicines. We determined intracellular iron with a calcein quenching method (more intracellular iron results in higher calcein quenching). Cellular uptake differed substantially between the various iron products (Fig. 5A). In correspondence to our hTLR activation studies in the same cell-type, ferric gluconate and iron sucrose were taken up more efficiently than ferric carboxymaltose and iron isomaltoside 1,000.

Endocytic pathway analysis on HEK293T cells revealed that uptake by all different formulations was completely inhibited by methyl-beta-cyclodextrin, indicating that uptake of iron nanomedicines occurred through the cholesterol mediated pathway. Partial inhibition was observed when the cells were pre-incubated with chlorpromazine and transferrin.

Peripheral blood mononuclear cells (PBMC) are important blood-borne mediator cells of innate immune responses and express varies Toll-like receptors. We investigated whether PBMC are able to take up iron nanomedicines. PBMC from healthy donors (n=5) were incubated for 1, 3 and 7 hours. Ferric gluconate and iron sucrose were taken up more effectively than ferric carboxymaltose and iron isomaltoside 1,000, and this difference remained upon 7 hours incubation (Fig. 6A–F). Uptake by PBMC occurred preferentially by monocytes.

3.5. PBMC cell viability

PBMC obtained from 3 healthy donors were used to study cell viability after 24 or 48 hours incubation. Ferric gluconate and iron sucrose induced a slight decrease in cell viability at 1.0 and 0.1 mg/mL (supporting information S4). No decrease was observed when the cells were incubated with either ferric carboxymaltose or iron isomaltoside 1,000.

3.6. Iron nanomedicines trigger cytokine release

Increased cytokine levels in both healthy donors and patients have been reported upon iron administration [15,16,23]. We investigated the release of IL-1β and IL-6 in whole blood supplemented with DMEM containing 4.5 g/L glucose and L-glutamine from healthy donors. IL-1β is a well-known inflammatory marker associated with TLR activation [24]. IL-6 was investigated as increased levels have been reported in patients treated with iron nanomedicines [15].

At baseline, none of the 9 donors had any detectable IL-1β in plasma (data not shown). Most IL-1β production was observed after 48 hours incubation when incubated with ferric gluconate and iron sucrose (Fig. 7A–D). No linear dose dependency was observed, instead IL-1β followed an optimum production at 100 μg iron/mL upon incubation with ferric gluconate and at 320 μg iron/mL upon incubation with iron sucrose.

Subsequently, plasma IL-6 levels were analyzed after 24 hours incubation. While IL-1β production mainly occurred when whole blood was incubated with either ferric gluconate or iron sucrose, increased levels of IL-6 were only measured upon incubation with ferric carboxymaltose and iron isomaltoside 1,000 (Fig. 8A–D). Here, IL-6 production also did not follow a linear dose dependent relation as an optimum production was found at 100 μg iron/mL upon incubation with iron isomaltoside 1,000 and at 320 μg iron/mL upon incubation with ferric carboxymaltose.

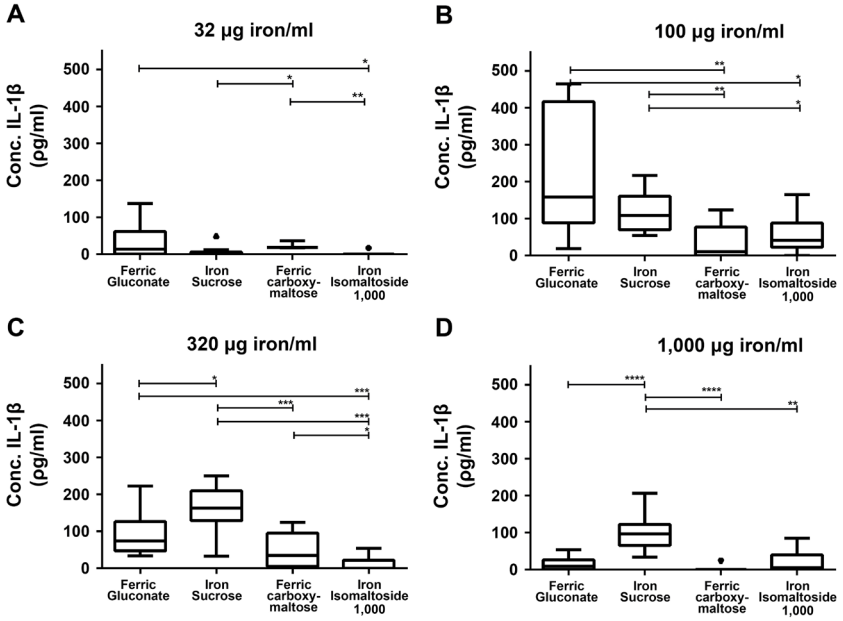

Fig. 7. IL-1β levels in whole blood incubated with various iron nanomedicines. IL-1β release in the extracellular environment was determined upon 48 hours incubation of whole blood from healthy donors (n=9) with the various iron nanomedicines at different concentrations iron (A-D). Statistical analysis was performed by the Mann-Whitney test.

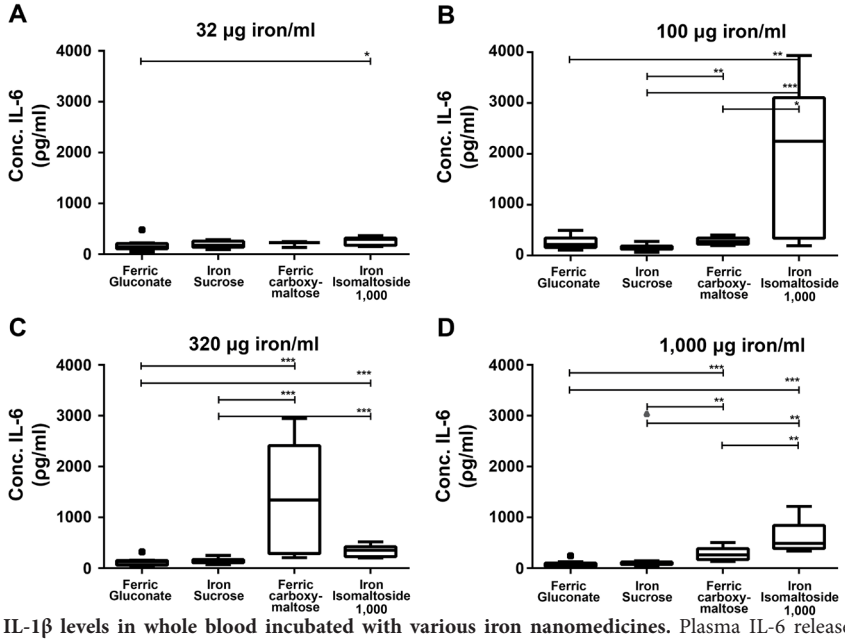

Fig. 8. IL-1β levels in whole blood incubated with various iron nanomedicines. Plasma IL-6 release in the extracellular environment was determined upon 24 hours incubation of whole blood from healthy donors (n=9) with the various iron nanomedicines at different concentrations iron (A-D). Statistical analysis was performed by the Mann-Whitney test.

4. Discussion

During the last two decades over a dozen of intravenous iron nanomedicines have entered the clinic to treat iron deficiency (anemia), a nutritional disorder affecting almost 30% of the world population [1,4]. All these formulations are within the lower nanometre size range and consist of a polynuclear Fe(III)-oxyhydroxide/oxide core surrounded by carbohydrates [4]. Between products, iron cores are not identical and the carbohydrates used to shield the core may differ.

Although administered for many decades, these products are not without safety concerns. For instance, high molecular weight iron dextran products are no longer sold due to severe and sometimes fatal hypersensitivity reactions [5]. In 2013 the European Medicines Agency's Committee for Medicinal Products for Human Use (CHMP) updated their guidelines for all iron nanomedicines with a warning for increased risk of hypersensitivity-like and even fatal reactions as well as the necessity to take adequate measures to minimize these reactions [12]. As the rate of new iron nanomedicines entering the market has been increasing over the last decade, it is essential to understand what drives these allergic reactions and how to properly manage them.

The exact mechanisms behind the hypersensitivity-like reactions have not been identified. The induction of radical oxygen species (ROS) as a results of labile iron release has been investigated, but does not appear strictly related and cannot explain these safety issues alone [25]. Pai et al. showed that although iron sucrose and iron dextran show differences in the amount of non-transferrin bound iron in serum, cytokine activation and intracellular ROS generation were essentially similar in PBMC of end-stage renal disease patients [15].

Here, the interaction of four different iron nanomedicines with the innate immune system was investigated as well as their physico-chemical properties. The iron cores of the formulations were in the lower nano-size range and were either spherical or rot-shaped. Size, shape and charge of the iron nanomedicines did not associate with any of the immunological parameters investigated in this paper. However, aggregation behavior associated with substantial hTLR- and complement activation, as well as with cellular uptake and the production of IL-1β, but not IL-6.

Ferric gluconate and iron sucrose appeared as aggregated iron cores when dried onto a grid for STEM analysis. These products induced activation of the endosomal receptors hTLR3 and -7 and were preferentially taken up by both HEK293T cells and PBMC. Surprisingly, ferric gluconate and iron sucrose did not interact directly with hTLRs as no activation was observed when these products were incubated in serum free medium. We hypothesized that these products adsorb serum proteins and opsonins which subsequently can cross-react with endosomal hTLRs.

Ferric gluconate and iron sucrose are known to contain less stable bound carbohydrates which more easily dissociate upon dilution [4]. Ferric carboxymaltose and iron isomaltoside 1,000 contain stable bound carbohydrates and are as such shielded against iron core aggregation [4,26]. When products with less stable bound carbohydrates are incubated in serum it is believed that the exposed iron cores adsorb serum proteins and opsonins such as IgG, complement factors and fibrinogen by means of hydrophobic interactions [27–29]. This

is supported by the fact that these iron nanomedicines induce complement activation and can scavenge specific positive control hTLR agonists resulting in diminished hTLR activation when incubated together.

Complement activation was assessed by measurement of SC5b-9 levels, a general complement activation marker released upon activation by any of the three complement pathways. We found that ferric gluconate and iron sucrose are able to induce complement activation indicated by elevated levels of SC5b-9. Pathway analysis excluded that ferric gluconate and iron sucrose induce complement activation by the alternative pathway as no SC5b-9 levels were detected when calcium ions were chelated by EGTA. Whereas the classical pathway and mannose-binding lectin pathway require calcium, the alternative pathway requires magnesium. Exclusion of the alternative pathway was confirmed by the fact that no elevated Bb levels were measured, a specific alternative pathway marker. Complement activation therefore occurred either through the mannose-binding lectin- or the classical pathway. Analysis of the classical pathway is preferable performed in sera of treated patients with anti-drug antibodies, which were unavailable for this study. In addition, to our knowledge no reports have been published that identified antibodies against either ferric gluconate or iron sucrose. As such, it is believed that iron nanomedicines can activate the complement system by means of the mannose-binding lectin pathway. These findings are in line with the current concept explaining non-IgE mediated hypersensitivity like reactions observed with several types of nanomedicines, referred to as complement activation-related pseudo-allergy (CARPA) [19,30].

Incubation of these products in whole blood resulted in different pro-inflammatory cytokine responses. Whereas cells incubated with ferric gluconate and iron sucrose are more prone to secrete IL-1β; ferric carboxymaltose and iron isomaltoside 1,000 mainly secreted IL-6. The inflammatory marker IL-1β is known to be produced by activated PBMC in response to nanoparticulates, such as colloidal aluminum oxide, zinc oxide and urate crystals [24,31,32]. IL-1β is an important cytokine involved in cell proliferation, differentiation and apoptosis.

There is controversy on the exact methods how to characterize the size and charge of iron nanomedicines. As such, different diameters and zeta-potentials have been reported [33,34]. A study by Jahn et al. identified smaller z-averages than presented in this study [34]. In our study, z-averages were measured at higher iron concentration and the dilutions were individually chosen for each product to obtain the highest count rate. Dilution and count rate were found to have a bell curve relation, as dilution decreases both particle concentration and absorption of the laser. With our instrumental setup we found that higher than earlier reported concentrations were needed to obtain a reasonable count rate. Also, zeta-potential was analyzed with a novel method using the diffusion barrier method in 10 mM HEPES which enables a more controlled way of identifying zeta-potentials. This allowed the control of the electrical double layer in contrast to detection in distilled water as reported by others [34,35].

As we have shown in this paper, a head to head comparisons of four different iron nanomedicines showed that these products can interact with the innate immune system. We found that two out of the four formulations appeared as aggregates by Scanning Transmission Electron Microscopy analysis and were actively taken up by HEK293T- and peripheral blood

mononuclear cells in a cholesterol-dependent manner. These formulations triggered in vitro activation of intracellular TLR3, -7 and -9 in a dose-dependent manner which depended on a serum co-factor. These iron nanomedicines were also able to induce complement activation and were more prone to induce production of the pro-inflammatory cytokine IL-1beta, but not IL-6 when incubated in whole blood.

The findings in this study reveal another mechanism how iron nanomedicine interact with the immune system. Previous studies have shown that differences in degradation kinetics and the presence of elemental iron is not the sole driver for the hypersensitivity reactions observed in the clinic [15]. In line with this, the findings in this study shed light on the immunological potential of iron nanomedicines by their carbohydrate stability and deserves to be further investigated.

Supporting information

This material is available free of charge via the internet at the website of the Journal of Biomaterials.

Funding sources

The project was funded by a research grant from Vifor Pharma

References

[1] C. Gasche, M. C. E. Lomer, I. Cavill, and G. Weiss, "Iron, anaemia, and inflammatory bowel diseases," Gut, vol. 53, no. 8, pp. 1190–1197, Aug. 2004.

[2] J. Umbreit, "Iron deficiency: a concise review," Am. J. Hematol., vol. 78, no. 3, pp. 225–231, Mar. 2005.

[3] M. Auerbach et al., "Intravenous Iron Optimizes the Response to Recombinant Human Erythropoietin in Cancer Patients With Chemotherapy-Related Anemia: A Multicenter, Open-Label, Randomized Trial," J. Clin. Oncol., vol. 22, no. 7, pp. 1301–1307, Apr. 2004.

[4] P. Geisser and S. Burckhardt, "The pharmacokinetics and pharmacodynamics of iron preparations," Pharmaceutics, vol. 3, no. 1, pp. 12–33, 2011.

[5] M. Auerbach and H. Ballard, "Clinical use of intravenous iron: administration, efficacy, and safety," Hematol. Educ. Program Am. Soc. Hematol. Am. Soc. Hematol. Educ. Program, vol. 2010, pp. 338–347, 2010.

[6] B. G. Danielson, "Structure, chemistry, and pharmacokinetics of intravenous iron agents," J. Am. Soc. Nephrol. JASN, vol. 15 Suppl 2, pp. S93-98, Dec. 2004.

[7] G. R. Bailie and J.-J. Verhoef, "Differences in the reporting rates of serious allergic adverse events from intravenous iron by country and population," Clin. Adv. Hematol. Oncol. HO, vol. 10, no. 2, pp. 101–108, Feb. 2012.

[8] D. Rampton et al., "Hypersensitivity reactions to intravenous iron: guidance for risk minimization and management," Haematologica, vol. 99, no. 11, pp. 1671–1676, Nov. 2014.

[9] C. Wang et al., "Comparative Risk of Anaphylactic Reactions Associated With Intravenous Iron Products," JAMA, vol. 314, no. 19, pp. 2062–2068, Nov. 2015.

[10] A. J. Bircher and M. Auerbach, "Hypersensitivity from intravenous iron products," Immunol. Allergy Clin. North Am., vol. 34, no. 3, pp. 707–723, x–xi, Aug. 2014.

[11] J. Szebeni et al., "Hypersensitivity to intravenous iron: classification, terminology, mechanisms and management," Br. J. Pharmacol., vol. 172, no. 21, pp. 5025–5036, Nov. 2015.

[12] European Medicines Agency, "New recommendations to manage risk of allergic reactions with intravenous iron-containing medicines," 2013. [Online]. Available: http://www.ema.europa.eu/docs/en_GB/document_library/Referrals_document/IV_iron_31/WC500151308.pdf.

[13] R. D. Cançado and M. Muñoz, "Intravenous iron therapy: how far have we come?," Rev. Bras. Hematol. E Hemoter., vol. 33, no. 6, pp. 461–469, 2011.

[14] H. S. Novey, M. Pahl, I. Haydik, and N. D. Vaziri, "Immunologic studies of anaphylaxis to iron dextran in patients on renal dialysis," Ann. Allergy, vol. 72, no. 3, pp. 224–228, Mar. 1994.

[15] A. B. Pai, T. Conner, C. R. McQuade, J. Olp, and P. Hicks, "Non-transferrin bound iron, cytokine activation and intracellular reactive oxygen species generation in hemodialysis patients receiving intravenous iron dextran or iron sucrose," Biometals Int. J. Role Met. Ions Biol. Biochem. Med., vol. 24, no. 4, pp. 603–613, Aug. 2011.

[16] L. H. Fell, A. M. Zawada, K. S. Rogacev, S. Seiler, D. Fliser, and G. H. Heine, "Distinct immunologic effects of different intravenous iron preparations on monocytes," Nephrol. Dial. Transplant. Off. Publ. Eur. Dial. Transpl. Assoc. - Eur. Ren. Assoc., vol. 29, no. 4, pp. 809–822, Apr. 2014.

[17] Y. Ma, V. Abbate, and R. C. Hider, "Iron-sensitive fluorescent probes: monitoring intracellular iron pools," Metallomics, vol. 7, no. 2, pp. 212–222, Feb. 2015.

[18] O. Takeuchi and S. Akira, "Pattern Recognition Receptors and Inflammation," Cell, vol. 140, no. 6, pp. 805–820, Mar. 2010.

[19] J. Szebeni, "Complement activation-related pseudoallergy: A new class of drug-induced acute immune toxicity," Toxicology, vol. 216, no. 2–3, pp. 106–121, Dec. 2005.

[20] N. K. Banda et al., "Mechanisms of complement activation by dextran-coated superparamagnetic iron oxide (SPIO) nanoworms in mouse versus human serum," Part. Fibre Toxicol., vol. 11, p. 64, 2014.

[21] D. P. Fine, S. R. Marney, D. G. Colley, J. S. Sergent, and R. M. Des Prez, "C3 shunt activation in human serum chelated with EGTA," J. Immunol. Baltim. Md 1950, vol. 109, no. 4, pp. 807–809, Oct. 1972.

[22] I. Hamad, A. C. Hunter, J. Szebeni, and S. M. Moghimi, "Poly(ethylene glycol)s generate complement activation products in human serum through increased alternative pathway turnover and a MASP-2-dependent process," Mol. Immunol., vol. 46, no. 2, pp. 225–232, Dec. 2008.

[23] A. Gupta, J. Zhuo, J. Zha, S. Reddy, J. Olp, and A. Pai, "Effect of different intravenous iron preparations on lymphocyte intracellular reactive oxygen species generation and subpopulation survival," BMC Nephrol., vol. 11, p. 16, 2010.

[24] H. Li, S. B. Willingham, J. P.-Y. Ting, and F. Re, "Cutting Edge: Inflammasome Activation by Alum and Alum's Adjuvant Effect Are Mediated by NLRP3," J. Immunol., vol. 181, no. 1, pp. 17–21, Jul. 2008.

[25] A. B. Pai, A. V. Boyd, C. R. McQuade, A. Harford, J. P. Norenberg, and P. G. Zager, "Comparison of Oxidative Stress Markers After Intravenous Administration of Iron Dextran, Sodium Ferric Gluconate, and Iron Sucrose in Patients Undergoing Hemodialysis," Pharmacother. J. Hum. Pharmacol. Drug Ther., vol. 27, no. 3, pp. 343–350, Mar. 2007.

[26] P. A. Kalra, "Introducing iron isomaltoside 1000 (Monofer®)—development rationale and clinical experience," NDT Plus, vol. 4, no. Suppl 1, pp. i10–i13, Jun. 2011.

[27] D. E. Owens and N. A. Peppas, "Opsonization, biodistribution, and pharmacokinetics of polymeric nanoparticles," Int. J. Pharm., vol. 307, no. 1, pp. 93–102, Jan. 2006.

[28] H. Carrstensen, R. H. Müller, and B. W. Müller, "Particle size, surface hydrophobicity and interaction with serum of parenteral fat emulsions and model drug carriers as parameters related to RES uptake," Clin. Nutr. Edinb. Scotl., vol. 11, no. 5, pp. 289–297, Oct. 1992.

[29] P. Aggarwal, J. B. Hall, C. B. McLeland, M. A. Dobrovolskaia, and S. E. McNeil, "Nanoparticle interaction with plasma proteins as it relates to particle biodistribution, biocompatibility and therapeutic efficacy," Adv. Drug Deliv. Rev., vol. 61, no. 6, pp. 428–437, Jun. 2009.

[30] J. Szebeni, P. Bedőcs, D. Csukás, L. Rosivall, R. Bünger, and R. Urbanics, "A porcine model of complement-mediated infusion reactions to drug carrier nanosystems and other medicines," Adv. Drug Deliv. Rev., vol. 64, no. 15, pp. 1706–1716, Dec. 2012.

[31] S. C. Eisenbarth, O. R. Colegio, W. O'Connor, F. S. Sutterwala, and R. A. Flavell, "Crucial role for the Nalp3 inflammasome in the immunostimulatory properties of aluminium adjuvants," Nature, vol. 453, no. 7198, pp. 1122–1126, Jun. 2008.

[32] Y.-H. Luo, L. W. Chang, and P. Lin, "Metal-Based Nanoparticles and the Immune System: Activation, Inflammation, and Potential Applications," BioMed Res. Int., vol. 2015, p. 143720, 2015.

[33] Y. Wu et al., "Core size determination and structural characterization of intravenous iron complexes by cryogenic transmission electron microscopy," Int. J. Pharm., vol. 505, no. 1–2, pp. 167–174, May 2016.

[34] M. R. Jahn et al., "A comparative study of the physicochemical properties of iron isomaltoside 1000 (Monofer®), a new intravenous iron preparation and its clinical implications," Eur. J. Pharm. Biopharm., vol. 78, no. 3, pp. 480–491, Aug. 2011.

[35] R. B. Shah, Y. Yang, M. A. Khan, A. Raw, L. X. Yu, and P. J. Faustino, "Pharmaceutical characterization and thermodynamic stability assessment of a colloidal iron drug product: Iron sucrose," Int. J. Pharm., vol. 464, no. 1–2, pp. 46–52, Apr. 2014.

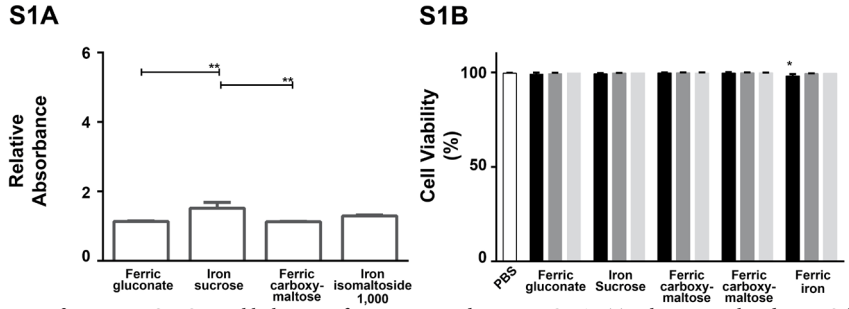

Supporting information S1. Optical behavior of iron nanomedicines in QUANTI-Blue normalized to PBS (A). Cell viability of HEK-Blue hTLR3 when incubated for 24 hours with the different iron nanomedicines (B). (black = 1.000 µg/mL, dark grey = 100 µg/mL, light grey 10 µg/mL).

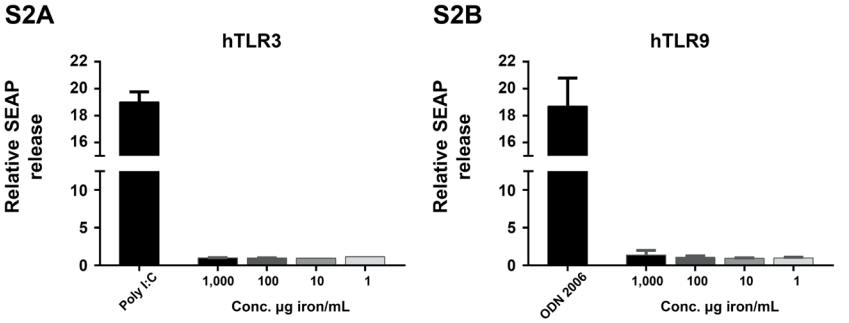

Supporting information S2. Lack of hTLR3 (S2A) and -9 (S2B) activation by ferric iron.

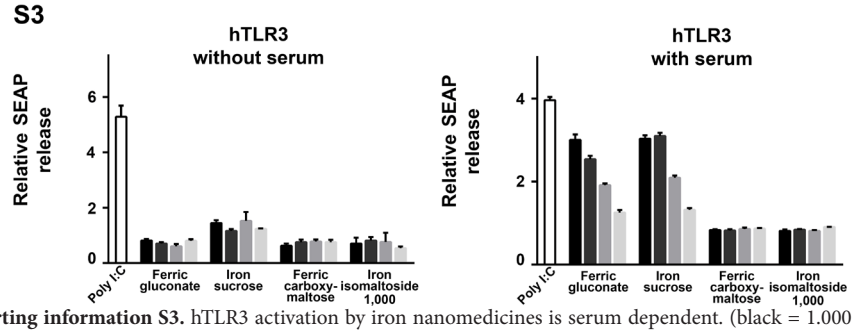

Supporting information S3. hTLR3 activation by iron nanomedicines is serum dependent. (black = 1.000 µg/mL, dark grey = 750 µg/mL, middle grey = 500 µg/mL, light grey 250 µg/mL).

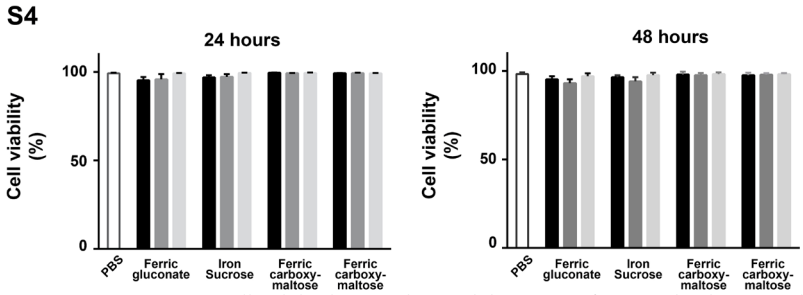

Supporting information S4. PBMC cell viability by propidium iodide staining after 24 and 48 hours incubation with the different iron nanomedicines. (black = 1.000 µg/mL, dark grey = 100 µg/mL, light grey 10 µg/mL).

Chapter | 4

A novel oral iron-complex formulation: Encapsulation of hemin in polymeric micelles and its *in vitro* Absorption

Verhoef JJF*, Span K*, Hunt H, van Nostrum CF, Brinks V, Schellekens H, Hennink, W

*Shared first authorship

Article published in:
Eur J Pharm Biopharm.
2016 Nov;108:226-234.
doi: 10.1016/j.ejpb.2016.09.002

Abstract

Anemia resulting from iron deficiency is one of the most prevalent diseases in the world. As iron has important roles in several biological processes such as oxygen transport, DNA synthesis and cell growth, there is a high need for iron therapies that result in high iron bioavailability with minimal toxic effects to treat patients suffering from anemia. This study aims to develop a novel oral iron-complex formulation based on hemin-loaded polymeric micelles composed of the biodegradable and thermosensitive polymer methoxy-poly(ethylene glycol)-*b*-poly[N-(2-hydroxypropyl) methacrylamide-dilactate], abbreviated as mPEG-*b*-p(HPMAm-Lac_2). Hemin-loaded micelles were prepared by addition of hemin dissolved in DMSO:DMF (1:9, one volume) to an aqueous polymer solution (nine volumes) of mPEG-*b*-p(HPMAm-Lac_2) followed by rapidly heating the mixture at 50°C to form hemin-loaded micelles that remain intact at room and physiological temperature. The highest loading capacity for hemin in mPEG-*b*-p(HPMAm-Lac_2) micelles was 3.9%. The average particle diameter of the hemin-micelles ranged from 75 to 140 nm, depending on the concentration of hemin solution that was used to prepare the micelles. The hemin-loaded micelles were stable at pH 2 for at least 3 hours which covers the residence time of the formulation in the stomach after oral administration and up to 17 hours at pH 7.4 which is sufficient time for uptake of the micelles by the enterocytes. Importantly, incubation of Caco-2 cells with hemin-micelles for 24 hours at 37°C resulted in ferritin levels of 2500 ng/mg protein which is about 10 fold higher than levels observed in cells incubated with iron sulfate under the same conditions. The hemin formulation also demonstrated superior cell viability compared to iron sulfate with and without ascorbic acid. The study presented here demonstrates the development of a promising novel iron complex for oral delivery.

1. Introduction

Anemia is one of the most common health problems at present. According to the World Health Organization the prevalence of anemia is dependent on ethnic groups and geographic location, but it is assumed that 50% of these cases is because of iron deficiency [1]. This occurrence is similar for both developing and developed nations and can arise due to various reasons such as pregnancy, growth in children and diseases that cause low iron bioavailability from the diet [2-4]. A healthy iron metabolism is important as iron is the main mineral involved in oxygen transport, DNA synthesis, cell growth and survival [5, 6]. The iron homeostasis is primarily regulated by intestinal absorption as the uptake of iron takes place predominately in the duodenum and upper jejunum by enterocytes. This absorption is regulated by the hormone hepcidin that is produced in hepatocytes of the liver and binds to the iron transporter protein ferroportin that carries iron from the duodenal enterocytes into the circulation [7]. It is known that hepcidin binding to the iron transporter leads to its degradation, therefore augmented hepcidin production results in less ferroportin and thus less iron transportation (export). As a consequence a decrease of iron absorption and efflux from the enterocytes occurs.

This incidence results in a disturbed iron homeostasis and ultimately could cause less iron in the circulation [8-10]. Due to the importance of a balanced iron metabolism, it is of interest to develop therapies that can remediate iron deficiency. There are two forms of dietary iron, namely non-heme iron that is present in vegetables and grains, and there is heme iron that is predominately found in red meat in the form of hemoglobin and myoglobin [11]. It is known that even though the prevalence of non-heme iron is higher than the heme form, the latter is being absorbed up to 30% more effectively [12]. Nevertheless, because non-heme iron supplements are relatively cheap and easy to produce, the pharmaceutical industry has developed several oral formulations based on iron salts such as iron sulfate. However, these formulations are associated with various side effects such as gastrointestinal disturbances which are probably caused by the redundant amount of iron in the preparations that remain unabsorbed in the colon [13]. There is consequently an urgent need for more advanced oral preparations with higher bioavailability and less side effects.

Many studies have explored the possibilities of novel therapies based on non-heme iron, but even though there are some heme-iron based oral iron medications on the market such as Proferrin (heme-iron polypeptide), far less research has been done exploiting heme-iron for oral supplementation [6, 14]. Unlike non-heme iron which is taken up by enterocytes via the divalent metal transporter 1 (DMT1), the exact uptake mechanism for heme remains elusive. It is, however, generally accepted that heme binds to the brush border membrane of the duodenum enterocytes and is subsequently transported by a different transporter as non-heme iron through the cell membrane to the cytoplasm [15-17]. The assumption that heme is recognized by a heme-transporter opens possibilities to investigate other sources for iron supplementation containing structures similar to heme such as ferric protoporphyrin IX chloride (hemin). Hemin in contrast to heme contains a chloro ligand attached to the iron center (structure is shown in figure 1). This compound is essentially insoluble in water of neutral pH and soluble in solutions of sodium hydroxide due to the substitution of the chloro ligand by a hydroxyl group resulting in the formation of hematin [18]. The prominent factors for the development of a novel oral therapy would be improving the stability, bioavailability and solubility of the iron supplement [19]. Thus, in order to exploit hemin for oral iron therapy, the

first challenge to tackle is to solubilize it in aqueous medium of physiological pH. Moreover a suitable formulation has to resist the harsh environment of the gastrointestinal tract.

In particular, nano-sized drug delivery systems have shown to be able to encapsulate several hydrophobic substances while increasing the uptake of the loaded drug and protecting it from degradation while passing through the gastrointestinal tract [20-22]. There is a wide range of nanoparticles based on liposomes and on natural as well as synthetic polymers that have been investigated for the encapsulation of hydrophobic drugs [23-25]. Within our department a novel class of thermosensitive biodegradable block copolymers based on methoxy-poly(ethylene glycol)-*b*-poly[N-(2-hydroxypropyl) methacrylamide-dilactate] (mPEG-*b*-p(HPMAm-Lac$_2$) has been developed , which under certain conditions form micelles consisting of a hydrophobic core, in which hydrophobic drugs can be solubilized and a hydrophilic corona, making these particles water dispersible [26, 27; 30, 31]. mPEG-b(HPMAm-Lac$_2$) consists of the hydrophilic polymer mPEG and poly(HPMAm-Lac$_2$). The latter polymer is thermosensitive and, when dissolved in water, exhibits a lower critical solution temperature (LCST) [27], as has also been described for polymers such as poly(N-isopropylacrylamide) and elastin-like peptides [28, 29]. Below the LCST poly(HPMAm-Lac$_2$) 13 °C, water molecules are bound to the polymer chains and prevents intra- and inter polymer interactions resulting in a water-soluble polymer. When the polymer solution is heated above its LCST, water is expelled and the polymer chains become hydrophobic resulting in precipitation [27]. Therefore, in the present study we investigated whether these micelles can also encapsulate the hydrophobic hemin and thus be used as a potential oral iron formulation. To this end, hemin was encapsulated in mPEG-*b*-p(HPMAm-Lac$_2$) micelles via a rapid heating method. The formed micelles were characterized for encapsulation efficiency, loading capacity and particle size. Furthermore, the stability of the loaded micelles at different pH and also the physical state of hemin within the micelles was investigated. Finally, Caco-2 cells were incubated with the micelles to assess iron uptake in comparison to the commonly used iron supplement, iron sulfate.

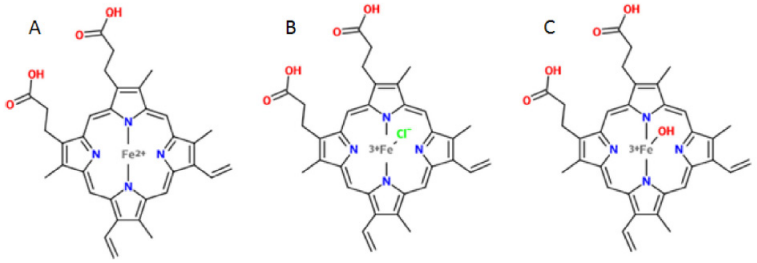

Figure 1. Molecular structure of (A) heme; (B) hemin and (C) hematin

2. Materials and Methods

2.1. Materials

Hemin (molecular weight = 651.9 g/mol), ammonium acetate, iron (II) sulfate heptahydrate; $FeSO_4.7H_2O$, sodium hydroxide, sodium bicarbonate, ascorbic acid, saponin and tetrazolium salt XTT (sodium 2,3-bis(2-methoxy-4-nitro-5-sulfophenyl)-2H-tetrazolium-5-carboxanilide) were all purchased from Sigma Aldrich (Zwijndrecht, The Netherlands). Dimethylsulfoxide (DMSO) and dimethylformamide (DMF) were obtained from Biosolve Ltd. (Valkenswaard, The Netherlands). Phosphate buffered saline (PBS) pH 7.4 containing per

liter 8.2 g NaCl, 3.1 g $Na_2HPO_4 \cdot 12H_2O$ and 0.3 g $NaH_2PO_4.2H_2O$ was from Braun Melsungen AG (Melsungen, Germany). Methoxy-poly(ethylene glycol)-*b*-poly[*N*-(2-hydroxypropyl) methacrylamide-dilactate] (abbreviated as mPEG-*b*- (HPMAm-Lac_2); Molecular weight of mPEG = 5000 g/mol) was synthesized as described by Soga et al. [26]. Regenerated cellulose syringe filters (0.45 μm) were purchased from Grace Davision Discovery Science. Vivaspin centrifugal concentrator tubes with 50,000 MWCO filter were obtained from Sartorius AG (Goettingen, Germany). The Caco-2 cell line was generously provided by M.A.M Oosterveer-van der Doelen (Faculty of Veterinary Medicine, Utrecht University). Dulbecco's Modified Eagle's Medium, Minimum Essential Medium, antibiotic antimycotic cell culture solution consisting of amphotericin B and penicillin, non-essential amino acids and RIPA buffer were obtained from Invitrogen (Breda, The Netherlands). Micro BCA protein assay and Ferritin Human ELISA kit (ab108837) were purchased from Pierce (Rockford, USA) and Abcam (Cambridge, United Kingdom). Rabbit polyclonal Anti-LAMP1 IgG - Lysosome Marker (ab24170) and Goat polyclonal Anti-Rabbit IgG H&L (Alexa Fluor® 488) (ab150077) were purchased from Abcam (Cambridge, United Kingdom). Methacryloxyethyl thiocarnamoyl rhodamine B was purchased from Polysciences Europe. Leica Confocal microscopy with Leica application suite advanced fluorescence (LAS AF) light software was used to visualize cellular uptake of labelled micelles.

2.2. Preparation and charaterization of hemin-loaded micelles

Hemin-loaded mPEG-*b*-p(HPMAm-Lac_2) micelles were prepared via the "rapid heating method" essentially as described by Neradovic et al. [32] and by Rijcken et al. [27] with some modifications. In short, the polymer was dissolved at a concentration of 2 mg/mL in 120 mM ammonium acetate pH 5 in a glass vial and stirred on ice for 1 hour. 120 mM ammonium acetate pH 5 was prepared by dissolving 0.925 grams of ammonium acetate in 100 mL purified water. The pH of this solution was subsequently adjusted with 0.1 N HCl to pH 5. This solvent was used as at this pH the hydrolysis of the lactate groups is limited, resulting in a high stability of the micelles [36]. Next the mixture was stored overnight at 4 °C and subsequently stirred for 15 minutes on ice and kept on ice until the micelles were made. This procedure was followed to ensure that the polymer solution remained below the critical micelle temperature (CMT) of 4 °C. Solutions of 0.4 - 2 mg/mL hemin in a mixture of DMSO:DMF (1:9 v/v) were freshly made and also kept on ice. Subsequently, 0.1 mL of hemin solution was added to 0.9 mL of polymer solution, vortexed for 4 seconds and the hemin/polymer mixture was then transferred into a water bath of 50 °C and hemin loaded micelles were formed under vigorous shaking for 1 minute. Finally, after cooling to room temperature, the hemin-loaded micelles were filtered through a 0.45 μm filter to remove precipitated, non-encapsulated, hemin.

The concentration of hemin encapsulated in the micelles was measured via UVspectrophotometric analysis (Spectrostar BMG Labtech). A sample of the micellar dispersion was diluted 10x in DMSO to disintegrate the micelles and solubilize the encapsulated hemin. A calibration curve of hemin standards was made in a concentration range of 0-50 μg/mL in DMSO. The samples and the standards were measured at a wavelength of 388 nm and the concentration of encapsulated hemin was determined using the calibration curve. The encapsulation efficiency (EE%) and the loading capacity (LC%) were calculated as follows:

$$EE = \frac{\text{concentration hemin measured}}{\text{concentration of the hemin added}} \times 100\%$$

$$LC = \frac{\text{concentration hemin measured}}{\text{concentration (hemin measured + polymer added)}} \times 100\%$$

The size and polydispersity index of the micelles were measured using dynamic light scattering (DLS) using a Malvern ALV CGS-3 (Malvern Ltd, Malvern UK) with a JDS Uniphase laser functioning at a wavelength of 632.8 nm, an optical fiber-based detector, a digital ALV/LSE 5003 correlator and a temperature controller set at 25°C. The refractive index and viscosity used for the data treatment were respectively 1.333 and 0.89 cp. All measurements were performed at a 90° angle. The Z-average mean particle size (Zave) and the polydispersity were calculated using the ALV-60 0 V.3.X software. The samples were made by diluting 10 to 20 µL micelle dispersion in 1 mL of 120 mM ammonium acetate pH 5.

Hemin-loaded micelles with the highest loading capacity and encapsulation efficiency were made as described in section 2.2. In detail, 0.1 mL of 120 µg/mL hemin in DMSO:DMF (1:9) was added to 0.9 mL of 1.8 mg/mL mPEG-*b*-p(HPMAm-Lac$_2$) in 120 mM ammonium acetate pH 5. Hemin was also dissolved in DMSO to obtain the same hemin concentration as the diluted micelle sample. UV-VIS spectra (λ 200 – 700 nm) of the solutions were recorded.

The stability of hemin-loaded micelles at pH 2 and pH 7.4 at 37 °C was determined by measuring the particle size (Zave) and polydispersity for 17 hours. For the stability at pH 2, the hemin-loaded micelles were formed in 120 mM ammonium acetate Ph 5 as described in section 2.2 followed by lowering to pH 2 by addition of 4 M HCl. To determine the stability of the hemin-loaded micelles at pH 7.4, the polymer was dissolved in PBS pH 7.4 containing 8.2 g NaCl, 3.1 g $Na_2HPO_4 \cdot 12H_2O$ and 0.3g NaH_2PO_4 $2H_2O$ per liter.

2.3. Synthesis of mPEG-*b*-p((HPMAm-Lac$_2$)-co-RhodMA

Rhodamine labeled mPEG-*b*-p(HPMAm-Lac$_2$) was synthesized according to a previously reported polymerization procedure [33, 34]. In short, methacryloxyethyl thiocarnamoyl rhodamine B and HMPA-Lac$_2$ (molar ratio 1:99) together with (mPEG)2 – ABCPA macroinitiator in a molar ratio of initiator to monomer of 1:150 were dissolved in 3 mL acetronitril (ACN) at a scale of 700 mg monomer. The mixture was flushed for 15 minutes with nitrogen at room temperature and subsequently stirred overnight at 70 °C. Next, the formed polymer was precipitated in diethyl ether and then dissolved in water. Dialysis was done for two days against ACN: H_2O (1:1), three days against THF:H_2O (1:1) and 4 days against H_2O in order to purify the polymer and remove low molecular weight impurities. The dialysis medium was refreshed 3 times a day. After dialysis, the rhodamine labeled polymer was recovered by lyophilization and characterized via 1H NMR and GPC as described by Soga et al. [26] and Rijcken et al. [27].

2.4. In-vitro cell uptake studies

The Caco-2 cells were cultured in Dulbecco´s Modified Eagle´s Medium (DMEM) containing 3.7 g/L sodium bicarbonate, 4.5 g/L glucose completed with 10 % fetal bovine

serum (FBS), 1 % antibiotics/antimycotics (100 IU penicillin G sodium/mL, 100 µg/mL streptomycin sulfate and 0.25 µg/mL amphotericin B) and 1 % nonessential amino acids. The cells were seeded at a density of 100,000 cells per cm2 on polystyrene well plates at 37 °C in a humidified atmosphere containing 5 % CO_2 and were allowed to differentiate for 14 days prior the experiments. Medium was replaced every 2-3 days.

For cellular uptake studies, hemin-loaded micelles with the highest loading capacity and encapsulation efficiency were made as described in section 2.2 and 2.3. Multiple dispersions of 1 mL were pooled and concentrated using viva spin centrifugal concentrator tubes (cut-off 50.000 kDa, Santorius Stedim, Germany) for 40 minutes at 4,000 x g, resulting in micellar dispersions concentrated around 70 times. The concentration of hemin in the micellar concentrate was determined by diluting the micellar dispersion 40x in PBS and then further diluting 10x in DMSO. Next, UVspectroscopy at 388 nm was used to determine the hemin concentration. This hemin-loaded micellar dispersion was used to perform dose response and time dependent cellular uptake as well as cytotoxicity studies. The volume of the micellar dispersion needed for the dose response and time dependent uptake studies was adjusted to 150 µL with PBS and mixed with 1350 µL cell culture medium to obtain 1.5 mL sample mixtures with concentrations of 10 – 200 µM hemin. The hemin micellar formulations were added to the Caco-2 cells and incubated for 24 hours, unless otherwise stated, at 37 °C humidified atmosphere containing 5 % CO_2. For the iron sulfate samples or iron sulfate combined with ascorbic acid in a molar ratio of (1:5), the necessary amount was dissolved in 150 µL PBS and mixed with 1350 µL cell culture medium to obtain iron sulfate solutions with concentration ranging from 10 to 200 µM.

After incubation of the Caco-2 cells with hemin-loaded micelles and iron sulfate formulations for 24 hours, the medium was removed and the cells were washed with PBS. The cells were then lysed with 350 µL RIPA buffer supplemented with a 1 % proteinase inhibitor cocktail. The lysed cells were stored at -20 °C until analyzed. Prior to analysis, the cells were thawed and spun down at 20.000 rpm for 15 minutes. Next, the protein concentration of the samples was measured using a Micro BCA protein assay kit (Pierce, Rockford USA). A dilution range of 1-200 µg/mL bovine serum albumin was used for calibration. In order to assess the iron uptake, the total ferritin content of the cell lysates was measured using a double sandwiched ELISA against human ferritin kit (ab 108837 Abcam, Cambridge United Kingdom). Both the protein and ferritin assays were performed according to the manufacturer's protocol.

2.5. Cell viability

The viability of the Caco-2 cells after incubation with the different formulations was assessed using a yellow tetrazolium salt XTT colorimetric assay that measures the metabolic activity of cells as first described by Scudiero et al. [35]. In short, Caco-2 cells were seeded at a density of 20,000 cells/well in a 96 well plate and incubated at 37 °C. After 24 hours, the cell culture medium was removed and replaced by an iron sample mixture of 150 µL, consisting of 100 µL medium and 50 µL made up of a volume of the different iron sample needed to obtain different concentrations adjusted with PBS. The cells were incubated for 24 hours and then washed with PBS. Next, 50 µL of fresh medium and 50 µL of XTT solution were added to the cells, which were subsequently incubated for 1 hour at 37 °C. Finally, the plates were measured using UV-spectroscopy at a wavelength of 490 nm and the relative cell survival after 24 hours treatment was compared to non-treated Caco-2 cells.

2.6. Intracellular localization of hemin-loaded micelles

A rhodamine labeled polymer was synthesized as described in section 2.7 and the hemin loaded (mPEG-*b*-p((HPMAm-Lac$_2$)-co-RhodMA) micelles were prepared as described in section 2.2 except that the rhodamine labeled polymer was dissolved in PBS pH 7.4 instead of 120 mM ammonium acetate. The Caco-2 cells were seeded at a density of 50,000 cells/well in a 16-well glass chamber slide system (Lab-Tek; chamber slide™ system 178599) and grown for 5 days in an incubator at 37 °C to reach 80% confluency. The rhodamine micelles dispersion was then diluted 4x with phenol red free DMEM culture medium. Next, the cells were incubated with the diluted dispersion for 3 hours and subsequently the medium was replaced and the cells were washed twice with PBS. The Caco-2 cells were subsequently fixed with 4% paraformaldehyde for 30 minutes, the fixative was then discarded and the cells were washed again twice with PBS. Binding buffer was made by preparing a stock solution of 50 mg Saponin from Sigma Aldrich and 100 mg BSA in 50 mL PBS. After the Caco-2 cells were fixed they were quenched for 10 minutes with 50 nM NH4Cl dissolved in water and washed twice with PBS. The binding buffer was then added to the cells and incubated for 30 minutes at room temperature. Next the primary antibody LAMP-1 to stain lysosomes, was dissolved in binding buffer (1 µg/mL). This antibody solution was then pipetted onto the cells and incubated for 60 minutes at room temperature. Subsequently, the secondary antibody Alexa-488 was used to detect the binding of the primary antibody and was dissolved in binding buffer (10 µg/mL). After 60 minutes of incubation with the primary antibody at room temperature, the Caco-2 cells were washed 4 x with PBS and the secondary antibody conjugated to Alexa-488 was added and incubated for 60 minutes. Finally, the cells were washed 3 times with PBS and once with Milli-Q ultrapure water and then mounted on the glass chamber slide system using FluorSave from Calbiochem, San Diego. Confocal microscopy was used to visualize the uptake of the rhodamine labeled micelles by measuring the red color within the cells and also to visualize lysosomes as the LAMP-1 antibody staining produced a green color.

3. Results and Discussion

3.1. Characterization of mPEG-*b*-p(HPMAm-Lac$_2$) block copolymer

Synthesis and characterization of mPEG(5000)-*b*-p(HPMAm-Lac$_2$) block copolymer was performed and characterized as described by Soga et al., [26, 36]. The polymer was obtained in a yield of 73 % and the number average molecular weight as determined by NMR analysis was 17400 g/mol. GPC analysis of the polymer (using PEG calibration) gave a number average molecular weight of 18500 g/mol, the weight average molecular weight was 37200 g/mol and the dispersity (Đ) was 2.0 which is close to earlier reported data [36].

3.2. Preparation and characterization of hemin loaded micelles

Hemin-loaded micelles with different loadings of hemin were prepared as described in section 2.2 by addition of a small volume of hemin in DMSO to a cold aqueous polymer solution (1.8 mg/mL, which is far above the critical micelle concentration (CMC) of 0.015 mg/mL as reported for this polymer [36]), followed by rapidly heating the solution to 50 °C. After filtration to remove non-encapsulated hemin, the obtained particles were characterized for hemin loading, size and size distribution. When no polymer was present, the addition of the DMSO/hemin solution to water resulted in the formation of large aggregates as shown

in figure 2C. In contrast, when adding the hemin solution to the polymer solution the encapsulation capacity of the micelles was obvious since a brownish micellar dispersion free of aggregates was obtained (figure 2D).

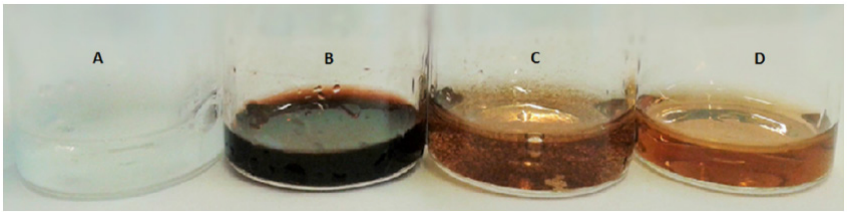

Figure 2. (A) mPEG-p(HPMAm-Lac$_2$) dissolved in 120 mM ammonium acetate (2 mg/mL); (B) Hemin dissolved in DMSO : DMF 1:9 (1.2 mg/mL); (C) Hemin in DMSO : DMF 1:9 (1.2mg/mL) of which 0.1 mL was added to 0.9 mL of 120 mM ammonium acetate; (D) Hemin- loaded micelles prepared by addition of 0.1 mL of 120 µg/mL of hemin in DMSO:DMF 1:9 to 0.9 mL of 1.8 mg/mL mPEG-*b*-p(HPMAm-Lac$_2$).

Figure 3 shows the loading of hemin in mPEG-*b*-p(HPMAm-Lac$_2$) micelles for three independently prepared micellar dispersions per hemin concentration with corresponding standard deviations in order to obtain insight in the batch-to-batch variability. Figure 3A demonstrates that the highest encapsulation was achieved by adding 120 µg/mL of hemin in DMSO to 1.8 mg/mL polymer solution in water. The loading capacity (LC) and encapsulation efficiency (EE) for this formulation were 3.9% and 61.4%, respectively. Figure 3A also shows that a higher concentration of hemin resulted in a decreasing EE. This is probably due to the fact that there is not enough polymer present to encapsulate the hemin, therefore resulting in saturation of the micelles with hemin and the formation of hemin aggregates with the excess hemin subsequently being filtered away [37, 38].

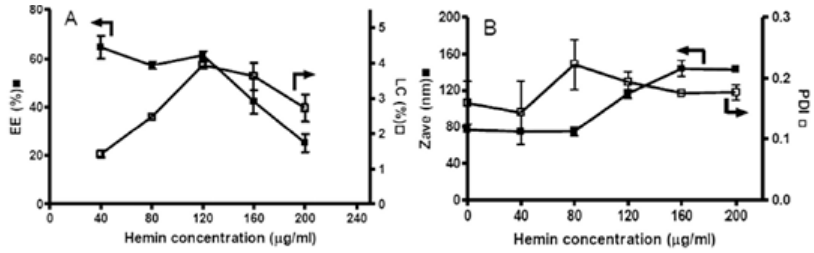

Figure 3. Loading of hemin in mPEG-*b*-p(HPMAm-Lac$_2$) micelles; (A) encapsulation efficiency on the left axis and loading capacity on the right axis and (B) Z-average diameter and polydispersity of hemin loaded micelles. Results represent mean ± standard deviation of three independently prepared samples.

Figure 3A further shows that the loading capacity increased from 2.5% at a hemin concentration of 40 µg/mL to 3.9% at a hemin concentration of 120 µg/mL and then leveled off, which is probably due to saturation of the micelles with hemin. Figure 3B demonstrates that when increasing the hemin concentration, the average size of the micelles also increased from 75 nm to 140 nm. The particle size at the highest hemin encapsulation was 116 nm and the polydispersity index was 0.19.

3.3. Physical state of hemin in micelles

Hemin loaded-micelles were prepared as described in section 2.2 and subsequently diluted ten times with ammonium acetate pH 5 to obtain a dispersion with a hemin concentration of 11.4 µM and a polymer concentration of 0.18 mg/mL. The polymer

concentration was above the CMC of 0.015 mg/mL [36], in order to ensure that the micelles remain intact during measurement. As control, hemin was dissolved in DMSO to obtain molecularly dissolved hemin at the same concentration as the diluted micelle sample.

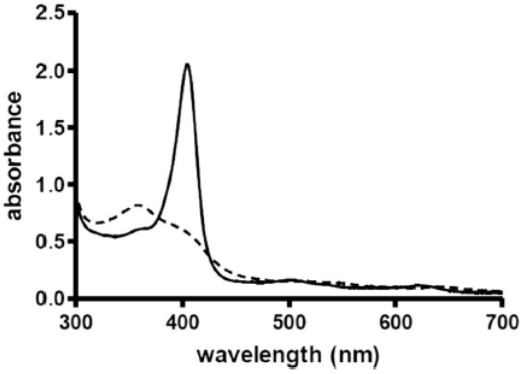

Figure 4. UV-Vis spectra of hemin ; (—) hemin (11.4 μM) in DMSO, (- -) hemin loaded micelles (11.4 μM of hemin) in 120 mM ammonium acetate pH 5.

Figure 4 shows for hemin dissolved in DMSO a so called Soret- or B band at a maximum of 404 nm, which is common for metalloporphyrins [39, 40]. Figure 4 further shows that the absorption for hemin loaded micelles is significantly broadened as compared to the absorption of hemin solubilized in DMSO. This can be ascribed to the aggregation of hemin in the micelles as previously reported for a silicon phthalocyanine photosensitizer loaded in mPEG-*b*-p(HPMAm-Lac$_2$) micelles [34]. Furthermore, the soret band for the hemin loaded-micelles shifted to lower wavelengths of respectively 385 nm compared to hemin dissolved in DMSO (404 nm). This shift is also known as a hypsochromic shift and is indicative for H-aggregation. Metalloporphyrins that form H-aggregates which are caused by strong metal to porphyrin orbital interaction are also called hypsoporphyrins. This interaction results in an enhanced porphyrin π-π* energy separation which subsequently leads to the hypsochromic shift as observed in figure 4 [41, 42]. The results presented in figure 4 imply that hemin is most likely present in an aggregate state within the micelles which can be beneficial as premature release of hemin when transiting through the digestive system is retarded.

3.4. Stability of hemin-loaded mPEG-*b*-p(HPMAm-Lac$_2$) micelles

In order for the hemin micelles to be effective for therapy, they should not disintegrate in the upper part of the digestive system and therefore the stability of the particles was examined at both pH 2 (stomach) and pH 7.4 (duodenum). Hemin loaded mPEG-*b*-p(HPMAm-Lac$_2$) micelles with the highest encapsulation and loading capacity (figure 3A) were used for these studies.

Figure 5A illustrates that at pH 2 the size of the micelles slightly increases from 143 to 199 nm upon incubation for 17 hours at 37 °C, whereas at pH 7.4 (figure 5B) the size remained constant in time. The polydispersity remained constant in time at both pH's, at an average of 0.18 at pH 2 and 0.21 at pH 7.4. The scattered intensity data provided as supporting information (figure S2) demonstrates that at pH 2 the scattered intensity slowly decreases in time indicating slow degradation of the micelles, while at pH 7.4 the scattered intensity of the micelles remains constant throughout the measurement. However, during the first three hours which covers the common transit time in the stomach [43, 44], the average size and scattered

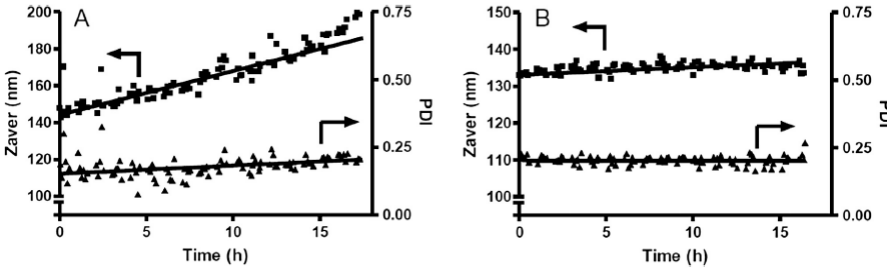

Figure 5. Z-average size (Zave) and polydispersity (PDI) of hemin micelles at 37 °C as a function of time at pH 2 (figure 5A) and at pH 7.4 (figure 5B); Figure 5A: micelles were prepared at pH 5 as described in section micellar preparation and then adjusted to pH 2 with 4 M HCl; Figure 5B: micelles were prepared using a polymer solution in PBS pH 7.4 as described in section micellar stability.

intensity remained almost constant at pH 2. At pH 7.4 the micelles were stable up to 17 hours which could be beneficial for the uptake by the enterocytes after their oral administration.

3.5. Cellular in-vitro uptake of hemin-loaded mPEG-*b*-p(HPMAm-Lac$_2$) micelles.

To study the feasibility of hemin-loaded micelles as formulation for oral iron delivery, several experiments were performed on Caco-2 cell cultures. The Caco-2 cell line has been extensively used to study nutrient and drug transport, as these cells upon differentiation express a comparable microvilli brush border with functionality similar to the enterocytes present in the small intestines [45, 46]. Ferritin is also a well-known marker for cellular iron uptake as it is the protein that stores iron when not needed elsewhere in the organism [47]. Once the Hemin loaded micelles are internalized by cells and the hemin is released, it is degraded by the enzyme heme oxygenase which is present on the endoplasmic reticulum resulting in the formation of Fe^{2+}, biliverdin and carbon monoxide [48]. Subsequently the iron in the cytoplasm enters the common iron pool and is then transported to the bloodstream via the protein ferroportin. The excess iron which is not required to enter in the circulatory system is stored in the cytosolic protein ferritin [8, 49]. The regulation of ferritin synthesis occurs via the translation of ferritin H and L mRNA's in presence of accessible iron in the labile iron pool which can be defined as a cell chelatable pool consisting of mainly Fe^{2+} associated with various ligands with an affinity for iron [50-52]. This results in an increase or decrease of ferritin synthesis and thus ferritin expression when iron levels are high or down regulated when iron levels are low [8,53]. In the present study, Caco-2 cells were incubated with dispersions of hemin loaded micelles with different concentrations, as well as with iron sulfate or iron sulfate in combination with ascorbic acid. Also, a cytotoxicity assay was done to assess the cytocompatibility of the formulations.

3.6. Uptake of hemin-loaded mPEG-*b*-p(HPMAm-Lac$_2$) micelles by Caco-2 cells

In order to study uptake of hemin-loaded micelles, mPEG-*b*-p((HPMAm-Lac$_2$)-co-RhodMA) was synthesized as described is section 2.7. GPC analysis (figure 6) equipped with both a RI- and UV-detector was performed to determine the number average molecular weight and the amount of free rhodamine in the sample. The number average molecular weight (Mn) using PEG standards for calibration was 23500 g/mol; Mw/Mn = 2.0. Furthermore GPC analysis showed that the amount of free label was less than 3 %.

In order to observe whether hemin-loaded micelles were taken up by the Caco-2 cells, confocal microscopy was performed using rhodamine labelled hemin-micelles and the commonly used lysosome marker LAMP-1 [54]. Figure 7B depicts that after an incubation time of 3 hours, the cells take up the labelled micelles, but Figure 7C shows that most of the green fluorescence of the lysosomes does not overlap with the red rhodamine fluorescence. This indicates that the rhodamine micelles were not present in lysosomal vesicles as would be expected if the uptake mechanism was via endocytosis [53]. Similar results were also obtained by Rijcken et al. [34] who incubated murine melanoma B16F10 cells with (mPEG-*b*-p((HPMAm-Lac$_2$)-co-RhodMA) micelles to investigate the cellular uptake of these particles. Furthermore, the particles studied in this paper had an average size of 116 nm as shown in figure 3B, which is well above the optimal particle size of 25-30 nm for endocytosis according to a study performed by Zhang et al. [56]. Nevertheless uptake of hemin into the cells in its free form is not expected because of its low aqueous solubility and therefore the high levels of ferritin that are formed after incubation of the hemin micelles with the cells, as shown in the section below, are probably due to the internalized micelles. Talelli et al. [57], also demonstrated that similar rhodamine labeled micelles, both non-targeted as well as EGa1 nanobody targeted were indeed taken up by 14C cells. Sahay et al., [58] discussed the various pathways that nanoparticles composed of different materials use to enter cells, including nanomaterials that are able to bypass early endosomes and lysosomes. However some of these mechanisms are not fully understood, but up to date any of the endocytic pathways are considered the main cellular uptake mechanism for micelles [59].

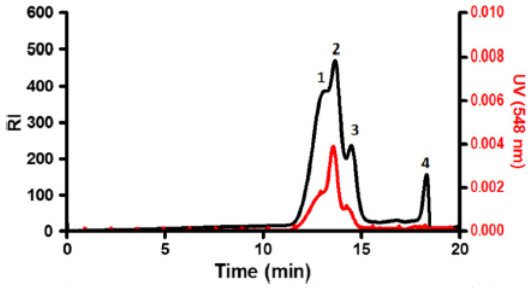

Figure 6. GPC profile (1) mPEG-*b*-p((HPMAm-Lac$_2$)-co-RhodMA; (2) traces of the PEG-macroinitiator;(3) free PEG; (4) injection peak. The red line is the UV signal at 548 nm and black line is RI signal.

3.7. Ferritin expression after in-vitro uptake of iron complex

Figure 8 presents the ferritin expression after incubating the Caco-2 cells for 24 hours with dispersions of hemin-loaded micelles or iron sulfate. After incubating the cells with medium containing iron sulfate in various concentrations, ferritin values reached a maximum of 250 ng/mg protein at a concentration of 150 μM. It can also be observed that at this iron sulfate concentration the expression of intracellular ferritin reached a plateau.

Importantly, when the cells were incubated with medium containing hemin-loaded micelles, ferritin values of 2500 ng/mg protein were observed, which are more than 10 fold higher than obtained when incubating the cells with iron sulfate. This observation is in accordance with a previous study in which it has been reported that heme iron is probably being taken up more efficiently by Caco-2 cells than nonheme iron such as iron salts [11].

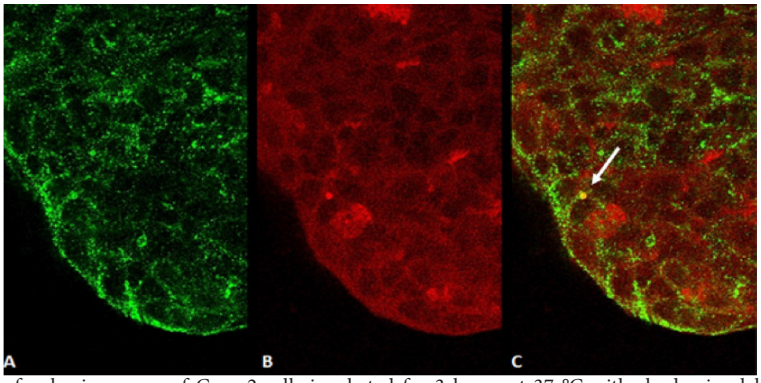

Figure 7. Confocal microscopy of Caco-2 cells incubated for 3 hours at 37 °C with rhodamine labeled hemin-micelles. Figure 7A: lysosome staining in green; figure 7B: rhodamine labelled micelles in red; figure 7C: overlap of lysosome staining and rhodamine.

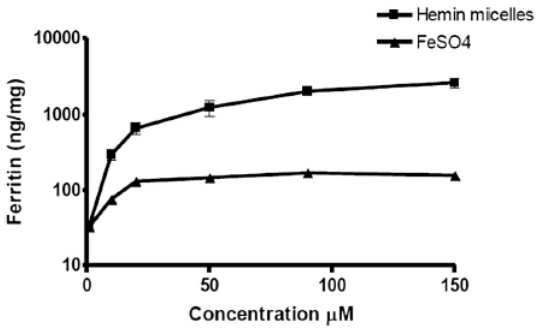

Figure 8. Formation of ferritin (in ng/mg cellular protein) by Caco-2 cells upon incubation with hemin or iron sulfate for 24 hours at 37 °C. Results represent mean ± standard deviation of three experiments.

Additional experiments were performed to study the effect of combining ascorbic acid (vitamin C), a vitamin that beneficially enhances iron uptake [60]. Figure 9 shows that when ascorbic acid was added to the medium, a substantial higher ferritin formation was observed, confirming literature claims [60]. Furthermore, it can be observed that there were no significant differences between ferritin expressed by cells incubated with iron sulfate supplemented with ascorbic acid or hemin loaded micelles. However, ascorbic acid is a strong reductant which in excess could lead to the formation of undesired high Fe^{2+} amounts and result in possible pro-oxidative activity [61, 62]. In addition, we investigated possible cytotoxic effects of the different iron formulations using the XTT assay. The results shown in figure 10 demonstrate that incubating Caco-2 cells with hemin–loaded micelles with a concentration up to 150 µM, has no effect on the cell viability whereas iron sulfate combined with ascorbic acid was clearly cytotoxic, with an IC50 value of 50 µM.

3.8. Kinetics of ferritin formation in Caco-2 cells after incubation of iron samples

The kinetics of ferritin formation was investigated by incubating the Caco-2 cells with iron sulfate and hemin-loaded micelles with a concentration of 150 µM. The hemin-loaded micellar dispersion was made from 120 µg hemin/mL in 1.8 mg/mL polymer. Figure 11 illustrates that the amount of ferritin reached a maximum already after 3 hours upon incubation with both formulations at 37 °C. After this incubation time there is no significant difference in formation of ferritin.

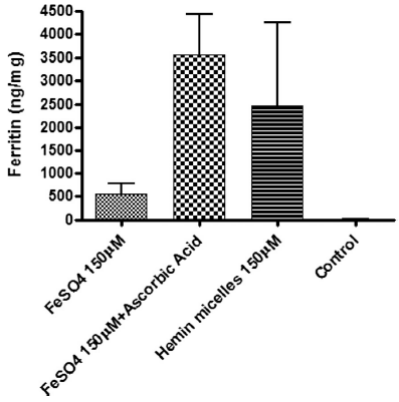

Figure 9. Formation of ferritin (in ng/mg cellular protein) by Caco-2 cells after 24 hours of incubation with 150 µM of hemin loaded mPEG-*b*-p(HPMAm-Lac$_2$) micelles, iron sulfate, iron sulfate plus ascorbic acid in a molar ratio of 1:5, and DMEM medium only. Results represent mean ± standard deviation of three experiments.

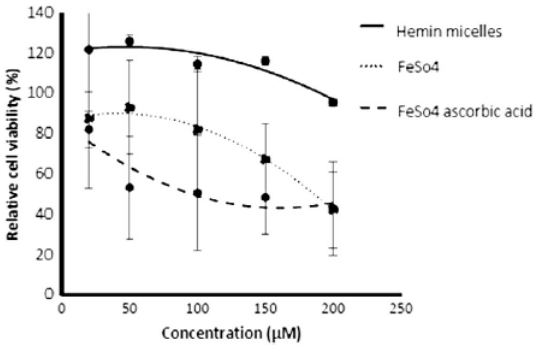

Figure 10. Viability of Caco-2 cells upon incubation of different concentrations of Hemin-loaded micelles; Iron sulfate; Iron sulfate : Ascorbic acid (1:5) and empty micelles. Results represent mean ± standard deviation of three experiments

In many previous studies using Caco-2 cells as a model cell line to investigate iron uptake, the cells were harvested after 24 hours upon incubation with iron supplements in order to allow ferritin formation [47, 63]. However, here we demonstrate that 3 hours is sufficient to reach a maximum of ferritin formation upon incubation with both hemin-loaded micelles as well as iron sulfate.

4. Conclusions

The present study shows that hemin can successfully be loaded in mPEG-bp(HPMAm-Lac$_2$) micelles forming water dispersible particles with an average size of around 100 nm. The hemin-loaded micelles demonstrated to remain stable up to 3 hours at pH 2 and 17 hours at pH 7.4. Importantly, upon incubation in Caco-2 cells the hemin-loaded micelles gave superior ferritin formation up to 10x times higher than when compared to the commonly used iron supplement iron sulfate. The new hemin formulation presented in this paper is therefore a promising formulation for iron oral delivery.

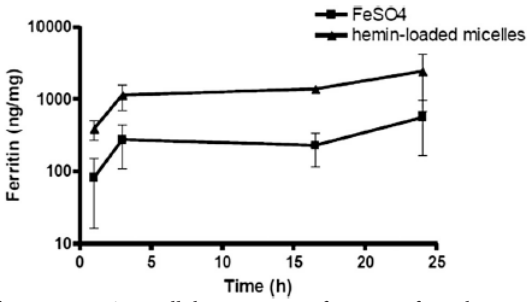

Figure 11. Formation of ferritin in ng/mg cellular protein as function of incubation time of Caco-2 cells with hemin-loaded micelles (150 μM) and iron sulfate (150 μM). Results represent mean ± standard deviation of three experiments.

Acknowledgements

This research was financially supported by Vifor Pharma.

References

[1] Benoist de, Bruno., McLean, Erin., Egli, Ines., Cogswell., 2008. Worldwide prevalence of anaemia 1993-2005: WHO global database on anaemia, ISBN 978 92 4 159665 7

[2] S. Yun, J.P. Habicht, D.D. Miller, R.P. Glahn, An In Vitro digestion/Caco-2 cell culture system accurately predicts the effects of ascorbic acid and polyphenolic compounds on iron bioavailability in humans, J. Nutr. 134 (2004) 2717–2721.

[3] E.C. Theil, Iron homeostasis and nutritional iron deficiency, J. Nutr. 141 (2011) 724S–728S.

[4] R.P. Glahn, M. Rassier, M.I. Goldman, O.A. Lee, J. Cha, A comparison of iron availability from commercial iron preparations using an in vitro digestion/Caco-2 cell culture model, J. Nutr. Biochem. 11 (2000) 62–68.

[5] G.J. Anderson, D.M. Frazer, G.D. McLaren, Iron absorption and metabolism, Curr. Opin. Gastroenterol. 25 (2009) 129–135.

[6] P. Santiago, Ferrous versus ferric oral iron formulations for the treatment of iron Deficiency: A clinical overview, Sci. World J. 2012 (2012) 5.

[7] B.K. Fuqua, C.D. Vulpe, G.J. Anderson, Intestinal iron absorption, J. Trace Elem. Med. Biol. 26 (2012) 115–119.

[8] R. Evstatiev, C. Gasche, Iron sensing and signalling, Gut 61 (2012) 933–952.

[9] J. Wang, K. Pantopoulos, Regulation of cellular iron metabolism, Biochem. J. 434 (2011) 365–381.

[10] A.A. Khan, J.G. Quigley, Control of intracellular heme levels: Heme transporters and heme oxygenases, Biochim. Biophys. Acta - Mol. Cell Res. 1813 (2011) 668–682.

[11] S. Miret, S. Tascioglu, M. van der Burg, L. Frenken, W. Klaffke, In vitro bioavailability of iron from the heme analogue sodium iron chlorophyllin, J. Agric. Food Chem. 58 (2010) 1327–1332.

[12] P. Villarroel, S. Flores, F. Pizarro, D. de Romaña, M. Arredondo, Effect of dietary protein on heme iron uptake by Caco-2 cells, Eur. J. Nutr. 50 (2011) 637–643.

[13] D.S. Kalinowski, D.R. Richardson, The evolution of iron chelators for the treatment of iron overload disease and cancer, Pharmacol. Rev. 57 (2005) 547–583.

[14] Comparison of oral iron supplements. Pharmacist's Letter/Prescriber's Letter 2008; 24 (8):240811.

[15] M. Shayeghi, G.O. Latunde-Dada, J.S. Oakhill, A.H. Laftah, K. Takeuchi, N. Halliday, et al., Identification of an intestinal heme transporter, Cell 122 (n.d.) 789–801.

[16] C. Cao, C. Thomas, K. Insogna, K. O'Brien, Duodenal expression of heme and non-heme iron transporters and tissue partitioning of dietary heme and non-heme iron in a rat mode of iron overload, FASEB J. 28 (2014), meeting abstract 246.8

[17] T. Korolnek, I. Hamza, Like iron in the blood of the people: The requirement for eme trafficking in iron metabolism, Front. Pharmacol. 5 (2014) 126.

[18] T.J. Egan, E. Hempelmann, W.W. Mavuso, Characterisation of synthetic β-haematin and effects of the antimalarial drugs quinidine, halofantrine, desbutylhalofantrine and mefloquine on its formation, J. Inorg. Biochem. 73 (1999) 101–107.

[19] A.C. Hunter, J. Elsom, P.P. Wibroe, S.M. Moghimi, Polymeric particulate technologies for oral drug delivery and targeting: a pathophysiological perspective, Nanomedicine 8 (2012) S5–S20.

[20] S. Mazzaferro, K. Bouchemal, G. Ponchel, Oral delivery of anticancer drugs III: formulation using drug delivery systems, Drug Discov. Today 18 (2013) 99–104.

[21] G. Gaucher, P. Satturwar, M.-C. Jones, A. Furtos, J.-C. Leroux, Polymeric micelles for oral drug delivery, Eur. J. Pharm. Biopharm. 76 (2010) 147–158.

[22] K. Thanki, R.P. Gangwal, A.T. Sangamwar, S. Jain, Oral delivery of anticancer drugs: Challenges and opportunities, J. Control. Release 170 (2013) 15–40.

[23] L. Zhang, S. Wang, M. Zhang, J. Sun, Nanocarriers for oral drug delivery, J. Drug Target. 21 (2013) 515–527.

[24] L. Mei, Z. Zhang, L. Zhao, L. Huang, X.-L. Yang, J. Tang, et al., Pharmaceutical nanotechnology for oral delivery of anticancer drugs, Adv. Drug Deliv. Rev. 65 (2013) 880–890.

[25] C. Deng, Y. Jiang, R. Cheng, F. Meng, Z. Zhong, Biodegradable polymeric micelles for targeted and controlled anticancer drug delivery: Promises, progress and prospects, Nano Today 7 (2012) 467–480.

[26] O. Soga, C.F. van Nostrum, W.E. Hennink, Poly(N-(2-hydroxypropyl) methacrylamide mono/di Lactate): A new class of biodegradable polymers with tuneable thermosensitivity, Biomacromolecules 5 (2004) 818–821.

[27] C.J.F. Rijcken, T.F.J. Veldhuis, A. Ramzi, J.D. Meeldijk, C.F. van Nostrum, W.E. Hennink, Novel fast degradable thermosensitive polymeric micelles based on PEG-block-poly(N-(2-hydroxyethyl) methacrylamide-oligolactates), Biomacromolecules 6 (2005) 2343–2351.

[28] D. Schmaljohann, Thermo- and pH-responsive polymers in drug delivery. Advanced Drug Delivery Reviews 58 (2006) 1655-1670.

[29] S.R. MacEwanand A. Chilkoti, Applications of elastin-like polypeptides in drug delivery, Journal of Controlled Release 190 (2014) 314-330.

[30] M. Talelli, C.J.F. Rijcken, T. Lammers, P.R. Seevinck, G. Storm, C.F. van Nostrum, et al., Superparamagnetic iron oxide nanoparticles encapsulated in biodegradable thermosensitive polymeric micelles: toward a targeted nanomedicine suitable for image-guided drug delivery, Langmuir 25 (2009) 2060–2067.

[31] O. Naksuriya, Y. Shi, C.F. van Nostrum, S. Anuchapreeda, W.E. Hennink, S. Okonogi, HPMA-based polymeric micelles for curcumin solubilization and inhibition of cancer cell growth, Eur. J. Pharm. Biopharm. 94 (2015) 501–512.

[32] D. Neradovic, O. Soga, C.F. Van Nostrum, W.E. Hennink, The effect of the processing and formulation parameters on the size of nanoparticles based on block copolymers of poly(ethylene glycol) and poly(N-isopropylacrylamide) with and without hydrolytically sensitive groups, Biomaterials 25 (2004) 2409–2418.

[33] O. Soga, C.F. van Nostrum, M. Fens, C.J.F. Rijcken, R.M. Schiffelers, G. Storm, et al., Thermosensitive and biodegradable polymeric micelles for paclitaxel delivery, J. Control. Release 103 (2005) 341–353.

[34] C.J.F. Rijcken, J.-W. Hofman, F. van Zeeland, W.E. Hennink, C.F. van Nostrum, Photosensitiser-loaded biodegradable polymeric micelles: Preparation, characterisation and in vitro PDT efficacy, J. Control. Release 124 (2007) 144–153.

[35] D.A. Scudiero, R.H. Shoemaker, K.D. Paull, A. Monks, S. Tierney, T.H. Nofziger, et al., Evaluation of a soluble tetrazolium/formazan assay for cell growth and drug sensitivity in culture using human and other tumor cell lines, Cancer Res. 48 (1988) 4827–4833.

[36] O. Soga, C.F. van Nostrum, A. Ramzi, T. Visser, F. Soulimani, P.M. Frederik, et al., Physicochemical characterization of degradable thermosensitive polymeric micelles, Langmuir 20 (2004) 9388–9395.

[37] M.C. Jones, J.C. Leroux, Polymeric micelles – a new generation of colloidal drug carriers, Eur. J. Pharm. Biopharm. 48 (1999) 101–111.

[38] M. Yokoyama, A. Satoh, Y. Sakurai, T. Okano, Y. Matsumura, T. Kakizoe, et al., Incorporation of water-insoluble anticancer drug into polymeric micelles and control of their particle size, J. Control. Release 55 (1998) 219–229.

[39] V. Srinivas, Ch. Mohan Rao, Time profile of hemin aggregation: an analysis. Biochemistry International 21 (1990) 849-855

[40] M.E. Lombardo, L.S. Araujo, A.B. Ciccarelli, A. Batlle, A spectrophotometric method for estimating hemin in biological systems, Anal. Biochem. 341 (2005) 199–203.

[41] S. Hirohara, M. Obata, S. Ogata, K. Kajiwara, C. Ohtsuki, M. Tanihara, et al., Sugar-dependent aggregation of glycoconjugated chlorins and its effect on photocytotoxicity in HeLa cells, J. Photochem. Photobiol. B Biol. 84 (2006) 56–63.

[42] M. Prushan, Absorption and Fluorescence spectroscopy of tetraphenyl porphyrin and metallo-tertraphenylporphyrin. (2005) 1–9. http://www.lasalle.edu/

[43] M. Camilleri, L.J. Colemont, S.F. Phillips, M.L. Brown, G.M. Thomforde, N. Chapman, and A.R. Zinsmeister. Human gastric emptying and colonic filling of solids characterized by a new method. Am J Physiol. - Gastrointestinal and Liver Physiology 257 (1989) G284-G290.

[44] L.P. Degen, S.F. Phillips, Variability of gastrointestinal transit in healthy women and men, Gut 39 (1996) 299–305.

[45] M. Pinto, S. Robine-Leon, M. Appay, M. Kedinger, N. Triadou, E. Dussaulx, B. Lacroix, P. Simon-Assmann, K. Haffen, J. Fogh, A. Zweibaum, Biology of the Cell (1983) 47, 323-330.

[46] B. Press, D. Di Grandi, Permeability for intestinal absorption: Caco-2 assay and related issues, Curr. Drug Metab. 9 (2008) 893–900.

[47] R.P. Glahn, O.A. Lee, A. Yeung, M.I. Goldman, D.D. Miller, Caco-2 cell ferritin formation predicts nonradiolabeled food iron availability in an in vitro digestion/Caco-2 cell culture model, J. Nutr. 128 (1998) 1555–1561.

[48] G. Kikuchi, T. Yoshida, M. Noguchi, Heme oxygenase and heme degradation, Biochem. Biophys. Res. Commun. 338 (2005) 558–567.

[49] J. Hooda, A. Shah, L. Zhang, Heme, an essential nutrient from dietary proteins, critically impacts diverse physiological and pathological processes, Nutrients 6 (2014) 1080–1102.

[50] O. Kakhlon, Z.I. Cabantchik, The labile iron pool: characterization, measurement, and participation in cellular, Free Radic. Biol. Med. 33 (2002) 1037–1046.

[51] M. Kruszewski, Labile iron pool: the main determinant of cellular response to oxidative stress, Mutat. Res. Mol. Mech. Mutagen. 531 (2003) 81–92.

[52] R.C. Hider, X. Kong. Iron speciation in the cytosol: an overview. Dalton Transactions. 42 (2013) 220-3229.

[53] F.M. Torti and S.V. Torti. Regulation of ferritin genes and protein. Blood 99 (2002) 3505-3516.

[54] T.G. Iversen, T. Skotland, K. Sandvig, Endocytosis and intracellular transport of nanoparticles: Present knowledge and need for future studies, Nano Today 6 (2011) 176–185.

[55] I. Mellman, Endocytosis and molecular, Annu. Rev. Cell Dev. Biol. 12 (1996) 575–625.

[56] S. Zhang, J. Li, G. Lykotrafitis, G. Bao, S. Suresh, Size-dependent endocytosis of nanoparticles, Adv. Mater. 21 (2009) 419–424.

[57] M. Talelli, C.J.F. Rijcken, S. Oliveira, R. van der Meel, P.M.P. van Bergen en Henegouwen, T. Lammers, et al., Nanobody — Shell functionalized thermosensitive core-crosslinked polymeric micelles for active drug targeting, J. Control. Release 151 (2011) 183–192.

[58] G. Sahay, D.Y. Alakhova, A. V Kabanov, Endocytosis of nanomedicines, J. Control. Release 145 (2010) 182–195.

[59] I. Pepić, J. Lovrić, J. Filipović-Grčić, How do polymeric micelles cross epithelial barriers?, Eur. J. Pharm. Sci. 50 (2013) 42–55.

[60] J.D. Cook, M.B. Reddy, Effect of ascorbic acid intake on nonheme-iron absorption from a complete diet, Am. J. Clin. Nutr. 73 (2001) 93–98.

[61] B. Sturm, H. Laggner, N. Ternes, H. Goldenberg, B. Scheiber-Mojdehkar, Intravenous iron preparations and ascorbic acid: Effects on chelatable and bioavailable iron, Kidney Int. 67 (2005) 1161–1170.

[62] I.D. Podmore, H. R. Griffiths, K. E. Herbert, N. Mistry, P. Mistry and J. Lunec, Nature 392 (1998), 559-559.

[63] B.I. Mergler, E. Roth, S.F.A. Bruggraber, J.J Powell, D.I.A Pereira, Development of the Caco-2 Model for assessment of iron absorption and utilisation at supplemental levels. J. Pharm. Nutr. Sci. 2 (2012), 26-33.

Chapter | 5

Potential induction of anti-PEG antibodies and complement activation towards PEGylated therapeutics

Verhoef JJF, Carpenter JF, Anchordoquy TJ, Schellekens H

Article published in:
Drug Discovery Today
2014 Dec;19:1945-52.
doi: 10.1016/j.drudis.2014.08.015

Abstract

Conjugation of poly(ethyleneglycol) (PEG) to therapeutics has proven to be an effective and safe approach to increase the serum half-life of a therapeutic by reducing both renal clearance and uptake by the mononuclear phagocyte system, an obstacle that has hindered the wide introduction and application of several therapeutics. Despite the fact that many patients are treated with PEGylated therapeutics, an increasing number of unexpected immunogenicity issues have been reported. Several researchers have claimed that these are caused by anti-PEG antibodies responsible for the rapid clearance of a subsequent dose. Even more concerning is the notion that PEGylation can result in the activation of the complement system with the potential to induce severe hypersensitivity reactions. Opposed to the anti-PEG antibody theory, several researchers have opted that no such claims can be made as these assays were not validated and lacked specificity. As the matter is getting more attention, it is of utmost importance that the discussion be based on well-grounded science. This review therefore discusses clinical data and, where needed, expresses concerns regarding the interpretation of data. In addition, a mechanism is proposed by which conjugation of PEG can induce complement activation and the potential induction of anti-PEG antibodies.

1. Introduction

Advances in biotechnology and drug delivery research have produced many novel protein and liposomal therapeutics and hold the promise of even more-innovative products for areas in which few or no therapies exist. Despite these advances, many of these therapeutics have several shortcomings that limit their clinical utility, such as short circulation times, direct toxicity, rapid renal clearance and propensity to induce antidrug antibodies [1]. To overcome these shortcomings, many strategies have been applied to protein therapeutics such as changing the amino acid sequence or conjugation to a fusion protein. Although useful in certain applications, these methods also have their own limitations such as reduced affinity and activity and a higher tendency to aggregate [2,3].

Another strategy that has been investigated extensively is the attachment of polymers to therapeutic proteins. The polymer polyethylene glycol (PEG), a linear and nonionic polyether diol with the molecular formula $HO–(CH_2–CH_2–O)_n–H$, hhas been used extensively in the development of drug delivery systems as well as for protein modifications since its introduction in the 1970s. Its use in protein modification was first described by Abuchowsky et al. who showed that by PEGylation – the covalent attachment of PEG to form a conjugate – a protein could be modified extensively while maintaining its biological activity. They reported that with increased levels of attached PEG the immunogenicity of bovine serum albumin (BSA) and liver catalase can be reduced in rabbits 4 and 5. The authors also showed that, in contrast to native liver catalase, clearance and immunogenicity of PEGylated catalase remained unchanged after multiple injections [5]. These findings ultimately led to a whole new discipline in drug development that has resulted in the marketing authorization of several PEGylated proteins including four blockbusters: PegIntron® (Schering-Plough, USA), Pegasys® (Hoffmann-La Roche, USA), Neulasta® (Amgen, USA) and Mircera® (Hoffmann-La Roche, USA).

PEGylation is also extensively applied in other fields of drug delivery research to increase serum half-life of therapeutics [6]. An example is PEGylated liposomes referred to as 'stealth liposomes', which accumulate less extensively in the liver than their non-PEGylated counterparts [7]. However, despite the so-called stealth properties of PEGylated liposomal therapeutics, Doxil® (Johnson and Johnson, USA; Schering Plough, Europe) is currently the only approved PEGylated liposomal drug delivery system that has reached the market [8].

In addition to a large molecular size, the beneficial properties of PEGylation are also caused by the ability to attract a water shell around the polymer because each ethylene glycol subunit attracts two or three water molecules [1]. The attraction of water can increase the hydrodynamic size by a factor of five-to-ten, attenuating rapid renal clearance of therapeutics. In addition, PEGylation via steric hindrance shields the drug component from enzymatic degradation and opsonization with serum proteins, the binding of certain proteins that interact with the immune system 1 and 9. Consequently, PEGylation can reduce uptake by the mononuclear phagocyte system (MPS), an obstacle that has hindered the wide introduction and application of many therapeutic proteins [1,10-12]. As a result, PEGylated therapeutics are thought to be more stable, induce fewer adverse events and have improved pharmacokinetics compared with their non-PEGylated counterparts [1].

However, in contrast to this, several papers from the past decade suggested that PEG – therapeutics are actually capable of inducing anti-PEG antibodies involved in rapid clearance of a subsequent dose [8,10,13]. Although the immunogenicity of PEG has not gained much attention in the field of protein therapeutics, the potential negative side-effects of PEG in other drug delivery systems have gained widespread attention [11,14]. Several research groups have shown that anti-PEG antibodies are associated with the rapid clearance of subsequent doses of PEGylated liposomes and micelles, referred to as the accelerated blood clearance (ABC) phenomenon [10,15,16]. In addition, several animal studies as well as clinical observations with the use of Doxil® have shown that PEGylated liposomes can activate the complement system and potentially cause hypersensitivity reactions [14,17,18]. Because PEGylation of therapeutics is currently considered to be one of the most favorable approaches in reducing immunogenicity and obtaining favorable pharmacokinetics, the existence and implications of anti-PEG antibodies as well as PEG-induced complement activation require thorough investigation.

2. Clinical symptoms and implication of PEGylated therapeutics

Although the immunogenicity of PEG is gaining increased attention, it should be noted that several PEGylated therapeutics have reached the market, most of which have not been linked to serious immunogenicity issues. For instance Pegintron®, which is now the standard treatment option for hepatitis C virus (HCV) infection, induces antidrug antibodies in ~10% of patients, but only results in diminished clinical outcome in ~1% of all patients [19]. It is therefore not surprising that many question the immunogenicity of PEG. Indeed, besides PEGylated liposomes only a few therapeutics have been associated with anti-PEG antibodies, such as PEGloticase (Krystexxa®, Savient, USA) and PEGasparginase (Oncaspar®, Ovation, USA) [20]. Importantly, PEGinesatide (Omontys®, Affymax and Takeda, USA) was recently withdrawn from the market owing to severe hypersensitivity reactions with even fatal consequences, which could be related to PEG [21,22]. Although anti-PEG antibodies and PEG-induced complement activation have only been studied by a few research groups and some PEGylated therapeutic proteins have been used apparently safely for several years, one should realize that PEGylation can result in a conjugate that is highly immunogenic. Indeed, one of the explanations why the immunogenicity of PEG has not obtained much attention is that most studies have only investigated immune responses against the active protein and therefore any immunogenicity issues most often have been attributed to the therapeutic itself [23,24]. Although the study of anti-PEG can be overlooked by researchers owing to the perception that PEG is biologically inert, analysis of anti-PEG antibodies is also extremely difficult as mentioned in a previous review paper by our group [25]. This is mainly caused by the fact that no available assay has been thoroughly investigated for its sensitivity and specificity. In addition, standards are often not well described or their extrapolation to titers measured in the assays. This also includes the commercially available double-antigen bridging ELISA described by Liu and colleagues [26]. Essential information is not provided such as the specificity and characterization of their monoclonal ANPEG-1 mouse IgM antibody used for quantification of samples and quality control [25]. As such, these assays can only be interpreted as semiquantitative. Although a validated assay format is not available, the FDA recently updated their guidelines to screen for anti-PEG antibodies during (pre)clinical trials as a precautionary measure.

The first report concerning an immune response against the PEG portion of a PEGylated protein was published in 1983 by Richter and Akerblom, who observed rapid clearance of a second dose of PEGylated ovalbumin in mice was related to increased levels of anti-PEG IgM antibodies [27]. One year later, the authors were also the first to report the induction of anti-PEG IgM in humans [28]. They reported that 50% of patients being treated with PEGylated ragweed extract and PEGylated honeybee venom developed anti-PEG antibody titers after their first dose. However, in contrast to their findings in mice, no changes in response rates were observed within the two years of treatment and the percentage of patients testing positive for anti-PEG decreased to 28.5% [28]. Unfortunately no information regarding the assays is available. The authors concluded that the anti-PEG antibodies were not of clinical significance because they can bind to PEG but do not neutralize the compound activity due to phagocytosis by macrophages of the MPS [28]. These findings played an important part in establishing the perception that PEG is nonimmunogenic, which contributed to the widespread use of PEG in drug development.

2.1. Liposomal doxorubicin

The PEGylated liposomal formulation of doxorubicin Doxil® is being used for the treatment of ovarian cancer and AIDS-related Kaposi's sarcoma. Although Doxil® reduces the cardiac toxicity observed with free doxorubicin, Doxil® itself also has some serious adverse effects such as the hand–foot syndrome and high incidence of infusion reactions [29]. These infusion reactions are thought to be caused by the complement system [30]. Hypersensitivity reactions (HSR) have been reported in up to 25% of patients in some studies, with an average of 8% across all published studies [30].

Although Doxil® is known to induce complement activation it has never been associated with the ABC phenomenon. Indeed, only PEGylated liposomes without cytostatic drugs have been shown to be associated with the ABC phenomenon. Dams et al. were the first to report that a second dose of empty PEGylated liposomes was rapidly eliminated when injected 5 days later [15]. The ABC phenomenon of empty PEG-liposomes has since been extensively studied in animals and revealed a negative correlation between the dose and lipid content on the clearance rate; meaning that the higher the dose and/or lipid content of the first administration the lower the ABC phenomenon and anti-PEG IgM production [31]. By contrast, encapsulation of doxorubicin into PEGylated liposomes induced a substantial reduction in the amount of anti-PEG IgM and a concomitantly reduced complement activation in the sera of rats [32]. It is assumed that cytotoxic agents released from the liposomes accumulating in the spleen impair the production of anti-PEG IgM as a result of inhibition of B cell proliferation and/or killing of B cells in the marginal zone (see below) [11,33].

2.2. PEGinesatide

The FDA approved peginesatide (Omontys®, Affymax and Takeda, USA) in December 2011 for the treatment of anemia in adult patients with chronic kidney disease (CKD) on hemodialysis [34 ,35]. Peginesatide, a dimeric peptide that is covalently attached to PEG, was the first erythropoietin-stimulating agent (ESA) that had no structural similarity to recombinant human erythropoietin (rhuEPO) and did cross-react with anti-rhuEPO antibodies [22]. Although clinical trials concluded that the product was nonimmunogenic, peginesatide was voluntarily withdrawn from the market in February 2013 owing to serious HSR; including anaphylaxis which was life-threatening and in some cases fatal [21]. Fatal

reactions occurred in ~0.02% of patients within 30 min of the start of their first intravenous administration [21]. Interestingly, no cases of HSR were observed for patients who obtained multiple doses or completed their dialysis session [21]. No patient-related data have been published explaining the mechanisms behind the HSR. However, the fact that all reactions occurred during the first dose suggests a potential role for non-antibody-mediated complement activation. Although this view is in contrast to the general perception of acute HSR, recent studies have confirmed that PEGylated therapeutics are indeed able to induce complement activation that is not triggered by antibodies directly (see below) [30,36]. By contrast, because no immunogenicity data have been published, the presence of any cross-reactive antibodies in these patients cannot be excluded.

2.3. PEGylated asparaginase

The enzyme asparaginase is used as a therapeutic protein for the treatment of acute lymphoblastic leukemia. In contrast to normal cells, these tumor cells are unable to synthesize the nonessential amino acid asparagine [37]. Asparaginase catalyzes the conversion of asparagine and glutamine into aspartic acid and ammonia, thereby depriving leukemic cells of circulating asparagines [37,38]. To reduce the immunogenicity of asparaginase, PEGylated asparginase (PEG-ASNase) (Oncaspar®, Ovation, USA) was developed in an effort to mask antigenic epitopes.

Armstrong et al. reported that in pediatric patients treated with PEG-ASNase for acute lymphoblastic leukemia 32% developed anti-PEG antibodies as measured by serology and 46% as determined by a flow-cytometry-based assay [20]. Furthermore, anti-PEG antibody titers, mainly IgM, were closely related to the rapid clearance of subsequent doses [20]. Surprisingly, 13% of patients treated with unmodified ASNase in the same study were also positive for anti-PEG antibodies, but no association was observed between serum ASNase activity and anti-PEG antibody levels [20].

The occurrence of anti-PEG antibodies in patients with no history of treatment with a PEGylated therapeutic was also addressed by the same authors. They showed that 25% of healthy volunteers who had never been treated with a PEGylated drug had anti-PEG antibodies in serum. Their assays were based on agglutination of mPEG-SPA red blood cells and also flow cytometry using Tenta-Gel-OH beads grafted with 60–70% PEG chains [39]. This high percentage is explained by some researchers as a result of the large amount of PEG that is present in cosmetics and food products, which might actually induce anti-PEG antibodies [8]. However, this high percentage could be questioned despite a study by Tillmann et al. who reported the occurrence of anti-PEG antibodies in 44% of patients with HCV before treatment with PEG–interferon (IFN), no other clinical trials have reported anti-PEG antibody titers in healthy patients [40].

2.4. PEGylated uricase

In September 2010, PEGylated uricase (pegloticase) (Krystexxa®, Savient, USA) was approved by the FDA for the treatment of gout, a purine metabolic disorder that results in urate deposition in tissues and can lead to arthritis [41]. Unfortunately, the unpegylated enzyme is a foreign protein for patients and highly immunogenic because humans do not express this enzyme [42].

Response rates of pegloticase in two Phase III clinical trials were between 38% and 47% in the biweekly group and between 20% and 49% in the monthly group [23]. Anti-pegloticase and anti-PEG antibodies were detected in 88% and 32%, respectively, of subjects, and titers were correlated with the rapid clearance of pegloticase [43]. Of the anti-pegloticase-positive patients, 78% had IgG and IgM antibodies, 20% only IgM and 2% were only positive for IgG [43]. In addition, patients having IgG and IgM antibodies normally had the highest levels, and IgM only titers usually preceded that of IgG [43]. Anti-pegloticase and anti-PEG antibodies were detected using ELISA wells coated with either pegloticase or PEG. Anti-pegloticase antibodies bound other PEGylated proteins, including PEG–asparaginase, PEG–catalase, PEG–chymotrypsin and PEG–subtilisin as well as PEG–superoxide-dismutase, from which the authors concluded that antipegloticase antibodies were primarily directed against the PEG portion of the protein 43 and 44. Although the authors reported that these antibodies were unable to reduce activity in their in vitro neutralizing assay, a strong correlation between rapid clearance, antipegloticase antibodies and complement activation were reported [23,43].

A strong relation between infusion reactions, high antipegloticase titers and complement activation was also observed [43,45]. Furthermore, more than 50% of transient responders who had activated complement appeared to have one or more signs of an infusion reaction of which only a small portion could be explained by IgE antibodies [23,43]. Because mainly IgM antibodies against pegloticase developed in these patients, a potential role of complement activation responsible for these infusion reactions cannot be excluded. It is well known that patients with gout can have activated complement levels owing to high levels of urate crystals [46]. When urate crystals activate the complement system, binding of IgM to pegloticase can further activate the complement systems at lower binding levels as a result of synergetic properties and this could explain why infusion reactions are more common in patients with high IgM antibody titers.

The specificity of the antipegloticase antibodies remains however uncertain. Approximately 88% of attenuated responders developed antipegloticase antibodies that were able to cross-react with the PEG portion of other PEGylated proteins. However their specific anti-PEG ELISA only detected anti-PEG antibodies in 32% of patients. This could be explained by the much lower assay sensitivity of the anti-PEG ELISA in which PEG was coated to the plate compared with the antipegloticase assay, but it underpins the problems with anti-PEG ELISA assays as recently mentioned by Schellekens and colleagues. They state that current assays are not well validated for their specificity because of the absence of positive controls and well-defined dose–response curves [25]. In addition, the data on the specificity and affinity of anti-PEG antibodies in the anti-PEG assay raise questions because antibodies measured in the anti-PEG competition ELISA had higher affinity toward pegloticase than to free PEG polymers [43]. We therefore propose two possible mechanisms by which anti-PEG antibodies can bind to the PEG portion of a therapeutic. The first being that anti-PEG antibodies are directed against the PEG protein conjugation site and not to the PEG chain solely, as also suggested in other studies [10]. Unfortunately no data were published regarding the assay design, but binding in the anti-PEG ELISA could be explained by binding to PEG and the linker between the PEG and the well plate. It is possible that PEG itself is indeed not immunogenic but instead behaves as a hapten, meaning that it can become immunogenic when bound to a specific conjugate (see below). The second hypothesis is that anti-PEG antibodies are actually antipegloticase antibodies that cross-react with PEG. Because anti-

PEG antibodies were only present in patients with high antibody titers and only appeared after antipegloticase antibodies were developed, it is possible that antipegloticase antibodies possess cross-reactivity toward PEG with lower avidity than to pegloticase [43]. The ELISA data of pegloticase are often referred to in discussions around anti-PEG antibodies. Owing to the poorly defined ELISA and the fact that the native protein is highly immunogenic, it is warranted to underpin the argument that PEG itself is able to induce an immune response by this example.

2.5. PEGylated IFN therapeutics

IFNs are a family of naturally occurring proteins produced by cells of the immune system. IFN therapeutics are clinically used for the treatment of: viral infections such as hepatitis B virus (HBV) and HCV; the primary treatment for several malignancies, such as melanoma, hairy cell leukemia and non-Hodgkin's lymphoma; and the treatment of autoimmune diseases such as multiple sclerosis [47]. Although these treatments are very effective, the percentage of non-responders is relatively high. The immunogenicity of these therapeutics has therefore been studied extensively [48].

Currently, two PEGylated IFN products have gained marketing authorization: PEGylated IFN alfa-2b (Pegintron®, Schering-Plough, USA) for the treatment of HCV; and PEGylated IFN alfa-2a (Pegasys®, Hoffmann-La Roche, USA) for the treatment of HBV. Both products are considered to have relatively longer circulating times and decreased immunogenicity than their non-PEGylated counterparts [49 ,50]. However, overall effectiveness remains relatively low for both products with response rates ~50% [1,49]. The number of studies reporting immunogenicity data is limited, and little research has been performed to determine the specificity of these antibodies. Most studies were performed using ELISA against either PEG–IFN or IFN [24,51] and only a few studies have investigated the potential existence of anti-PEG antibodies. For instance, Tillmann et al. evaluated the development, frequency and impact of anti-PEG antibodies in patients with HCV before and after treatment with either PEG–IFN-a2a or PEG–IFN-a2b. Anti-PEG antibodies were tested with an ELISA well coated with either pegloticase or 10 kDa PEG, and by competition with free PEG [40]. Anti-PEG antibody prevalence before therapy was 44% in HCV patients, which was significantly higher than the 6.9% in healthy controls [40]. However, the authors concluded that anti-PEG antibodies did not result in impaired response because sustained antiviral response was still achieved in 60% of anti-PEG-positive patients [40]. In 2010, a PEGylated INF-beta-1a (PEG–IFN-b1a, Biogen, USA) was investigated in two clinical Phase I trials for the treatment of relapsing multiple sclerosis. The study showed response rates of ~40%, and none of the subjects developed antibodies or neutralizing antibodies (NABs) against the IFN-b1a portion in the multiple dose group. By contrast, 8% of patients developed anti-PEG antibodies after a single dose [52].

Despite PEGylation, Pegintron® and Pegasys® can still induce antidrug antibodies just like their non-PEGylated counterparts. The clinical implications of this immunogenicity are unknown, and unfortunately only a few studies examined the specificity of these antibodies to be directed against the PEG chain [24,53]. Because these two products are both blockbusters and more PEGylated IFN products will enter clinical trials, it is of great importance to study the potential induction of anti-PEG antibodies and their clinical impact. Besides, no articles were found that studied the interaction of antibodies with the immune system in detail. Indeed, only binding capacity was assessed by determining antibody titers using ELISA and their neutralizing capacity in HCV-replicon IFN assays. However, many studies reported that anti-PEG antibodies

can induce endocytosis by phagocytic cells owing to the activation of the complement system. Because it is hypothesized that non-NABs can further activate the immune system, in vitro and in situ complement activation studies as well as in situ phagocytic uptake studies deserve more attention [16].

3. Mechanisms of immunogenicity

Although PEGylated therapeutics are generally less immunogenic than their non-PEGylated counterparts, many clinically approved PEGylated therapeutics can still induce an immune response in a significant fraction of patients. The exact immunogenicity mechanisms are unknown, and little is known regarding a potential immune response against the PEG portion in PEGylated protein therapeutics. However, extensive research regarding the immunogenicity of PEGylated liposomes has been performed, which is described below.

3.1. Innate Immune response by splenic B-cells

Several groups have elucidated that anti-PEG IgM antibodies, produced by the spleen in response to an administered first dose of PEGylated liposomes, are responsible for the rapid clearance of a second dose administered several days later [16,54,55]. Production of anti-PEG IgM is believed to occur in the spleen. Several studies have shown that splenectomized mice do not produce anti-PEG IgM nor do they clear a second administered dose of PEGylated liposomes [11,13,31,55]. Anti-PEG antibodies are elicited without the stimulation of helper T cells because BALB/cnu/nu (T-cell-deficient) mice are capable of producing anti-PEG IgM [55]. These results provide strong evidence that anti-PEG IgM is secreted by splenic B cells by a mechanism that is not dependent on T cells.

Although the follicle region in the spleen is the main compartment for B cells, several studies have shown that PEGylated liposomes mainly bind B cells in the marginal zone [11]. It is thought that upon stimulation the marginal zone B cells (MZ B cells) rapidly proliferate and differentiate into either antigen-presenting cells or into IgM-secreting plasma cells [11]. Production of anti-PEG IgM behaves in a wave pattern, meaning that after the first injection anti-PEG IgM titers increase at day 3, peak at day 5 and then gradually decrease until undetectable at day 28 [13,16,33,56]. Indeed, Li et al. showed that intravenous administration of PEGylated liposomes in beagles only resulted in the ABC phenomenon when a second dose was administered within 3 weeks. A second dose was not rapidly cleared when the time interval was prolonged to 4 weeks [57].

Because immune memory is not established, antibody production seems to be mediated by the innate immune system. This is one of the evolutionarily older systems that can produce antibodies without the help from T cells in response to pathogen-specific antigens consisting of repeating structures, such as lipopolysaccharides on the cell walls of Gram-negative bacteria [58]. The innate immune response is thought to be due to two types of thymus-independent (TI) B cells, depending on co-stimulating factors and the ability to cross-link [59]. A type 1 response occurs when B cells bind to an antigen and receive secondary activation by Toll-like receptors, and a type 2 response occurs when enough B cells can simultaneously cross-link antigens [11,59,60]. Owing to the multireactivity properties of B cells and their strong response to membrane-associated antigens, B cells probably recognize the PEG conjugate in a type 2 manner owing to its composition of multiple repeating structures [61].

3.2. Antibody classification and antigenic determinant

Anti-PEG antibodies have been found to be mainly IgM, especially in the studies identifying antibodies responsible for the rapid clearance of PEGylated liposomes [32,55,61,62]. However, most studies make use of an ELISA format in which lipids such as DSPE–PEG are being used as the antigen. The exact specificity of anti-PEG antibodies is still unknown; but, as mentioned above, several studies have shown that anti-PEG antibodies produced in response to a certain PEG – therapeutic can also bind other PEGylated therapeutics in vitro and in vivo [43,62,63]. In addition, Armstrong reported that the antigenic determinant of anti-PEG antibodies found in 25% of healthy volunteers was directed toward the PEG chain. Agglutination in the red cell assay was completely inhibited by PEG polymers sized from 300 to 20,000 Da, polypropylene glycol 2000 Da and tri- and tetra-(ethylene glycol)dimethyl ether and penta(ethylene glycol) [64]. From these results they concluded that the minimum epitope of recognition by anti-PEG antibodies is 4–5 repeated oxyethylene units [64].

Although this result might imply that PEG itself is the immunogenic determinant, several studies have shown that a single injection of PEG polymers alone does not induce an anti-PEG immune response [11,27]. This phenomenon is explained by the hypothesis that the production of antibodies only occurs against PEG conjugates in a haptogenic manner; meaning that PEG only elucidates an immune response when conjugated [10,28,65]. The haptogenic properties of PEG fit well with the clinical data and depend on its molecular weight, the immunogenicity of the conjugated protein or nanocarrier, the presence of adjuvants and potentially by the terminal end-group of PEG [27,28,65,66]. Besides, it is thought that MZ B cells possess a stronger response to membrane-associated antigens than to soluble antigens [11,67]. In addition, the conjugate itself does need to be immunogenic to induce a haptogenic immune response. The literature implies that, although PEG could be the antigenic determinant for anti-PEG antibodies based on their cross-reactive properties, anti-PEG antibodies can only be induced when the PEG conjugate behaves as a hapten.

3.3. Anti-PEG antibodies versus dose

The induction of anti-PEG IgM and the subsequent accelerated clearance of PEGylated liposomes seem to have an inverse relationship with the quantity of the first dose. The same relationship is seen for the accumulation of PEGylated nanocarriers in the marginal zone of spleen after a second dose. More PEGylated nanocarriers associate with marginal B cells when a low first dose was administered compared with a high first dose [16]. This observation implies that an optimal amount of TI-2 antigens need to cross-link with B cells to induce an antibody response. It is proposed that, when a high dose is administered as a first dose, the density of TI-2 antigens is too high and this causes splenic MZ B cells to induce immune tolerance or anergy [11]. In addition, it has been shown that subsequent receptor signaling is needed to maintain anergy of B cells [68]. Because higher doses lead to prolonged circulation, it is thought that PEGylated therapeutics are in increased contact with MZ B cells, which again can contribute to immune tolerance or anergy [16].

4. Complement activation

To summarize the above discussion, it is thought that PEGylated therapeutics can be recogniTo summarize the above discussion, it is thought that PEGylated therapeutics can be recognized by splenic B cells, which are activated by a thymus-independent mechanism, as a

result of cross-linking of multiple B cells to either PEG or the PEG–therapeutic conjugation site. As a result, these B cells produce anti-PEG IgM, which has been shown to correlate with the clearance of a second administered dose.

However, IgM antibodies are unable to promote phagocytosis directly because IgM is not an opsonizing antibody as a result of the absence of Fc receptors for IgM on the surface of macrophages [69]. Instead, binding of IgM can trigger opsonization of complement factors that subsequently promote phagocytosis by Kupffer cells bearing complement receptors [69,70]. Several of these complement factors are known to have an important role in HSR toward certain therapeutics. Indeed, clinical studies have linked elevated complement factors to infusion reactions in response to PEGylated proteins and nanocarriers such as PEGylated asparaginase and the liposomal formulation Doxil® [14,71].

4.1. Complement activation in response to PEGylated therapeutics

Indications that complement factors are involved in the ABC phenomenon by IgM antibodies arose when Dams et al. showed that rats that had undergone a transfusion of serum from rats pretreated with PEGylated liposomes were able to clear the dose rapidly when they were treated with PEGylated liposomes for the first time [15]. In addition, the phenomenon could be abolished by pre-heating the serum at 56°C for 30 min before transfusion, the temperature at which complement is deactivated [15,18].

Several studies have indicated that the molecular weight and concentration of PEG is a crucial factor for complement activation. For instance in situ studies by Shimizu et al. showed that PEG30000–BSA induced higher anti-PEG IgM titers and greater complement activation than PEG2000–BSA; and extensive research on masking red blood cells by PEG has shown that cell lysis caused by complement activation was actually enhanced with increased concentrations of PEG [16,72,73].

4.2. Non-antibody mediated complement activation

In contrast to complement activation through the classical pathway, several studies have reported that PEGylated therapeutics can activate the complement system after a first dose [21,29,30]. Until recently, acute allergic reactions were believed to be mainly IgE-mediated as defined by the Gell and Coombs classification of HSR [36]. However, data from the past decade have shown that more than 75% of acute allergic reactions are actually not initiated or mediated by IgE antibodies, and are referred to as pseudoallergic reactions [74]. Although the exact mechanisms are not well understood, there is evidence that most of these HSR are triggered by complement activation and caused by anaphylatoxins [74]. However the role of cross-reactive IgM or IgG antibodies has never fully been investigated to exclude the influence of an antibody-mediated response in these pseudoallergic reactions.

Extensive research by Szebeni et al. has shown that complement activation has a causal relation with the infusion reactions observed in up to 25% of patients treated with Doxil®, which were non-IgE-mediated [29,71,74]. In contrast to the general perception, they have also shown that these reactions can occur after a first administration, which implies that Doxil® can directly activate the complement system by the mannose-binding lectin pathway or the

alternative pathway [17]. Furthermore, vesicles of the same size and composition as Doxil® that did not bear doxorubicin were also able to trigger complement activation in vitro [75]. In addition, it was recently reported that highly concentrated free PEG or polysorbate 80 are able to generate complement activation in serum within minutes [14,76]. It remains however unclear whether complement activation in response to a first dose is able to induce phagocytosis besides the generation of anaphylatoxins, as Chanan-Khan et al. reported that the ABC phenomenon was not present in 92% of patients treated with Doxil® despite having elevated SC5b-9 levels [30]. It seems that phagocytosis only occurs with the presence of antibodies, which in the case of PEGylated nanocarriers containing cytostatic drugs does not occur as a result of its toxicity toward MZ B cells [31,77].

As extensive research on Doxil® implies that PEGylation can directly activate the complement system during a first dose, it is hypothesized that other PEGylated therapeutics can activate complement in a non-antibody-mediated manner. For instance, peginesatide has been withdrawn from the market owing to anaphylaxis, of which some cases resulted in death [21]. Unfortunately no hematologic data have been published, but the clinical symptoms as well as the fact that all cases occurred within 30 min of the start of the first administration suggests non-antibody-mediated complement activation [22].

5. Concluding remarks and recommendations

PEGylation is being applied in many different therapeutic fields because of its promising properties for increasing pharmacokinetics because of increased hydrodynamic size and shielding against immunogenic epitopes by means of steric hindrance against the MPS [1]. For instance, its shielding properties have enabled non-human proteins such as uricase and asparginase to be administered to humans. However, despite the belief that PEGylation can reduce immunogenicity of non-human proteins in human patients, a significant fraction of patients still produce antidrug antibodies. Immunogenicity against PEGylated proteins is often explained by an immune response against the protein component, but thorough studies investigating the specificity of these antibodies are rarely performed. Anti-PEG antibodies induced by PEGylated nanocarriers such as liposomes is a phenomenon becoming more accepted as the perpetrator of the ABC phenomenon. These antibodies are capable of rapidly clearing a subsequent dose injected a few days later. Although it appears that the production of these anti-PEG antibodies does not result in immunological memory, doses administered within 3–4 weeks of the first dose can still be cleared [56].

The FDA recently updated their guidelines to screen for anti-PEG antibodies during clinical trials of PEGylated therapeutics. Although several studies have implied that PEGylated protein therapeutics can induce anti-PEG antibodies responsible for an attenuated response, too few studies have investigated the specificity of these antibodies to conclude if anti-PEG antibodies can influence the pharmacokinetics of PEGylated proteins [16,43].

An important obstacle regarding immunogenicity studies is that no validated anti-PEG assay, including appropriate standards, has yet been developed. Few results have been published regarding the sensitivity and selectivity of these assays [25]. These deficiencies have led to a discussion among scientists about how to interpret anti-PEG antibody data, including potential cross-reactivity with other PEGylated therapeutics as well as polysorbates [64,78]. In addition, different results have been reported on the pre-treatment occurrence of anti-

PEG in humans as well as the amount of anti-PEG produced in response to PEGylated therapeutics [23,43,65]. It is therefore recommended that a fully validated assay is developed by collaboration between different research groups as soon as possible. Because it is believed that anti-PEG antibodies are developed against the PEG chain and its conjugate, the biggest challenge will be to develop a standard that can be used to analyze samples from patients treated with different products. Anti-PEG antibodies developed in patients treated with pegloticase also bound other PEGylated proteins. Although the affinity of these antibodies toward these products was not mentioned, it provides some hope that a commercial mono- or poly-clonal anti-PEG standard can be developed. It is therefore highly recommended that parties developing such an assay show specificity and affinity data toward different kinds of PEGylated products.

It is also recommended to analyze the activation of complement thoroughly in vitro and in vivo. Because it seems that mainly anti-PEG IgM is produced against the PEG–therapeutic conjugation site, another component of the immune system needs to be involved because IgM antibodies cannot induce phagocytosis directly [69]. Until a validated anti-PEG assay is developed, studying complement activation in patients might provide an alternative method to gain insight into the immunogenicity and HSR caused by PEGylated therapeutics.

References

[1] Harris, J. M. & Chess, R. B. Effect of PEGylation on pharmaceuticals. Nat. Rev. Drug Discov. 2, 214–221 (2003).

[2] Jenkins, N. Modifications of therapeutic proteins: challenges and prospects. Cytotechnology 53, 121–125 (2007).

[3] Carter, P. J. Introduction to current and future protein therapeutics: a protein engineering perspective. Exp. Cell Res. 317, 1261–1269 (2011).

[4] Abuchowski, A., van Es, T., Palczuk, N. C. & Davis, F. F. Alteration of immunological properties of bovine serum albumin by covalent attachment of polyethylene glycol. J. Biol. Chem. 252, 3578–3581 (1977).

[5] Abuchowski, A., McCoy, J. R., Palczuk, N. C., van Es, T. & Davis, F. F. Effect of covalent attachment of polyethylene glycol on immunogenicity and circulating life of bovine liver catalase. J. Biol. Chem. 252, 3582–3586 (1977).

[6] Verhoef, J. J. F. & Anchordoquy, T. J. Questioning the use of PEGylation for drug delivery. Drug Deliv. Transl. Res. 3, 499–503 (2013).

[7] Allen, T. M. & Chonn, A. Large unilamellar liposomes with low uptake into the reticuloendothelial system. FEBS Lett. 223, 42–46 (1987).

[8] Garay, R. P., El-Gewely, R., Armstrong, J. K., Garratty, G. & Richette, P. Antibodies against polyethylene glycol in healthy subjects and in patients treated with PEG-conjugated agents. Expert Opin. Drug Deliv. 9, 1319–1323 (2012).

[9] Pisal, D. S., Kosloski, M. P. & Balu-Iyer, S. V. Delivery of therapeutic proteins. J. Pharm. Sci. 99, 2557–2575 (2010).

[10] Ishida, T. & Kiwada, H. Anti-polyethyleneglycol Antibody Response to PEGylated Substances. Biol. Pharm. Bull. 36, 889–891 (2013).

[11] Shimizu, T., Ishida, T. & Kiwada, H. Transport of PEGylated liposomes from the splenic marginal zone to the follicle in the induction phase of the accelerated blood clearance phenomenon. Immunobiology 218, 725–732 (2013).

[12] Schellekens, H. Immunogenicity of therapeutic proteins: Clinical implications and future prospects. Clin. Ther. 24, 1720–1740 (2002).

[13] Koide, H. et al. T cell-independent B cell response is responsible for ABC phenomenon induced by repeated injection of PEGylated liposomes. Int. J. Pharm. 392, 218–223 (2010).

[14] Hamad, I., Hunter, A. C., Szebeni, J. & Moghimi, S. M. Poly(ethylene glycol)s generate complement activation products in human serum through increased alternative pathway turnover and a MASP-2-dependent process. Mol. Immunol. 46, 225–232 (2008).

[15] Dams, E. T. et al. Accelerated blood clearance and altered biodistribution of repeated injections of sterically stabilized liposomes. J. Pharmacol. Exp. Ther. 292, 1071–1079 (2000).

[16] Shimizu, T. et al. Intravenous administration of polyethylene glycol-coated (PEGylated) proteins and PEGylated adenovirus elicits an anti-PEG immunoglobulin M response. Biol. Pharm. Bull. 35, 1336–1342 (2012).

[17] Szebeni, J., Muggia, F., Gabizon, A. & Barenholz, Y. Activation of complement by therapeutic liposomes and other lipid excipient-based therapeutic products: prediction and prevention. Adv. Drug Deliv. Rev. 63, 1020–1030 (2011).

[18] Ishida, T., Kashima, S. & Kiwada, H. The contribution of phagocytic activity of liver macrophages to the accelerated blood clearance (ABC) phenomenon of PEGylated liposomes in rats. J. Controlled Release 126, 162–165 (2008).

[19] European Medicines Agency. PegIntron : EPAR - Summary for the public. (2012). at <http://www.ema.europa.eu/docs/en_GB/document_library/EPAR_-_Product_Information/human/000280/WC500039388.pdf>

[20] Armstrong, J. K. et al. Antibody against poly(ethylene glycol) adversely affects PEG-asparaginase therapy in acute lymphoblastic leukemia patients. Cancer 110, 103–111 (2007).

[21] Eckardt, K.-U. Anaemia: The safety and efficacy of peginesatide in patients with CKD. Nat. Rev. Nephrol. 9, 192–193 (2013).

[22] Mikhail, A. Profile of peginesatide and its potential for the treatment of anemia in adults with chronic kidney disease who are on dialysis. J. Blood Med. 3, 25–31 (2012).

[23] Sundy, J. S. et al. Efficacy and tolerability of pegloticase for the treatment of chronic gout in patients refractory to conventional treatment: two randomized controlled trials. JAMA J. Am. Med. Assoc. 306, 711–720 (2011).

[24] Scagnolari, C. et al. Development and specificities of anti-interferon neutralizing antibodies in patients with chronic hepatitis C treated with pegylated interferon-α. Clin. Microbiol. Infect. 18, 1033–1039 (2012).

[25] Schellekens, H., Hennink, W. E. & Brinks, V. The immunogenicity of polyethylene glycol: facts and fiction. Pharm. Res. 30, 1729–1734 (2013).

[26] Liu, Y. et al. A double antigen bridging immunogenicity ELISA for the detection of antibodies to polyethylene glycol polymers. J. Pharmacol. Toxicol. Methods 64, 238–245 (2011).

[27] Richter, A. W. & Akerblom, E. Antibodies against polyethylene glycol produced in animals by immunization with monomethoxy polyethyleneglycol modified proteins. Int. Arch. Allergy Appl. Immunol. 70, 124–131 (1983).

[28] Richter, A. W. & Akerblom, E. Polyethylene glycol reactive antibodies in man: titer distribution in allergic patients treated with monomethoxy polyethylene glycol modified allergens or placebo, and in healthy blood donors. Int. Arch. Allergy Appl. Immunol. 74, 36–39 (1984).

[29] Szebeni, J. et al. Liposome-induced complement activation and related cardiopulmonary distress in pigs: factors promoting reactogenicity of Doxil and AmBisome. Nanomedicine Nanotechnol. Biol. Med. 8, 176–184 (2012).

[30] Chanan-Khan, A. et al. Complement activation following first exposure to pegylated liposomal doxorubicin (Doxil®): possible role in hypersensitivity reactions. Ann. Oncol. 14, 1430–1437 (2003).

[31] Wang, X., Ishida, T. & Kiwada, H. Anti-PEG IgM elicited by injection of liposomes is involved in the enhanced blood clearance of a subsequent dose of PEGylated liposomes. J. Controlled Release 119, 236–244 (2007).

[32] Ishida, T. et al. Injection of PEGylated liposomes in rats elicits PEG-specific IgM, which is responsible for rapid elimination of a second dose of PEGylated liposomes. J. Controlled Release 112, 15–25 (2006).

[33] Nagao, A., Abu Lila, A. S., Ishida, T. & Kiwada, H. Abrogation of the accelerated blood clearance phenomenon by SOXL regimen: Promise for clinical application. Int. J. Pharm. 441, 395–401 (2013).

[34] Macdougall, I. C. et al. Peginesatide for Anemia in Patients with Chronic Kidney Disease Not Receiving Dialysis. N. Engl. J. Med. 368, 320–332 (2013).

[35] Fishbane, S. et al. Peginesatide in patients with anemia undergoing hemodialysis. N. Engl. J. Med. 368, 307–319 (2013).

[36] Gell, P. G. H. & Coombs, R. R. A. Clinical Aspects of Immunology. xxvi + 883 pp. (1963).

[37] Steiner, M. et al. Distinct fluctuations of ammonia levels during asparaginase therapy for childhood acute l eukemia. Pediatr. Blood Cancer 49, 640–642 (2007).

[38] Pieters, R. et al. L-asparaginase treatment in acute lymphoblastic leukemia: a focus on Erwinia asparaginase. Cancer 117, 238–249 (2011).

[39] Narta, U. K., Kanwar, S. S. & Azmi, W. Pharmacological and clinical evaluation of l-asparaginase in the treatment of leukemia. Crit. Rev. Oncol. Hematol. 61, 208–221 (2007).

[40] Garratty, G. Progress in modulating the RBC membrane to produce transfusable universal/stealth donor RBCs. Transfus. Med. Rev. 18, 245–256 (2004).

[41] Tillmann, H. et al. 307 High prevalence of pre-existing antibodies against polyethylene glycol (PEG in hepatitis C (HCV) patients which is not associated with impaired response to PEG-interferon. J. Hepatol. 52, S129–S129 (2010).

[42] Eggebeen, A. T. Gout: an update. Am. Fam. Physician 76, 801–808 (2007).

[43] Bomalaski, J. S., Holtsberg, F. W., Ensor, C. M. & Clark, M. A. Uricase formulated with polyethylene glycol (uricase-PEG 20): biochemical rationale and preclinical studies. J. Rheumatol. 29, 1942–1949 (2002).

[44] Food and Drug Administration. KRYSTEXXATM (pegloticase) for intravenous infusion BLA No. 125293. (2009). at <http://www.fda.gov/downloads/AdvisoryCommittees/CommitteesMeetingMaterials/Drugs/ArthritisAdvisoryCommittee/UCM165814.pdf>

[45] Ganson, N. J., Kelly, S. J., Scarlett, E., Sundy, J. S. & Hershfield, M. S. Control of hyperuricemia in subjects with refractory gout, and induction of antibody against poly(ethylene glycol) (PEG), in a phase I trial of subcutaneous PEGylated urate oxidase. Arthritis Res. Ther. 8, R12 (2006).

[46] Lipsky, P. E. et al. Pegloticase immunogenicity: the relationship between efficacy and antibody development in patients treated for refractory chronic gout. Arthritis Res. Ther. 16, R60 (2014).

[47] Chen, C.-J. et al. MyD88-dependent IL-1 receptor signaling is essential for gouty inflammation stimulated by monosodium urate crystals. J. Clin. Invest. 116, 2262–2271 (2006).

[48] Meyer, O. Interferons and autoimmune disorders. Joint Bone Spine 76, 464–473 (2009).

[49] Maher, S. G., Romero-Weaver, A. L., Scarzello, A. J. & Gamero, A. M. Interferon: cellular executioner or white knight? Curr. Med. Chem. 14, 1279–1289 (2007).

[50] Tovey, M. G. & Lallemand, C. Safety, Tolerability, and Immunogenicity of Interferons. Pharmaceuticals 3, 1162–1186 (2010).

[51] Manns, M. P. et al. Peginterferon alfa-2b plus ribavirin compared with interferon alfa-2b plus ribavirin for initial treatment of chronic hepatitis C: a randomised trial. The Lancet 358, 958–965 (2001).

[52] Bailon, P. et al. Rational Design of a Potent, Long-Lasting Form of Interferon: A 40 kDa Branched Polyethylene Glycol-Conjugated Interferon α-2a for the Treatment of Hepatitis C. Bioconjug. Chem. 12, 195–202 (2001).

[53] Santantonio, T., Milella, M., Antonelli, G. & Scagnolari, C. Neutralizing antibodies to interferon alpha in a chronic hepatitis C patient non-responder to pegylated interferon. J. Hepatol. 45, 759–761 (2006).

[54] Hu, X. et al. A Novel PEGylated Interferon Beta-1a for Multiple Sclerosis: Safety, Pharmacology, and Biology. J. Clin. Pharmacol. 52, 798–808 (2012).

[55] Van der Eijk, A. A., Vrolijk, J. M. & Haagmans, B. L. Antibodies neutralizing peginterferon alfa during retreatment of hepatitis C. N. Engl. J. Med. 354, 1323–1324 (2006).

[56] Antonelli, G. Biological basis for a proper clinical application of alpha interferons. New Microbiol. 31, 305–318 (2008).

[57] Abu Lila, A. S., Kiwada, H. & Ishida, T. The accelerated blood clearance (ABC) phenomenon: Clinical challenge and approaches to manage. J. Controlled Release doi:10.1016/j.jconrel.2013.07.026

[58] Ishida, T., Wang, X., Shimizu, T., Nawata, K. & Kiwada, H. PEGylated liposomes elicit an anti-PEG IgM response in a T cell-independent manner. J. Controlled Release 122, 349–355 (2007).

[59] Ishihara, T. et al. Accelerated Blood Clearance Phenomenon Upon Repeated Injection of PEG-modified PLA-nanoparticles. Pharm. Res. 26, 2270–2279 (2009).

[60] Li, C. et al. Prolongation of time interval between doses could eliminate accelerated blood clearance phenomenon induced by pegylated liposomal topotecan. Int. J. Pharm. 443, 17–25 (2013).

[61] Cerutti, A., Cols, M. & Puga, I. Marginal zone B cells: virtues of innate-like antibody-producing lymphocytes. Nat. Rev. Immunol. 13, 118–132 (2013).

[62] Vinuesa, C. G. & Chang, P.-P. Innate B cell helpers reveal novel types of antibody responses. Nat. Immunol. 14, 119–126 (2013).

[63] Porto, A. P. N. A. et al. Assessment of splenic function. Eur. J. Clin. Microbiol. Infect. Dis. 29, 1465–1473 (2010).

[64] Ichihara, M. et al. Anti-PEG IgM Response against PEGylated Liposomes in Mice and Rats. Pharmaceutics 3, 1–11 (2010).

[65] Cheng, T. L., Wu, P. Y., Wu, M. F., Chern, J. W. & Roffler, S. R. Accelerated clearance of polyethylene glycol-modified proteins by anti-polyethylene glycol IgM. Bioconjug. Chem. 10, 520–528 (1999).

[66] Sherman, M. R., Williams, L. D., Sobczyk, M. A., Michaels, S. J. & Saifer, M. G. P. Role of the Methoxy Group in Immune Responses to mPEG-Protein Conjugates. Bioconjug. Chem. 23, 485–499 (2012).

[67] Armstrong, J. K. in PEGylated Protein Drugs Basic Sci. Clin. Appl. (ed. Veronese, F. M.) 147–168 (Birkhäuser Basel, 2009). at <http://link.springer.com/chapter/10.1007/978-3-7643-8679-5_9>

[68] Garay, R. P. & Labaune, J.-P. Immunogenicity of Polyethylene Glycol (PEG). 2011 2, 1004–107

[69] Saifer, M. G. P., Williams, L. D., Sobczyk, M. A., Michaels, S. J. & Sherman, M. R. Selectivity of binding of PEGs and PEG-like oligomers to anti-PEG antibodies induced by methoxyPEG-proteins. Mol. Immunol. 57, 236–246 (2014).

[70] Carrasco, Y. R. & Batista, F. D. B cell recognition of membrane-bound antigen: an exquisite way of sensing ligands. Curr. Opin. Immunol. 18, 286–291 (2006).

[71] Gauld, S. B., Benschop, R. J., Merrell, K. T. & Cambier, J. C. Maintenance of B cell anergy requires constant antigen receptor occupancy and signaling. Nat. Immunol. 6, 1160–1167 (2005).

[72] Janeway, C. A., Travers, P., Walport, M. & et al. The Immune System in Health and Disease. (Garland Science, 2001).

[73] Helmy, K. Y. et al. CRIg: A Macrophage Complement Receptor Required for Phagocytosis of Circulating Pathogens. Cell 124, 915–927 (2006).

[74] Muller-Eberhard, H. J. Molecular Organization and Function of the Complement System. Annu. Rev. Biochem. 57, 321–347 (1988).

[75] Szebeni, J. et al. Prevention of infusion reactions to PEGylated liposomal doxorubicin via tachyphylaxis induction by placebo vesicles: A porcine model. J. Controlled Release 160, 382–387 (2012).

[76] Sicherer, S. H. & Leung, D. Y. M. Advances in allergic skin disease, anaphylaxis, and hypersensitivity reactions to foods, drugs, and insects in 2012. J. Allergy Clin. Immunol. 131, 55–66 (2013).

[77] Van den Hoven, J. M. et al. Complement activation by PEGylated liposomes containing prednisolone. Eur. J. Pharm. Sci. 49, 265–271 (2013).

[78] Bradley, A. J., Test, S. T., Murad, K. L., Mitsuyoshi, J. & Scott, M. D. Interactions of IgM ABO antibodies and complement with methoxy-PEG-modified human RBCs. Transfusion (Paris) 41, 1225–1233 (2001).

[79] Chapanian, R. et al. Influence of polymer architecture on antigens camouflage, CD47 protection and complement mediated lysis of surface grafted red blood cells. Biomaterials 33, 7871–7883 (2012).

[80] Szebeni, J. Complement activation-related pseudoallergy: a new class of drug-induced acute immune toxicity. Toxicology 216, 106–121 (2005).

[81] Moghimi, S. M. et al. Complement activation cascade triggered by PEG–PL engineered nanomedicines and carbon nanotubes: The challenges ahead. J. Controlled Release 146, 175–181 (2010).

[82] Qiu, S. et al. Complement activation associated with polysorbate 80 in beagle dogs. Int. Immunopharmacol. 15, 144–149 (2013).

[83] Ishida, T., Atobe, K., Wang, X. & Kiwada, H. Accelerated blood clearance of PEGylated liposomes upon repeated injections: Effect of doxorubicin-encapsulation and high-dose first injection. J. Controlled Release 115, 251–258 (2006).

[84] Veronese, F. M. PEGylated Protein Drugs: Basic Science and Clinical Applications. (Springer, 2009).

Chapter | 6

Specificity analysis of anti-PEG-asparaginase antibodies in patients treated with PEG-asparaginase

Verhoef JJF, Kloos R, van der Sluijs IM, Pieters R, Schellekens H

Article in preparation

Abstract

The immunogenicity of poly(ethyleneglycol) (PEG) has been heavily debated. Here, sera from patients treated with PEG-asparaginase who were positive for anti-PEG-asparaginase antibodies were investigated. Antibodies were screened for specificity against L-asparaginase, mPEG5k and the succinate linker between L-asparaginase and the conjugated mPEG5k polymer. All patients had antibodies against L-asparaginase, mPEG5k, and the succinate linker. However, anti-asparaginase and anti-linker antibodies could only be detected by a direct ELISA and not in a competition ELISA coated with PEG-asparaginase. This manuscript describes different ELISA formats that were used as well as its challenges. The results in this manuscript reveals the artifacts that occur when coating ELISA plates with PEGylated compounds which can have broader implications on previously reported anti-PEG antibody studies using similar ELISA formats. In addition, we report that the conjugated succinimidyl succinate mPEG5k is highly susceptible to hydrolysis and that these patients developed antibodies against this linker.

1. Introdction

Over the last decade an increasing number of publications have investigated an immunological response towards poly(ethyleneglycol) (PEG) [1]–[4].Generally, PEG is considered biological inert and is applied in pharmaceutical formulations to increase circulation half-lives. This is realized either by increasing the hydrodynamic size to prevent kidney clearance, or by preventing recognition by mononuclear phagocytic cells (MPS) by shielding immunogenic epitopes. These properties have resulted in the clinical approval of more than a dozen PEGylated therapeutics which include both PEGylated antibodies, enzymes, peptides, but also drug delivery systems, such as PEGylated liposomes and micelles [5].

Despite its clinical success, cases of anti-PEG antibodies have been reported. Cases of anti-PEG antibodies have been reported in patients treated with PEGylated ragweed pollen extract were already reported in 1983 by Richter and Akerblom [6]. Since, anti-PEG antibodies were reported mainly in patients treated with either PEGuricase or PEG-asparaginase [7]. As far, no anti-PEG antibodies have been described in patients treated with proteins, native to human; L-asparaginase and uricase are non-human enzymes.

The extent of the immunogenicity of PEG and its clinical consequences remain uncertain by the lack of standardized and well validated antibody assays [7], [8]. Here, sera from patients treated with PEG-asparaginase who were positive for anti-PEG-asparaginase antibodies were investigated. Antibodies were screened for specificity against L-asparaginase, mPEG5k and the succinate linker between L-asparaginase and the conjugated mPEG5k polymer.

2. Materials and Methods

2.1. Patient samples

Patient sera were obtained from the Erasmus University Medical Centre. Patients were selected on their rapid clearance of PEG-asparaginase doses and experienced hypersensitivity-like reactions. Serum from healthy donors was obtained from the Mini Donor Dienst at the University Medical Center Utrecht and collected in Serum Vacutainers (Becton, Dickinson and Company, Franklin Lakes, United States).

2.2. Anti-PEG-asparaginase ELISAs

Microlon 600 96-well plates, high binding (Greiner Bio-One, Alphen aan den Rijn, the Netherlands) were coated with 100 ul PBS containing 2.13 U/mL PEG-asparaginase (Oncaspar; Sigma-Tau, Gaithersburg, United States) in either Phosphate Buffer pH 7.4 (B-Braun, Meisungen, Germany) or 100 mM sodium carbonate buffer (Sigma-Aldrich, Zwijndrecht, the Netherlands) buffer pH 9.5, 5.6 U/mL L-Asparginase (Medac, Stirling, United Kingdom) in PBS pH 7.4 or 1 µg/mL Varicella Zoster Virus (VZV) antigen (Bio-Connect, Huissen, the Netherlands). Plates were incubated overnight at 4°C and subsequently washed 3x with 200 µl washing buffer containing 0.05% CHAPS (Sigma-Aldrich, Zwijndrecht, the Netherlands) in PBS. Plates were blocked with 2% Elk (Campina, Amersfoort, the Netherlands) for 2 hours and washed 5x. Serum samples were diluted in blocking buffer and incubated for 3 hours.

In competition assays samples were prior to incubation 1:1 diluted with competitor. Wells were 5x washed, incubated with 1:1000 anti-IgG-HRP Ab98605 (Abcam, Cambride, United Kingdom) United States) or anti-IgM-HRP Ab97205 (Abcam, Cambridge, United Kingdom) for 1 hour, washed 5x and detected by 100 ul TMB (Thermo Scientific, Rockford, United States). Reaction was stopped with 2M Sulfuric Acid (Sigma-Aldrich, Zwijndrecht, the Netherlands) when sufficient color developed.

2.3. Size-exclusion chromatography

PEG-asparaginase and L-asparaginase were diluted to 1.000 U/mL in 100 mM carbonate buffer pH 9.5. Size-exclusion chromatography was performed on a Waters 2695 Separations Module connected to a Waters 2414 Refractive Index Detector and a Waters 2487 Dual λ Absorbance Detector (Waters Corporation, Milford, MA) to which a PL Aquagel-OH mixed 8 µm column (Agilent Technologies, Santa Clara, United States) was attached. At specific time points 100 µl samples were injected over 30 minutes at 1 mL/minute flow rate of 100 mM carbonate buffer. Refractive Index and UV-absorbance at 280 nm were recorded.

2.4. BSA conjugation with mPEG5k and succinate

Bovine Serum Albumin (BSA) was conjugated with succinimidyl-succinate-mPEG5k and succinimidyl carbonate-mPEG5k (Creative PEGWorks, Chapel Hill, Unites States) according to Holtsberg et al. [9]. Conjugation was performed at 1:20 mol ratio in PBS under agitation for 3 hours. Solutions were dialyzed extensively in PBS to remove any unreacted PEG. PEGylation efficiency was determined by the number of unreacted amine groups in BSA using 5% w/v 2,4,6-trinitrobenzene sulfonic acid (TNBSA) (Thermo Scientific, Rockford, United States) and protein amount using the Pierce Protein BCA Assay (Thermo Scientific, Rockford, United States). PEGylation was also investigated by SDS-PAGE and Coomassie-Blue staining. Succinate BSA conjugate were prepared at 1:10 mol ratio in carbonate buffer at pH 8.5 by adding Succinic Anhydride (Sigma-Aldrich, Zwijndrecht, the Netherlands) over a 10 minute period to BSA in PBS. The pH was adjusted to 8.5, reacted for 2 hours at room temperature and subsequently dialyzed extensively. Coupling was determined using the TNBSA and Pierce BSA method.

3. Results

3.1. PEG hydrolysis from PEG-asparaginase

PEG-asparaginase consists out of L-Asparaginase E. Coli to which multiple 5 kDa linear PEG polymers are conjugated by a succinimidyl succinate linker that randomly reacts with amines on L-asparaginase. The succinate-succinimidyl linker is prone to hydrolysis [10]. Size-exclusion analysis revealed that PEG is rapidly hydrolyzed from L-asparaginase when incubated in sodium bicarbonate pH 9.0 (Figure 1A). Upon 15 hours incubation, 2.5x more free PEG is present in PEG-asparaginase pH 9.5 solution compared to pH 7.4 solution (Fig. 1B). Unfortunately, the amount of free mPEG5k at time-zero was not possible to be calculated due to the low sensitivity of our SEC analysis. However, these results indicate that PEG can hydrolyze under physiological conditions or when incubated in carbonate buffer for ELISA coating.

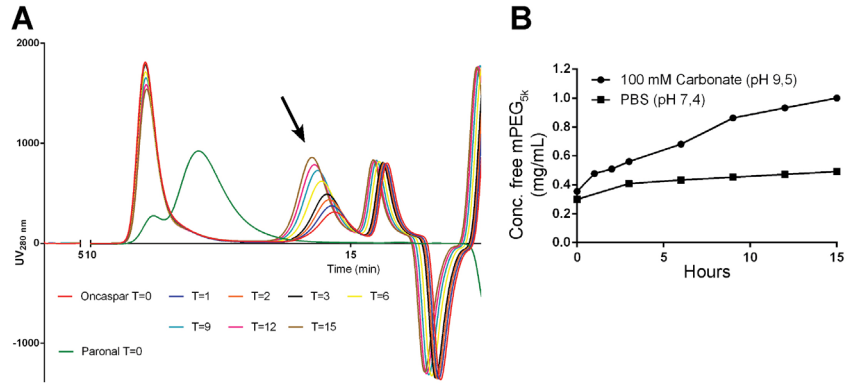

Figure 1. Size-exclusion chromatograms of PEG-Asparaginase and L-asparaginase upon incubation in 100 mM sodium carbonate buffer pH 9.5 for different time periods. Peak represent free mPEG5k (A). The concentration of free mPEG5k in solution in different buffers after different incubation times (B)

3.2. Anti-asparaginase antibodies

Diluted patient sera (2.000x) were analyzed for antibodies against PEG-asparaginase (Figure 2A,B; respectively anti-IgG, –IgM antibodies). Sera from donors 1 and 2 contained most antibodies against PEG-asparaginase. Subsequent analyses revealed that all donors were positive for anti-PEG-asparaginase antibodies when diluted at 1.000x dilution compared to negative control sera (not shown; titers were not determined due to limited amount of sera).

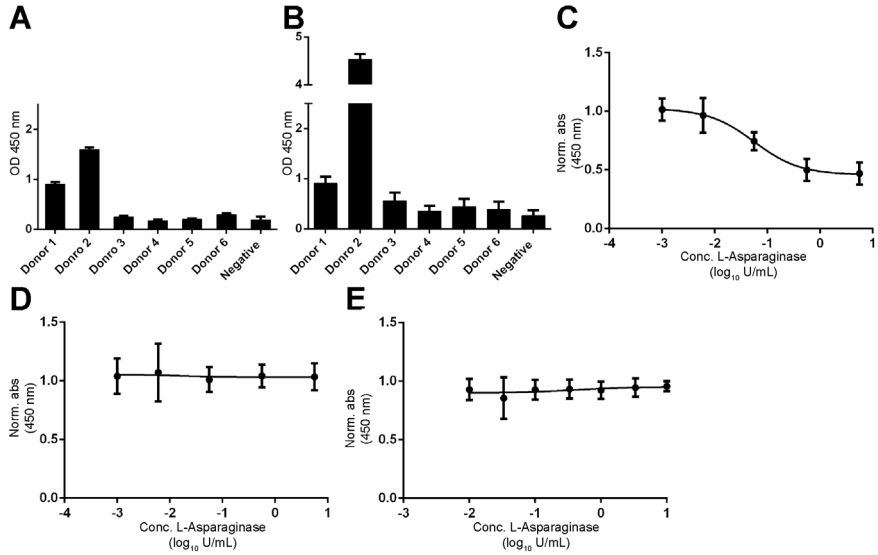

Figure 2. Anti-PEG-asparaginase antibodies in sera (2.000x dilution), respectively IgG and IgM (A,B). Anti-L-asparaginase antibodies were detected in a direct ELISA coated with L-asparaginase (C) and by competition by L-asparaginase on a PEG-asparaginase coated plate in either PBS (D) or carbonate buffer (E).

Specificity towards L-asparaginase was determined by a direct anti-L-asparaginase ELISA or by competition on a PEG-asparaginase coated plate. All patient sera contained anti-L-asparaginase antibodies detected on a L-asparaginase coated plate, IC50 value of 0.057 ± 0.008 IU/mL (Figure 2C). However, competition with L-asparaginase on a PEG-asparaginase

coated plate did not reduce binding in either a plate coated in PBS (Figure 2D) or in carbonate buffer to induce hydrolysis of PEG (Figure 2E).

3.3. Anti-PEG antibodies

Specificity of anti-PEG-asparaginase towards PEG was determined by a anti-PEG-asparaginase competition ELISA with either mPEG5k or PEG-BSA conjugates. PEG competition was first studied in a non-relevant ELISA to exclude dissociation of antibodies other than by affinity and specificity. An anti-varicella zoster virus (VZV) ELISA was developed and serum from healthy donors was incubated with buffer or PEG (Figure 3A). No decrease in anti-VZV binding occurred by the co-incubation with mPEG5k up to 2,000 µM confirming that PEG does not non-specifically dissociate antibodies. In patient sera, PEG reduced binding of anti-PEG-asparaginase coated plate, indicating antibodies binding to PEG (Figure 3B), IC50 83.9 µM. However, competition was also observed in 500x diluted serum from a healthy donor, (Figure 3C) (patient sera were diluted 5.00–25.000x). Anti-PEG-asparaginase binding was also inhibited by competition with both BSA-suc-PEG and BSA-car-PEG (Figure 3D,E), respectively IC50 values of 1.1 and 0.7 µM. Patients were also positive for antibodies against conjugated mPEG5k to BSA in a direct ELISA format (data not shown).

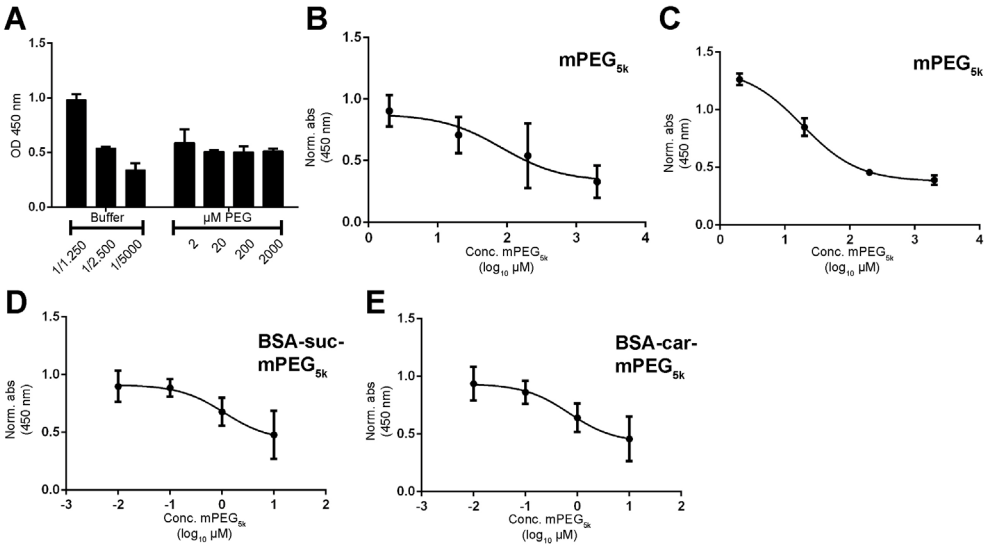

Figure 3. Serum dilutions of a healthy donor were screened for anti-varicella zoster virus antibodies as well as binding in the presence of different concentrations of mPEG5k (A). Specificity against mPEG5k was studied by an anti-PEGasparaginase ELISA in competition with mPEG5k in patient sera (B) and in a healthy donor (C). Anti-PEG antibodies were also studied in ELISAs coated with mPEG5k-BSA with either a succinimidul succinate (D) or succinimidyl carbonate linker (E).

3.4. Anti-linker antibodies

Specificity of anti-PEG-asparaginase antibodies towards the hydrolyzed linker, resulting in a succinate group on L-asparaginase, was determined by an anti-PEG-asparaginase competition ELISA and succinate BSA conjugate as well as by an anti-succinate BSA conjugate ELISA. Whereas competition of succinate BSA conjugate did not diminish binding to anti-PEG-asparaginase (Fig 4A), antibodies positive for the succinate linker were found in patients when the plate was coated with BSA-linker (Fig 4B).

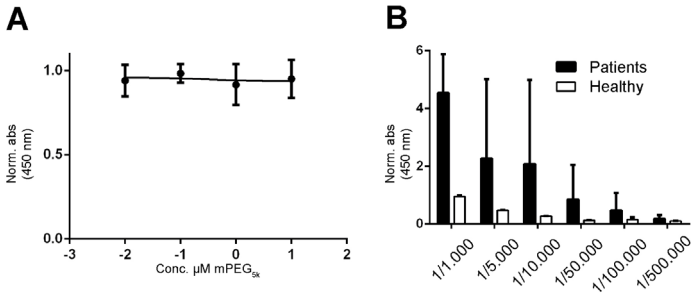

Figure 4. Anti-succinate linker antibodies were investigated on an ELISA plate coated with PEG-asparaginase in competition with BSA conjugated with succinic anhydride (A) and by a plate coated with this competitior to which dilutions of patient sera and healthy donor were incubated (B).

4. Discussion

The potential immunogenicity of PEG has gotten an increasing amount of attention. Despite its successful application in many different therapeutics, PEG is believed to be able to induce antibodies. As such, the use of PEG on novel formulations is questioned by both industry and regulatory authorities. We here performed our own anti-PEG investigation in sera from patients with acute lymphatic leukemia (ALL). These patients were all considered non-responders of which several experienced hypersensitivity-like reactions as well.

When screening sera for anti-PEG-asparaginase antibodies in a direct ELISA, we found that all patients had increased levels of binding antibodies to PEG-asparaginase compared to negative control sera of patients obtained before treatment. Also, all patients were positive for anti-asparaginase antibodies, but could only be identified in a direct ELISA against L-asparaginase. Surprisingly, anti-PEG-asparaginase antibodies did not compete with L-asparaginase when co-incubated. This indicates that antibodies bound in the anti-PEG-asparaginase ELISA are towards anything but the protein part. We hypothesize that 1) steric-hindrance of the PEG corona prevents antibodies to penetrate towards the protein surface or that 2) PEGylation is able to block all immunogenic epitopes on L-asparaginase completely. However, when PEGasparaginase was coated overnight in a carbonate buffer pH 9.5 to induce hydrolysis of PEG, also no competition by L-asparaginase was observed. Another hypothesize is that the conformational structure of PEGasparginase has been changed due to PEGylation or coating, shielding the immunogenic epitopes of L-asparaginase.

Anti-PEG-asparaginase antibodies were found to be directed against the mPEG5k polymer, identified by competition with either mPEG5k polymers or mPEG5k-conjugates. However, binding was not completely competed for in an excess of either mPEG5k polymer or BSA-conjugate. Affinity of these antibodies towards the succinate-linker was subsequently investigated as the ester group in mPEG5k-succiniate-L-asparaginase is prone to hydrolysis, exposing a succinate group on the enzyme. For the first time, we here report that anti-succinate antibodies can be induced upon administration of PEG-asparaginase. All patients had anti-succinate antibodies identified in a direct ELISA against succinate BSA conjugate. However, in a PEG-asparaginase ELISA binding could not be competed for. We hypothesize that when we coat the ELISA plate in PBS, little hydrolysis takes place and as such no or very little succinate epitopes are exposed.

Further investigation on the specificity of anti-PEG-asparaginase antibodies revealed that these antibodies bind PEG polymers. However, crucial experiments are missing to fully identify anti-PEG antibodies. When serum from a healthy donor was co-incubated with mPEG5k on a PEG-asparaginase coated plate, binding was also diminished. This would indicate that either 1) this donor was positive for anti-PEG antibodies or that 2) PEG-asparaginase coated surfaces have a high a matrix-effect, non-specifically absorption of proteins to the well. Although patient sera were incubated at much higher dilutions, understanding why PEG is able to inhibit binding in these samples is essential. When biomaterials or proteins are PEGylated, these PEG polymers attract serum proteins to form a protein-corona, including opsonins such as complement factors [11]. It is not clear if these antibodies bind directly to PEG polymers or actually to proteins, adsorbed into the PEG corona. Future experiments with purified IgG/IgM from patient sera should answer this hypothesis.

To this point, crucial experiments are missing to proof if PEG polymers can induce specific antibodies towards its C-C-O repertoire (anti-PEG). However, our data and other research papers make clear that PEGylation can induce antibodies directed against the polymer-corona with subsequent unbeneficial clinical outcomes. The specificity of these antibodies remains unknown and warrants further investigation before the existence of anti-PEG can be proven.

References

[1] T. J. Povsic et al., "Pre-existing anti-PEG antibodies are associated with severe immediate allergic reactions to pegnivacogin, a PEGylated aptamer," J. Allergy Clin. Immunol., Jul. 2016.

[2] H. Myler et al., "Anti-PEG antibody bioanalysis: a clinical case study with PEG-IFN-λ-1a and PEG-IFN-α2a in naive patients," Bioanalysis, vol. 7, no. 9, pp. 1093–1106, 2015.

[3] M. S. Hershfield, N. J. Ganson, S. J. Kelly, E. L. Scarlett, D. A. Jaggers, and J. S. Sundy, "Induced and pre-existing anti-polyethylene glycol antibody in a trial of every 3-week dosing of pegloticase for refractory gout, including in organ transplant recipients," Arthritis Res. Ther., vol. 16, no. 2, p. R63, Mar. 2014.

[4] J. K. Armstrong et al., "Antibody against poly(ethylene glycol) adversely affects PEG-asparaginase therapy in acute lymphoblastic leukemia patients," Cancer, vol. 110, no. 1, pp. 103–111, Jul. 2007.

[5] Y. Min, J. M. Caster, M. J. Eblan, and A. Z. Wang, "Clinical Translation of Nanomedicine," Chem. Rev., vol. 115, no. 19, pp. 11147–11190, Oct. 2015.

[6] A. W. Richter and E. Akerblom, "Antibodies against polyethylene glycol produced in animals by immunization with monomethoxy polyethylene glycol modified proteins," Int. Arch. Allergy Appl. Immunol., vol. 70, no. 2, pp. 124–131, 1983.

[7] J. J. F. Verhoef, J. F. Carpenter, T. J. Anchordoquy, and H. Schellekens, "Potential induction of anti-PEG antibodies and complement activation toward PEGylated therapeutics," Drug Discov. Today, vol. 19, no. 12, pp. 1945–1952, Dec. 2014.

[8] H. Schellekens, W. E. Hennink, and V. Brinks, "The immunogenicity of polyethylene glycol: facts and fiction," Pharm. Res., vol. 30, no. 7, pp. 1729–1734, Jul. 2013.

[9] F. W. Holtsberg, C. M. Ensor, M. R. Steiner, J. S. Bomalaski, and M. A. Clark, "Poly(ethylene glycol) (PEG) conjugated arginine deiminase: effects of PEG formulations on its pharmacological p roperties," J. Controlled Release, vol. 80, no. 1–3, pp. 259–271, Apr. 2002.

[10] G. T. Hermanson, Bioconjugate Techniques. Academic Press, 2013.

[11] I. Hamad, A. C. Hunter, J. Szebeni, and S. M. Moghimi, "Poly(ethylene glycol)s generate complement activation products in human serum through increased alternative pathway turnover and a MASP-2-dependent process," Mol. Immunol., vol. 46, no. 2, pp. 225–232, Dec. 2008.

Chapter | 7

Polyphosphate nanoparticles on the platelet surface trigger contact system activation

Verhoef JJF*, Barendrecht AD*, Nickel KF*,
Dijkxhoorn K, Kenne E, Labberton L, et al.

*Shared first authorship

Article in print:
Blood.
doi: 10.1182/blood-2016-08-734988

Abstract

Polyphosphate is an inorganic polymer that can potentiate several interactions in the blood coagulation system. Blood platelets contain polyphosphate, and the secretion of platelet-derived polyphosphate has been associated with increased thrombus formation and activation of coagulation factor XII. However, the small polymer size of secreted platelet polyphosphate limits its capacity to activate factor XII in vitro. Thus, the mechanism by which platelet polyphosphate contributes to thrombus formation remains unclear. Using live-cell imaging, confocal and electron microscopy, we show that activated platelets expose polyphosphate on their cell surface. The apparent polymer size of membrane-associated polyphosphate largely exceeds that of secreted polyphosphate. Ultracentrifugation fractionation experiments revealed that membrane-associated platelet polyphosphate is condensed into insoluble spherical nanoparticles with divalent metal ions. In contrast to soluble polyphosphate, membrane-associated polyphosphate nanoparticles potently activate factor XII. Our findings identify the presence of membrane-associated polyphosphate in a nanoparticle state on the surface of activated platelets. We propose that these polyphosphate nanoparticles mechanistically link the procoagulant activity of platelets with the activation of coagulation factor XII.

1. Introduction

Following the discovery of polyphosphate in mammalian cells, this inorganic, negatively charged polymer has been shown to be present in a variety of cell types, such as platelets [1], mast cells [2], and tumor cells [3]. Polyphosphate plays a role in a variety of hemostatic and thrombotic mechanisms. It enhances the binding of platelets to von Willebrand factor [4] (VWF), induces clustering of platelet factor 4 into antigenic complexes [5], acts as a cofactor for C1 esterase inhibitor (C1inh) [6], triggers activation of factor XII (FXII) [7], amplifies factor XI (FXI) activation by thrombin [8], accelerates factor V activation [9], inactivates tissue factor pathway inhibitor [10], inhibits fibrinolysis, and alters fibrin clot structure [11]. As a result, polyphosphate has been proposed as a potential druggable target to prevent thrombosis [12,13]. In preclinical in vivo studies using experimental models of thrombosis, selective depletion of (or deficiency in) coagulation FXII was consistently found to confer protection against thrombosis without increasing bleeding [14-17]. Collective evidence from decades of research had previously established that platelet activation is associated with activation of FXII [18-21] More recent studies implicate platelet polyphosphate as an endogenous trigger for FXII activation in thrombus formation in vivo [22]. However, when platelets become activated, only short polyphosphate polymers (60-100 residues) are secreted into the surrounding fluid. These short-chain soluble polyphosphates have a surprisingly low capacity for direct activation of FXII in vitro [23-25]. This observation suggests that we are lacking essential insight into the mechanistic link between platelet polyphosphates and FXII during thrombus formation in vivo.

In addition to polyphosphate (130 mM) [1], intracellular granules contain large amounts of inorganic compounds, such as adenosine triphosphate (400 mM), adenosine diphosphate (600 mM), pyrophosphate (300 mM), and serotonin (65 mM) [26] and are characterized by a low pH of ~5.4 [27]. Moreover, these organelles are rich in calcium (2.2 M) and other divalent metal ions. The steps involved in secretion of the content-dense granules are not fully defined. For polyphosphate, it is thought to be molecularly dissolved and directly released into the extracellular environment after platelet activation [28].

We report here that, in addition to soluble secreted polyphosphate, a previously unidentified second pool of polyphosphate exists in platelets. This species of polyphosphate forms nanoparticles, composed of polyphosphate and divalent metal ions, and remains associated with the platelet surface after degranulation. Platelet polyphosphate nanoparticles constitute a powerful activator of FXII, providing the "missing link" between primary hemostasis and activation of the contact pathway of coagulation.

2. Materials and methods

2.1. Platelet isolation

Platelets were isolated from citrated blood of healthy volunteers under approval of the local Medical Ethical Committee of the University Medical Center Utrecht by centrifugation as previously reported [16,17]. A detailed description of "Materials and methods" with additional information is provided in the supplemental data.

2.2. Production of recombinant exopolyphosphatase and a truncated variant

Exopolyphosphatase (PPX) or its polyphosphate-binding domains (PPX_Δ12) were expressed in *Escherichia coli* and purified as previously published with minor modifications [29] After purification, the PPX and the PPX_Δ12 were dialyzed against phosphate buffer (10 mM Na_2HPO_4, 10 mM NaH_2PO_4 500 mM NaCl, pH 7.4).

2.3. Live-cell imaging under flow

Washed platelet suspensions were supplemented with Alexa488-labeled anti-CD63 to visualize dense granule degranulation and 1.5 μM SYTOX Orange (Molecular Probes/ Life Technologies, Waltham, MA) or 5 μg/mL Alexa488-conjugated PPX_Δ12 to visualize polyphosphate, and subsequently perfused through a laminar-flow chamber [30] over VWF-coated cover glasses at low shear rates (25-50 s-1). In selected experiments, platelets were pre-incubated for 30 minutes at 37°C with 10 μg/mL 4',6-diamidino-2-phenylindole (DAPI; Sigma-Aldrich Chemie, Zwijndrecht, the Netherlands) and centrifuged at 400*g* for 30 minutes in the presence of 10 ng/mL prostacyclin to remove unbound dye. Where indicated, the effect of ethylenediaminetetraacetic acid (EDTA; 50-500mM), 10 μg/mL ribonuclease A (Invitrogen, Bleiswijk, the Netherlands), 10 μg/mL deoxyribonuclease I (Roche, Mannheim, Germany), or 500 μg/mL PPX was investigated. In plasma experiments, platelet adhesion, spreading, and degranulation were studied step-wise in the continuous presence of SYTOX Orange. First, platelet-rich plasma (PRP) was perfused over immobilized fibrinogen at a shear rate of 25 s^{-1} for 10 minutes. Next, unbound platelets were removed by perfusion with platelet-poor plasma for 5 minutes. Finally, adherent platelets were activated by perfusion with PAR4-activating peptide (Bachem, Bubendorf, Switzerland) in platelet-poor plasma for another 10 minutes. Polyphosphate deposition during thrombus formation was investigated by perfusing citrated whole blood over collagen-coated cover glasses at a high shear rate (1600 s^{-1}). Analyses were performed on a Zeiss Z1 microscope with Colibri LEDs and ZEN 2 Blue Edition software. Videos were captured at a magnification of 31000 for 20 to 40 minutes at a frame rate of 2 frames per minute. After perfusion experiments, cover glasses were removed from the flow chambers and studied further by confocal microscopy and scanning electron microscopy. A detailed description is provided in the supplemental data.

2.4. Platelet fractionation by density ultracentrifugation

Washed platelets (2.5×10^6/mL) were resuspended in lysis buffer (25 mM HEPES [*N*-2-hydroxyethylpiperazine-*N*'-2-ethanesulfonic acid), 250 mM sucrose, 12 mM sodium citrate, pH 6.5) with 1 mM sodium orthovanadate and 1:100 protease inhibitor cocktail (p8340; Sigma-Aldrich) and lysed by 3 pulses of mild sonication (5 seconds at 3 mV) on a Soniprep 150 (MSE, London, UK). Suspensions were subsequently centrifuged at 1000*g* for 15 minutes at 4°C; supernatants containing polyphosphate nanoparticles were collected on ice. The pelleted material was resuspended, sonicated, and centrifuged in 2 to 4 additional cycles until no more pellet was observed. Finally, the collected supernatants were combined and centrifuged at 19 000*g* for 20 minutes at 4°C. The pellet containing polyphosphate nanoparticles was diluted in 1.4 mL lysis buffer with 250 mM sucrose and supplemented with 5 μM SYTOX Orange. Where indicated, 250 mM EDTA was added. Samples were loaded on top of a sucrose gradient with 0.7 mL fractions ranging from 0.5 M to 2 M, diluted in lysis buffer without protease inhibitors. The gradient was centrifuged at 1 000 000*g* for 60 minutes

at 4°C using a Beckman SW40 rotor (without brake). Fractions of 350 mL were analyzed for SYTOX Orange fluorescence at 540/570 nm excitation/emission using a Spectramax 340 (Molecular Devices, Sunnyvale, CA) plate reader. The phosphate content in SYTOX Orange–rich fractions was determined by means of acid digestion and subsequent reaction with ammonium molybdate as described by Rouser et al [31].

2.5. Platelet polyphosphate extraction

Human pheresis platelets (~2.4×10^{11} platelets/pheresis unit) were obtained from the blood banks of Karolinska University Hospital and University Medical Center Hamburg and used for polyphosphate isolation within the expiry date (application in human transfusion). Polyphosphate was isolated by 2 different methods: (1) Isolation of soluble polyphosphate from lysed platelets by phenol/chloroform extraction was performed as previously described with minor modifications, described in the supplemental data. (2) Isolation of total polyphosphate from lysed platelets, including membrane-associated polyphosphate. A spin column anion exchanger method was performed as described [3] with some modifications, described in the supplemental data. Polyphosphate concentrations were measured after hydrolysis in 1 M HCl at 95°C for 60 minutes. The orthophosphate released by polyphosphate digestion was estimated using colorimetric phosphate assay kit (Abcam) according to the manufacturer's instructions, and absorbance was measured at 650 nm with a Multiskan GO Microplate Spectrophotometer (Thermo Scientific).

2.6. Polyphosphate electrophoresis

Polyphosphate (1 nmol/lane of platelet-purified polyphosphate; expressed as monophosphate units, or 100 ng/lane of synthetic polyphosphate; indicated in figure legends) was separated by electrophoresis on 10% polyacrylamide Tris-borate-EDTA buffer (TBE)-urea (7 M) gels and stained by DAPI-negative staining as previously described [3]. Alternatively, calcium-preadsorbed synthetic polyphosphate (70-mers; 40 μg/lane) was separated on 15% Urea-TBE gels [32] and stained with toluidine blue [33]. In some experiments, platelet polyphosphate extracts were incubated with alkaline phosphatase (PSP, 10 U/mL) in the presence of 5 mM $MgCl_2$ for 120 minutes at 37°C prior to separation. In other experiments, calcium-preadsorbed synthetic short polyphosphate (4 mg/mL) and PPX (concentration series) were dissolved in HT buffer containing 5 mM $MgCl_2$ and incubated at 37°C for 1 hour.

2.7. Plasma contact system activation with platelet polyphosphate

Venous blood was collected from healthy human volunteers into 3.2% trisodium citrate (9:1 blood-to-citrate ratio). The first 10 mL was discarded. Platelet-free plasma was prepared by 2 consecutive centrifugation steps at 3000*g* for 10 minutes. Plasma from individuals with congenital deficiency in FXII was purchased from George King Biomedical (Overland Park, KS). Either 1.5 μg/mL kaolin or 20 μM platelet-derived polyphosphate (expressed as monophosphate units) was used as a trigger. Optionally, 50 mM EDTA was added. Development of kallikrein-like activity was analyzed with 1 mM substrate S-2302 (sensitive to FXIIa and plasma kallikrein; Chromogenix, Mölndal, Sweden) at an absorbance wavelength of 405 nm in a Bio-Kinetics Reader (BioTek Instruments Inc) at 37°C.

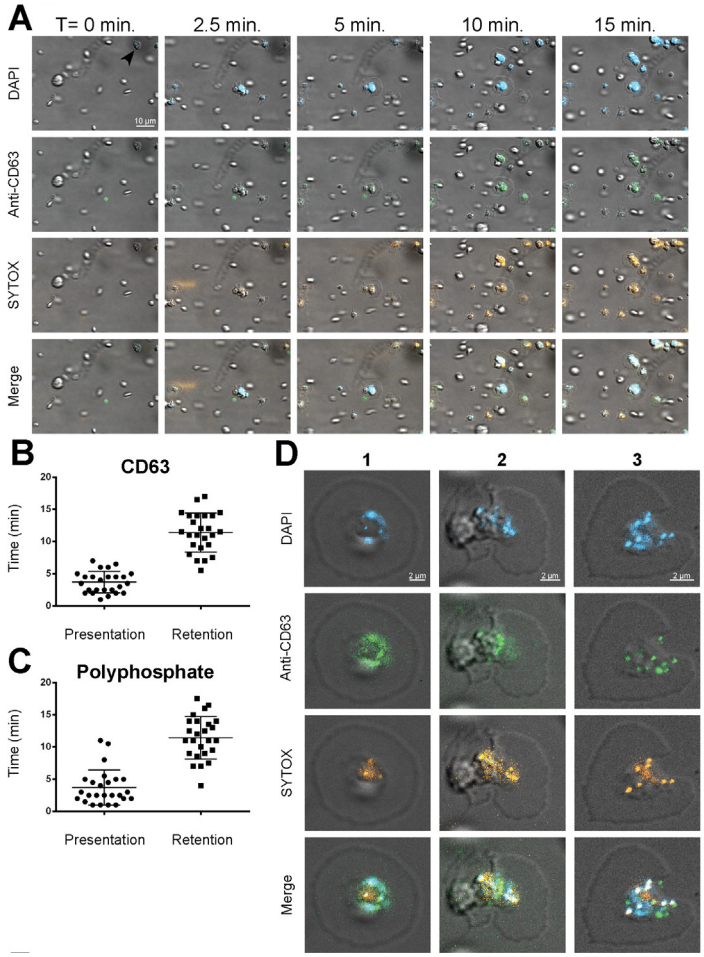

Figure 1. Polyphosphate is retained on the platelet surface after degranulation. (A) Time series of platelet adhesion and spreading on immobilized VWF under flow. Polyphosphate was tracked with DAPI (blue) and SYTOX (orange). Degranulation was detected by an anti-CD63 antibody (green). A scale bar is shown in the upper left panel (indicated by arrow in upper left panel) (10 mm). All images are shown at the same magnification. Times (above) represent the time course, starting from the moment of first stable platelet adhesion in the image field (indicated by arrow in upper left panel). (B-C) Individual spreading platelets were visually inspected (n = 25, derived from videos of >3 separate experiments). Approximately 4 minutes after initial adhesion, both CD63 and polyphosphate appeared on the platelet surface ("Presentation"). The fluorescence of both these markers persisted for the remainder of the experiments ("Retention"). (D) Localization of polyphosphate and CD63 on spreading platelets after >20 minutes. T, time.

Table 1. Colocalization between DAPI, SYTOX, and CD63 on the platelet surface

Anti-CD63 with SYTOX, %	DAPI with SYTOX, %	DAPI with anti-CD63, %
40 ± 8	50 ± 13	48 ± 12

Colocalization of anti-CD63, DAPI, and SYTOX staining was determined by means of pixel intensity correlation on confocal images.

2.8. Plasma activation with short polyphosphate (70-mers) and enzyme-C1inh complex ELISAs

Prewarmed citrated plasma was activated by addition of 50 μg/mL calcium preadsorbed polyphosphate [22]. Where indicated, 100 U/mL aprotinin was added prior to plasma activation. Where indicated, polyphosphate was incubated with EDTA, after which it was diluted to a final concentration of 50 μg/mL and 100 mM, respectively. Total kallikrein-like activity was monitored at 37°C by cleavage of the chromogenic substrate H-D-Pro-Phe-Arg-pNA (0.5 mM final concentration) at 405 nm. Alternatively, samples were collected in assay-specific buffer for analysis by enzyme-linked immunosorbent assay (ELISA). The C1inh-enzyme complex ELISA was performed as previously described [34].

3. Results

3.1. Polyphosphate mobilization to the platelet surface

It was previously reported that platelet polyphosphate can be visualized with the cell-permeable dye DAPI [1]. We perfused DAPI-treated washed human platelets over immobilized VWF at a venous shear rate (25 s^{-1}). Under these conditions, DAPI-positive platelets adhere without aggregating. The fluorescent DAPI staining of platelets was consistent with localization of polyphosphate in dense granules [1] and persisted over the complete course of our experiments (Figure 1A blue). However, CD63 exposure on the surface indicated that platelet degranulation was spontaneously taking place under these conditions [35] (Figure 1A green; quantification in Figure 1B). Unlike DAPI, SYTOX is a cell-membrane impermeable nucleic acid stain that is commonly used to distinguish extracellular from intracellular DNA [36]. During degranulation, platelets began to display SYTOX fluorescence (Figure 1A orange; supplemental Video 1A-B; without and with DAPI, respectively). SYTOX fluorescence was detected on the platelet surface for prolonged periods of time, suggesting that polyphosphate is exposed and retained on the cell surface under flow (Figure 1C). In the majority of experiments, SYTOX-positive structures with spherical morphology were observed on the platelet surface. SYTOX fluorescence on the platelet surface was unaffected by deoxyribonuclease I or ribonuclease A (supplemental Figure 1A-B), indicating that the contribution of nucleic acids to this cell surface staining was negligible. We confirmed the activity of these enzymes in control experiments (supplemental Figure 1C-D). Analyses of platelet cell surfaces after 20 minutes of perfusion showed partial colocalization between DAPI, SYTOX, and anti-CD63 (Figure 1D; Table 1). Furthermore, SYTOX fluorescence on the surface of activated platelets persisted in the presence of plasma, indicating resistance against plasma phosphatase activity (Figure 2A; supplemental Video 2A). SYTOX fluorescence also persisted in the presence of recombinant PPX (Figure 2B; supplemental Video 2B) during the course of our experiments. We confirmed the enzymatic activity of PPX in control experiments (supplemental Figure 1E). However, we found that the distribution of polyphosphate on the platelet surface slowly became less punctate, suggesting limited degradation by PPX. Furthermore, we observed that an anti-thrombotic variant of PPX, lacking its protease domain (PPX_Δ12) [29], bound to the surface of activated platelets (Figure 2C; supplemental Video 2C). The binding of this polyphosphate-specific probe further confirms that polyphosphate is retained on the membrane surface.

Finally, platelet aggregate formation in whole blood on immobilized collagen under high shear rates (1600 s^{-1}) revealed that polyphosphate was incorporated into the aggregates (Figure 2D-E). Supplemental Video 3A shows a sequence of microscopic images at varying

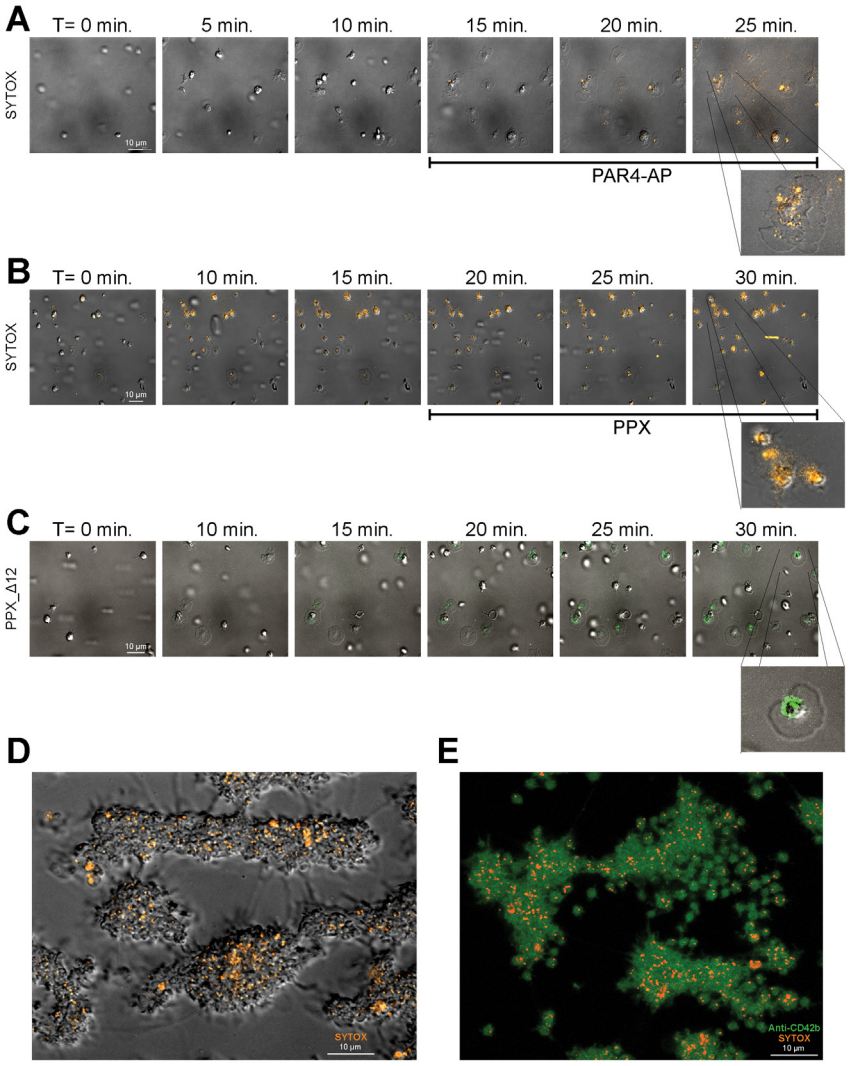

Figure 2. Membrane-associated polyphosphate is incorporated into platelet aggregates. Scale bar is shown in the left panels (10 **µ**m). All images are shown at the same magnification; insets show indicated areas at higher magnification. Times (above) represent the time course, starting from the moment of first stable platelet adhesion in the image field. (A) Time series of spreading and degranulation of platelets in citrated plasma on immobilized fibrinogen at 25 s^{-1} shear rate during activation by PAR4-activating peptide (PAR4-AP). Polyphosphate was visualized with SYTOX (orange); PAR4-AP enters the flow chamber after 15 minutes of perfusion (indicated below the images). (B) Time series of platelet adhesion and spreading on immobilized VWF under flow. Polyphosphate was visualized with SYTOX (orange); PPX (500 µg/mL) enters the flow chamber after 20 minutes of perfusion (indicated below the images). (C) Time series of platelet adhesion and spreading on immobilized VWF under flow. Polyphosphate was visualized with Alexa488-conjugated PPX_Δ12 (green). (D-E) Cross-section images of SYTOX-stained platelet aggregates, formed by perfusing citrated whole blood over immobilized collagen at 1600 s^{-1} shear rate for 10 minutes. (D, bright-field/fluorescence microscopy image of unfixed aggregates; E, confocal microscopy image of fixed aggregates) Green, anti-CD42b; orange, SYTOX. Images are representative of experiments that were performed >3 times.

distances from the surface (indicated above) of a SYTOX stained platelet aggregate. Supplemental Video 3B shows a 3-dimensional reconstruction of SYTOX-stained platelet aggregates, analyzed by confocal microscopy.

These results suggest that platelets not only secrete soluble polyphosphate polymers into the surrounding solution, as was demonstrated earlier [1,22], but also retain polyphosphate on their surface after degranulation. We subsequently went on to investigate the biochemical properties of platelet membrane-associated polyphosphate.

Table 2. Dynamic light scattering analyses of density fractions from platelet lysate

Fraction	I	II	III
Z-average (nm)	345	554	714
Polydispersity index	0.162	0.211	0.314

Mean hydrodynamic size (Z-average) in nanometers and polydispersity (0-1) of particles in subset of pooled fractions obtained after sucrose gradient ultracentrifugation of lysed platelets. Pooled fractions were derived from different density categories, as indicated in Figure 3D.

3.2. Platelet polyphosphate exists in 2 pools and displays nanoparticle-like behavior

Previous studies that identified platelet polyphosphate with a short polymer size in supernatant from platelets employed a phenol/chloroform extraction method for purification [22]. This extraction method is selective for soluble secreted molecules due to the removal of all cellular and cell-bound materials. Confirming our previous reports [3,22], we found polyphosphate polymers with an apparent size of 60 to 90 units in platelet lysates when extracted by phenol/chloroform extraction (Figure 3A).We subsequently extracted polyphosphate from complete platelet lysate by anion-exchange purification, which should purify all polyphosphate independently of polymer size, subcellular localization, or solubility. In this preparation, polyphosphate polymers displayed a larger apparent size and chain length distribution. Digestion of the extracted material with phosphatase (PSP) completely ablated the signal (Figure 3A). Moreover, polyphosphate with large apparent polymers sizes were found in multiple individual donors when isolated from complete platelet lysate by anion-exchange purification (Figure 3B).

We next investigated the contact system–activating properties of polyphosphate extracted by these 2 methods. Total platelet polyphosphate (Ion exc.; 20 μM, expressed as monophosphate units) strongly activated the plasma contact system, as determined in a chromogenic assay for kallikrein-like activity in plasma, while soluble polymers (phenol/chloroform; 20 μM, expressed as monophosphate units) were poor activators (Figure 3C). Plasma contact system activation was critically dependent on the presence of FXII (Figure 3C; ΔFXII indicates congenital FXII-deficient plasma). These findings indicate that, in addition to soluble short-chain polyphosphate polymers [1], a second polyphosphate pool with a higher apparent polymer size is present in platelets,which remains associated with the cell surface after secretion. To further investigate this concept, we lysed platelets in the presence of SYTOX. We then fractionated these lysates by sucrose density ultracentrifugation. SYTOX fluorescence was particularly enriched in a subset of fractions with higher sucrose densities (Figure 3D, group II). These, as well as surrounding control fractions (Figure 3D, group I and III), were collected for further analysis. In control experiments,we confirmed that SYTOX without platelet lysate (ie, unbound free dye) does not display any fluorescence or

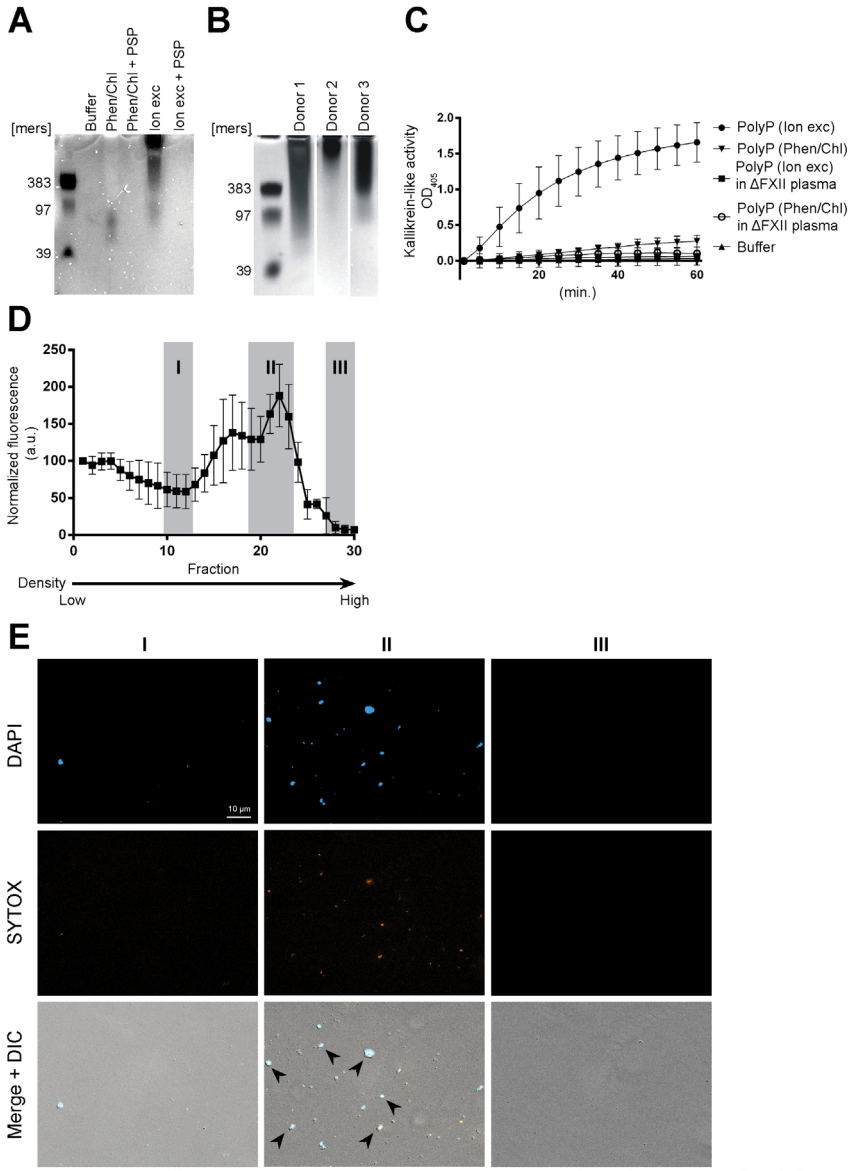

Figure 3. Platelet polyphosphate exists in 2 pools and displays nanoparticle-like behavior. (A) Gel electrophoresis of soluble platelet polyphosphate (Phen/Chl) or total platelet polyphosphate (Ion exc). Polyphosphate (1 nmol/lane; expressed as monophosphate units) was separated on 10% polyacrylamide TBE-urea (7 M) gels and visualized by DAPI-negative staining. PSP (10 U/mL) indicates phosphatase treatment prior to separation. Synthetic polyphosphate preparations with polymer sizes of 39, 97, and 383 phosphate units served as molecular size standard. A representative image for 3 separate experiments is shown. (B) Total platelet polyphosphate (Ion exc; 1 nmol/lane, expressed as monophosphate units) from 3 individual donors. (C) Kallikrein-like activity, triggered by platelet polyphosphate (PolyP), from 2 different sources (20 µM; expressed as monophosphate units). ΔFXII plasma indicates congenital FXII-deficient plasma. (D) Fractionation of SYTOX-supplemented platelet lysate by ultracentrifugation on sucrose density gradients. Data show normalized means 6 standard deviation of 3 independent fractionation studies. (E) Microscopic images of representative samples that were taken from fractions, indicated in panel D by roman numerals I-III. Polyphosphate was detected with DAPI (blue) and SYTOX (orange). Differential interference contrast microscopy; optical density at 405 nm.

sedimentation behavior (not shown). Determination of the average hydrodynamic diameter of particles in the collected fractions revealed that SYTOX fluorescence was mainly associated with a population of particles that had an average hydrodynamic size of 554 nm (Table 2). Pooled samples from SYTOX-rich fractions 21 to 25 (100-µLsamples from each fraction; 500 µL total volume) typically contained 820.1 µg phosphate. When we analyzed these fractions further by microscopy, particles were found with affinity for both DAPI and SYTOX (Figure 3E Roman numerals above the images refer to the fractions in Figure 3D).

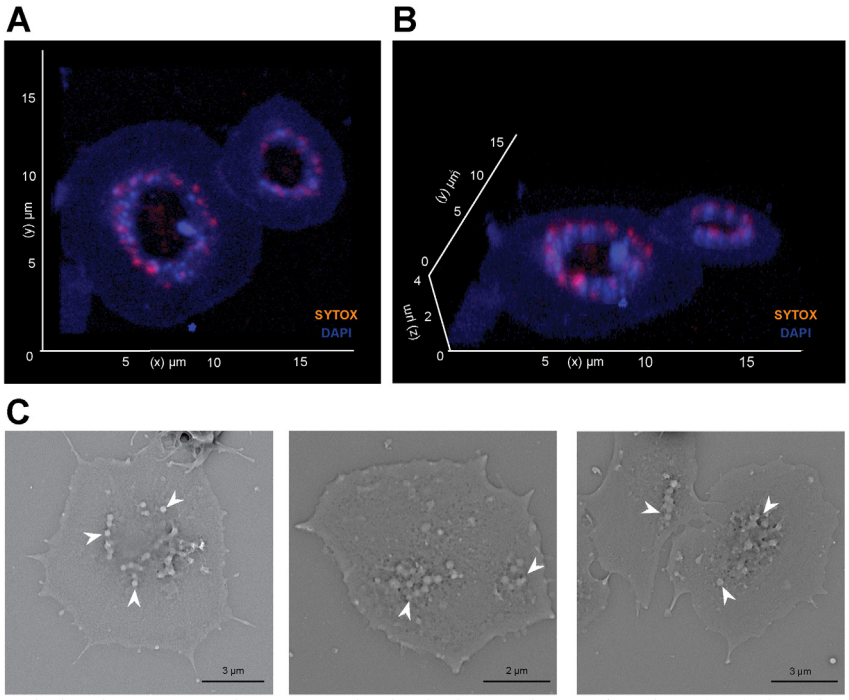

Figure 4. Polyphosphate nanoparticles are retained at the platelet granulomere after release. (A-B) Three-dimensional reconstruction of fixed spread platelets on immobilized VWF, analyzed by confocal microscopy. Blue, DAPI; orange, SYTOX. (C) Scanning electron microscopy of spreading platelets. Arrows indicate spherical structures.

3.3. Polyphosphate nanoparticles are retained at the platelet granulomere after release

Both our live-cell flow and fractionation studies indicated that platelet polyphosphate takes on a particulate state and accumulates on the surface of procoagulant platelets. We next analyzed the morphology and subcellular localization of platelet membrane-bound polyphosphate by confocal microscopy. Polyphosphate nanoparticles were positioned on top of the platelet granulomere of spread platelets (Figure 4A,B; supplemental Video 4; total polyphosphate in blue; extracellular polyphosphate in orange). Consistently, scanning electron microscopy revealed that spherical particles were present on the granulomere of spread platelets (Figure 4C). These particles range between 100 and 200 nm in diameter, which is comparable to particles formed by synthetic polyphosphate in the presence of calcium ions [28].

3.4. Polyphosphate nanoparticle formation depends on divalent metal ion incorporation

Polyphosphate precipitates with divalent metal ions that are known to be highly abundant in dense granules [27]. Furthermore, it has been reported that synthetic polyphosphate forms insoluble stable nanoparticles in the presence of calcium ions [28]. We therefore investigated the effect of EDTA (a chelator of divalent metal ions) on platelet polyphosphate complexes. The presence of EDTA strongly reduced migration of SYTOX into the deeper, sucrose-dense fractions during ultracentrifugation fractionation of platelet lysates (Figure 5A). The phosphate content in fractions 21 to 25 was typically reduced by ~50%(457.2 μg) in the presence of EDTA, compared with the control situation (820.1 μg). In the presence of EDTA, SYTOX fluorescence remained concentrated in fractions with low sucrose densities, which we assume to contain soluble polyphosphate. These experiments indicate that SYTOX fluorescence is associated with polyphosphate metal ion complexes.

We next investigated the properties of membrane-associated polyphosphate. Scanning electron microscopy revealed that spherical nanoparticles were no longer present on the platelet surface after exposure to EDTA (Figure 5B), underlining the role of divalent metal ions for polyphosphate nanoparticle formation. We next perfused washed platelets over immobilized VWF and tracked polyphosphate mobilization to the cell surface with SYTOX and subsequently exposed platelets to EDTA. As before, polyphosphate mobilization occurred after 4 to 5 minutes (Figure 5C; supplemental Video 5A). Exposure of these cells to EDTA after 15 to 20 minutes of perfusion resulted in immediate removal of polyphosphate from the platelet surface as visualized by SYTOX (Figure 5C; supplemental Video 5B). Similarly, PPX_Δ12 was unable to bind to the platelet surface after exposure to EDTA (Figure 5D; supplemental Video 5C-D).

3.5. Polyphosphate nanoparticle formation strongly promotes contact system activation.

Finally, we investigated whether platelet polyphosphate nanoparticle formation influenced the ability of polyphosphate to activate the plasma contact system. Hereto, we re-created calcium-polyphosphate nanoparticles with synthetic soluble polyphosphate (70-mers). In a calcium adsorbed state, this form of polyphosphate was capable of inducing kallikrein-like activity (Figure 5E). It is noteworthy that the apparent polymer size of short polyphosphate increases during calcium complexation, when analyzed in a gel-based assay (supplemental Figure 2). We found that plasma kallikrein-like activity was strongly diminished in the presence of EDTA and completely abrogated by the plasma kallikrein-inhibitor aprotinin, confirming the known importance of plasma kallikrein in contact activation (Figure 5E). We subsequently measured enzyme-C1inh complexes in plasma to investigate activation of the contact system enzymes as well as FXI in more detail. We found that calcium-adsorbed polyphosphate nanoparticles quickly triggered FXIIa-C1inh, PK-C1inh, and FXIa-C1inh complexes (Figure 4F; signals after 15 minutes of incubation; no complexes form in plasma without a trigger; not shown). Aprotinin completely blocked, and EDTA strongly reduced, formation of all these complexes. These findings indicate that the generation of kallikrein-like activity by polyphosphate nanoparticles in plasma is accompanied by activation of FXII, plasma prekallikrein, and FXI.

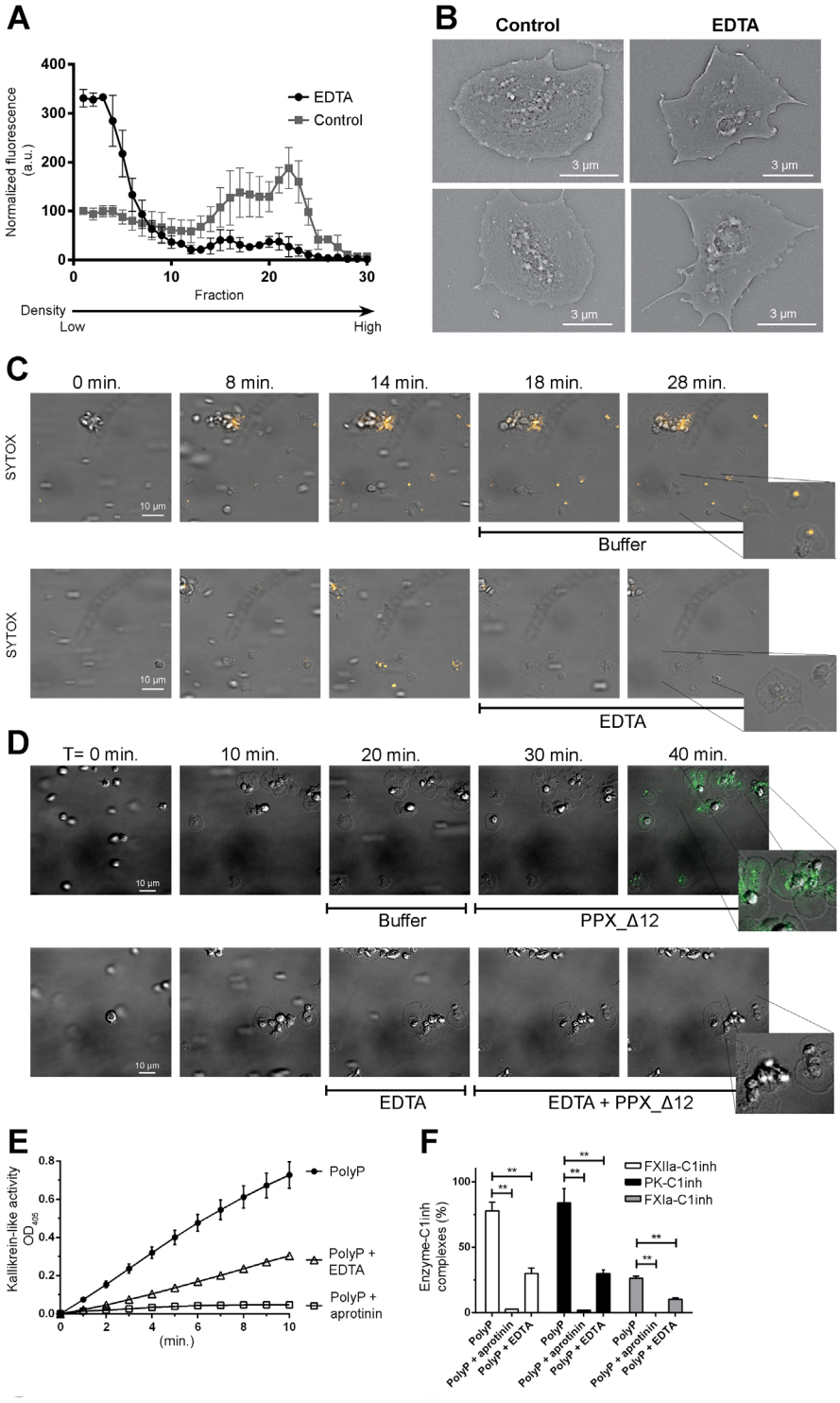
A
Normalized fluorescence (a.u.)
400
300
200
100
0
0
10
20
30
Fraction
EDTA
Control
Density
Low
High
B
Control
EDTA
3 µm
C
0 min.
8 min.
14 min.
18 min.
28 min.
SYTOX
10 µm
Buffer
EDTA
D
T= 0 min.
10 min.
20 min.
30 min.
40 min.
Buffer
PPX_Δ12
EDTA
EDTA + PPX_Δ12
E
Kallikrein-like activity
OD405
0.8
0.6
0.4
0.2
0.0
0
2
4
6
8
10
(min.)
PolyP
PolyP + EDTA
PolyP + aprotinin
F
Enzyme-C1inh complexes (%)
100
50
0
FXIIa-C1inh
PK-C1inh
FXIa-C1inh
**
PolyP
PolyP + aprotinin
PolyP + EDTA

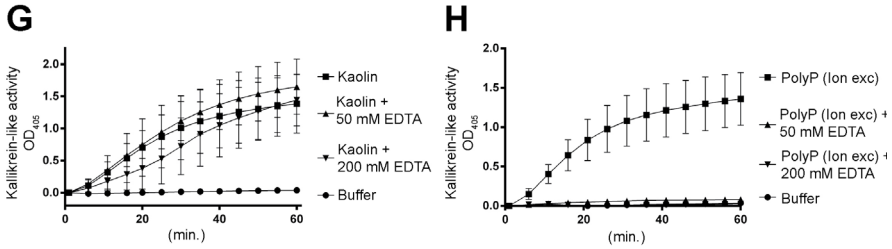

Figure 5. Polyphosphate nanoparticle formation depends on divalent metal ion incorporation and promotes contact system activation. (A) Fractionation of SYTOXsupplemented platelet lysate by ultracentrifugation on sucrose density gradients in the absence or presence of EDTA (250 mM). Data show normalized means ± standard deviation of 3 independent fractionation experiments. (B) Scanning electron microscopy of spreading platelets in the absence or presence of EDTA (250 mM). (C-D) Platelet adhesion and spreading on immobilized VWF under flow. A scale bar is shown in the left panel (10 μm). All images are shown at the same magnification; insets show indicated areas at higher magnification. Times (above) represent the time course, starting from the moment of first stable platelet adhesion in the image field. (C) Polyphosphate exposure was tracked with SYTOX (orange). After 15 minutes, either buffer or EDTA (50 mM) was perfused over spread platelets. (D) Polyphosphate exposure was detected by the binding of Alexa488-conjugated PPX_Δ12 (green) after 25 minutes of platelet spreading in the absence or presence of EDTA (250 mM). A scale bar (10 μm) is shown in the first panel of the series. All images are shown at the same magnification. Times (indicated above) represent the time course, starting from the first moment of stable platelet adhesion in the image field. Insets show indicated areas at higher magnification. Images are representative for experiments that were performed >3 times. (E-F) Plasma contact system activation by 50 μg/mL calcium-preadsorbed synthetic short-chain polyphosphate (PolyP; 70-mers). (E) Kallikrein-like activity was monitored by conversion of a chromogenic substrate and (F) formation of enzyme-C1 inhibitor complexes in plasma (after 15 minutes). Where indicated, contact system activation was triggered in the presence of aprotinin (100 U/mL) or by polyphosphate (PolyP) that was pretreated with EDTA (100 mM) for 10 minutes prior to contact system activation. 100% indicates the amount of complexes that are formed in plasma when exposed to positive control contact activators for 30 minutes. **P , .01, analyzed by unpaired Student t test. (G-H) Kaolin (1.5 μg/mL) or anion exchange–purified platelet polyphosphate (20 μM; expressed as monophosphate units) triggered kallikrein-like activity in the absence or presence of EDTA, monitored by chromogenic substrate conversion.

We then established that contact system activation by kaolin proceeds normally in the presence of EDTA, confirming that contact activation itself could take place without divalent metal ions as a prerequisite (Figure 5G). However, the contact system–activating potential of total platelet polyphosphate (isolated by ion exchange, 20 μM; expressed as monophosphate units) was fully abrogated in the presence of EDTA (Figure 5H). These experiments cumulatively suggest that membrane-associated polyphosphate nanoparticles constitute a powerful trigger for contact system activation.

4. Discussion

Polyphosphate is an ancient and diverse biological "multi-tool" that regulates a wide variety of biological processes ranging from cell proliferation to angiogenesis, apoptosis, osteoblast function, bone mineralization, energy metabolism, and tumor metastasis [37]. Platelet granules contain large amounts of polyphosphate, and patients with dense-granule defects have ~10 times less polyphosphate in their platelets [1,38]. Moreover, genetic targeting of inositol hexakisphosphate kinase 1 (a key enzyme in polyphosphate biosynthesis) in mice has been shown to reduce platelet polyphosphate content and granule numbers [39].

Over the past decades, several studies have reported that activated platelets promote coagulation in a FXII-dependent manner [18-21]. More recently, platelet polyphosphate was implicated as the molecular link between platelet activation and FXII activation in vitro [7] and in vivo [22]. These studies analyzed soluble polyphosphate in the supernatant of activated platelets and found that platelets release short-chain polyphosphate polymers. Confusingly, short-chain polyphosphate constitutes a weak activator of FXII [23,25]. At the same time, agents that block polyphosphate polymers have been shown to effectively interfere with platelet-driven thrombus formation without a therapy associated increased rate of hemorrhage [12,29]. These observations phenocopy the results observed in experimental models of thrombosis performed using either FXII-deficient mice [17] or an antibody that blocks the activation of FXI by FXIIa [14], suggesting that FXII activation by platelet polyphosphate promotes pathological thrombus formation in vivo. We here identify an additional, previously unidentified pool of platelet polyphosphate, which is retained on the cell surface during and after degranulation. The apparent polymer size of membrane associated polyphosphate largely exceeds that of secreted soluble polyphosphate polymers. Microscopic analyses as well as ultracentrifugation fractionation studies indicate that membrane-associated platelet polyphosphate adopts a nanoparticle state. The effects of the chelating agent EDTA show that divalent metals are essential for the stability and membrane association of polyphosphate nanoparticles. This observation corresponds well to the biochemical principle that phosphate forms insoluble complexes with divalent metal ions [40] as well as recent reports that synthetic polyphosphate precipitates into stable spherical nanoparticles in the presence of calcium [28,41]. It is attractive to hypothesize that intracellular calcium and other divalent metal ions are stored in a (poly)phosphate-complexed state to avoid the maintenance of steep osmolarity gradients over the phospholipid membrane of intracellular granules. Evidence from microscopy experiments supports this concept: sectioned platelets and isolated dense granules often appear as void lipid bilayers in electron microscopy studies [1].

FXII requires binding to a surface in order to effectively initiate blood coagulation; example surfaces include silica-based particulates such as glass or kaolin (reviewed in de Maat and Maas [42]). The archetypical FXII activator ellagic acid (a commonly used diagnostic reagent) is a surprising exception. Although this small molecule lacks the properties of a surface, it only triggers FXII activation and subsequent thrombin generation when precipitated into insoluble particles with divalent metal ions [43]. Our findings indicate that the FXII-activating properties of polyphosphate are also controlled by ion triggered precipitation, complementing the concept that the role of polyphosphate in coagulation is modulated by polymer size.

From previous studies, it has become clear that polyphosphate's polymer size deeply influences its hemostatic functions (as a soluble molecule) [23]. Our findings lead to the question of whether polyphosphate will actually meet the bloodstream in a soluble state.

It is often reported that platelets contain short polyphosphate polymers, whereas micro-organisms contain much larger polymers. During our studies, we recognized that calcium complexation strongly alters the migratory behavior of polyphosphate, leading to a higher apparent polymer size in gel-based electrophoresis experiments (supplemental Figure 2). In addition, the appearance of platelet membrane–associated polyphosphate in gel-based assays is strikingly similar (Figure 2A-B). These findings indicate that gel-based assays only

provide insight into apparent polymer size. However, the actual determination of polymer size requires more a sophisticated approach, such as nuclear magnetic resonance analyses [23].

Recently, polyphosphate was shown to be capable of dampening C1s-mediated activation of the classical pathway by acceleratingC1inh neutralization of C1s cleavage of C4 and C2 [6]. This study also visualized polyphosphate on activated platelet surfaces, consistent with our findings. Although speculative, it is attractive to hypothesize that polyphosphate nanoparticle formation enables concentration of C1inh on the platelet surface as C1inh co-localizes with polyphosphate.

Mast cells contain crystalline granules that store high levels of concentrated inflammatory mediators as well as heparin. Polyphosphate co-localizes with serotonin and calcium in the acidic secretory granules of mast cells (similar to platelet dense granules) and is released during mast cell activation [2]. In separate reports,mast cells were shown to secrete stable, solid particles that can deliver signals to remote lymphnodes [44]. Based on these combined observations, it is attractive to speculate that mast cells also contain solid polyphosphate nanoparticles. This hypothesis would provide a mechanistic explanation for the increased activity of the coagulation system [45] and activation of the plasma contact system [46,47] observed in mast cell–related disorders.

In conclusion, our findings may provide a new perspective on the procoagulant role of platelet polyphosphate as well as refine our view on the mechanisms by which platelets distribute their granular content.

Acknowledgments

The authors gratefully acknowledge the expertise and assistance of the Cell Microscopy Center Utrecht. The authors gratefully acknowledge financial support (C.M.) of the International Patient Organization for C1-Inhibitor Deficiencies, Stichting Vrienden van Het UMC Utrecht, and the Netherlands Organization for Scientific Research. T.R. was supported by the Hj¨art Lungfonden (20140741), Stockholms L¨ans Landsting (ALF; 20140464), Vetenskapsr°adet (K2013-65X-21462-04-5), the German Research Society (SFB877, TP A11 and SFB841, TP B8), and a European Research Council grant (ERC-StG-2012-311575_F-12). O.M. was supported by grants from the National Institutes of Health (National Heart, Lung, and Blood Institute, R01 HL101972, and National Institute of General Medical Sciences, R01 GM116184) and the American Heart Association (13EIA12630000).

Authorship

Contribution: J.J.F.V., A.D.B., K.F.N., K.D., S.d.M., E.K., L.L., A.P.H., and M.H.F. performed experiments; T.R., S.D.M., and C.M. designed the experiments; H.F.H., R.S. and H.S. provided critical reagents and expertise; and J.J.F.V., A.D.B., K.F.N., T.R., O.J.T.M., and C.M. drafted and edited the manuscript. All authors approved the final manuscript.

ORCID profiles: C.M., 0000-0003-4593-0976.

Correspondence: Coen Maas, Department of Clinical Chemistry and Haematology, University Medical Center Utrecht, Heidelberglaan 100, Room G.03.550, 3584CX, Utrecht, the Netherlands; e-mail: cmaas4@umcutrecht.nl.

References

[1] Ruiz FA, Lea CR, Oldfield E, Docampo R. Human platelet dense granules contain polyphosphate and are similar to acidocalcisomes of bacteria and unicellular eukaryotes. J Biol Chem. 2004; 279(43):44250-44257.

[2] Moreno-Sanchez D, Hernandez-Ruiz L, Ruiz FA, Docampo R. Polyphosphate is a novel proinflammatory regulator of mast cells and is located in acidocalcisomes. J Biol Chem. 2012;287(34): 28435-28444.

[3] Nickel KF, Ronquist G, Langer F, et al. The polyphosphate-factor XII pathway drives coagulation in prostate cancer-associated thrombosis. Blood. 2015;126(11):1379-1389.

[4] Montilla M, Hernández-Ruiz L, García-Cozar FJ, Alvarez-Laderas I, Rodríguez-Martorell J, Ruiz FA. Polyphosphate binds to human von Willebrand factor in vivo and modulates its interaction with glycoprotein Ib. J Thromb Haemost. 2012;10(11):2315-2323.

[5] Brandt S, Krauel K, Jaax M, et al. Polyphosphates form antigenic complexes with platelet factor 4 (PF4) and enhance PF4-binding to bacteria. Thromb Haemost. 2015;114(6):1189-1198.

[6] Wijeyewickrema LC, Lameignere E, Hor L, et al. Polyphosphate is a novel cofactor for regulation of complement by a serpin, C1 inhibitor. Blood. 2016;128(13):1766-1776.

[7] Smith SA, Mutch NJ, Baskar D, Rohloff P, Docampo R, Morrissey JH. Polyphosphate modulates blood coagulation and fibrinolysis. Proc Natl Acad Sci USA. 2006;103(4):903-908.

[8] Choi SH, Smith SA, Morrissey JH. Polyphosphate is a cofactor for the activation of factor XI by thrombin. Blood. 2011;118(26):6963-6970.

[9] Choi SH, Smith SA, Morrissey JH. Polyphosphate accelerates factor V activation by factor XIa. Thromb Haemost. 2015;113(3):599-604.

[10] Puy C, Tucker EI, Ivanov IS, et al. Platelet-derived short-chain polyphosphates enhance the inactivation of tissue factor pathway inhibitor by activated coagulation factor XI. PLoS One. 2016; 11(10):e0165172.

[11] Mutch NJ, Engel R, Uitte de Willige S, Philippou H, Ariëns RAS. Polyphosphate modifies the fibrin network and down-regulates fibrinolysis by attenuating binding of tPA and plasminogen to fibrin. Blood. 2010;115(19):3980-3988.

[12] Travers RJ, Shenoi RA, Kalathottukaren MT, Kizhakkedathu JN, Morrissey JH. Nontoxic polyphosphate inhibitors reduce thrombosis while sparing hemostasis. Blood. 2014;124(22): 3183-3190.

[13] Zhu S, Travers RJ, Morrissey JH, Diamond SL. FXIa and platelet polyphosphate as therapeutic targets during human blood clotting on collagen/tissue factor surfaces under flow. Blood. 2015 126(12):1494-1502.

[14] Matafonov A, Leung PY, Gailani AE, et al. Factor XII inhibition reduces thrombus formation in a primate thrombosis model. Blood. 2014;123(11): 1739-1746.

[15] Revenko AS, Gao D, Crosby JR, et al. Selective depletion of plasma prekallikrein or coagulation factor XII inhibits thrombosis in mice without increased risk of bleeding. Blood. 2011;118(19): 5302-5311.

[16] Yau JW, Liao P, Fredenburgh JC, et al. Selective depletion of factor XI or factor XII with antisense oligonucleotides attenuates catheter thrombosis in rabbits. Blood. 2014;123(13):2102-2107.

[17] Renné T, Pozgajová M, Grüner S, et al. Defective thrombus formation in mice lacking coagulation factor XII. J Exp Med. 2005;202(2):271-281.

[18] Castaldi PA, Larrieu MJ, Caen J. Availability of platelet Factor 3 and activation of factor XII in thrombasthenia. Nature. 1965;207(995):422-424.

[19] Walsh PN, Griffin JH. Platelet-coagulant protein interactions in contact activation. Ann N Y Acad Sci. 1981;370:241-252.

[20] Johne J, Blume C, Benz PM, et al. Platelets promote coagulation factor XII-mediated proteolytic cascade systems in plasma. Biol Chem. 2006;387(2):173-178.

[21] Bäck J, Sanchez J, Elgue G, Ekdahl KN, Nilsson B. Activated human platelets induce factor XIIamediated contact activation. Biochem Biophys Res Commun. 2010;391(1):11-17.

[22] Müller F, Mutch NJ, Schenk WA, et al. Platelet polyphosphates are proinflammatory and procoagulant mediators in vivo. Cell. 2009;139(6): 1143-1156.

[23] Smith SA, Choi SH, Davis-Harrison R, et al. Polyphosphate exerts differential effects on blood clotting, depending on polymer size [published correction appears in Blood. 2011;117(12):3477]. Blood. 2010;116(20):4353-4359.

{24} Morrissey JH, Smith SA. Polyphosphate as modulator of hemostasis, thrombosis, and inflammation. J Thromb. Haemost. 2015;13(Suppl 1): S92-S97.

[25] Puy C, Tucker EI, Wong ZC, et al. Factor XII promotes blood coagulation independent of factor XI in the presence of long-chain polyphosphates. J Thromb Haemost. 2013;11(7):1341-1352.

[26] Holmsen H, Weiss HJ. Secretable storage pools in platelets. Annu Rev Med. 1979;30:119-134.

[27] Fitch-Tewfik JL, Flaumenhaft R. Platelet granule exocytosis: a comparison with chromaffin cells. Front Endocrinol (Lausanne). 2013;4:77.

[28] Donovan AJ, Kalkowski J, Smith SA, Morrissey JH, Liu Y. Size-controlled synthesis of granular polyphosphate nanoparticles at physiologic salt concentrations for blood clotting. Biomacromolecules. 2014;15(11):3976-3984.

[29] Labberton L, Kenne E, Long AT, et al. Neutralizing blood-borne polyphosphate in vivo provides safe thromboprotection. Nat Commun. 2016;7:12616.

[30] Remijn JA, Wu YP, Ijsseldijk MJ, Zwaginga JJ, Sixma JJ, de Groot PG. Absence of fibrinogen in afibrinogenemia results in large but loosely packed thrombi under flow conditions. Thromb Haemost. 2001;85(4):736-742.

[31] Rouser G, Fkeischer S, Yamamoto A. Two dimensional then layer chromatographic separation of polar lipids and determination of phospholipids by phosphorus analysis of spots. Lipids. 1970;5(5):494-496.

[32] Summer H, Grämer R, Dröge P. Denaturing urea polyacrylamide gel electrophoresis (Urea PAGE). J. Vis. Exp. JoVE. 2009;(32):

[33] Smith SA, Morrissey JH. Sensitive fluorescence detection of polyphosphate in polyacrylamide gels using 4`,6-diamidino-2-phenylindol. Electrophoresis. 2007;28(19):3461-3465.

[34] de Maat S, Björkqvist J, Suffritti C, et al. Plasmin is a natural trigger for bradykinin production in patients with hereditary angioedema with factor XII mutations. J Allergy Clin Immunol. 2016;138(5): 1414-1423. e9.

[35] Nishibori M, Cham B, McNicol A, Shalev A, Jain N, Gerrard JM. The protein CD63 is in platelet dense granules, is deficient in a patient with Hermansky-Pudlak syndrome, and appears identical to granulophysin. J Clin Invest. 1993; 91(4):1775-1782.

[36] Fuchs TA, Brill A, Duerschmied D, et al. Extracellular DNA traps promote thrombosis. Proc Natl Acad Sci USA. 2010;107(36):15880-15885.

[37] Morrissey JH, Choi SH, Smith SA. Polyphosphate: an ancient molecule that links platelets, coagulation, and inflammation. Blood. 2012;119(25):5972-5979.

[38] Hernández-Ruiz L, Sáez-Benito A, Pujol-Moix N, Rodrïguez-Martorell J, Ruiz FA. Platelet inorganic polyphosphate decreases in patients with delta storage pool disease. J Thromb Haemost. 2009; 7(2):361-363.

[39] Ghosh S, Shukla D, Suman K, et al. Inositol hexakisphosphate kinase 1 maintains hemostasis in mice by regulating platelet polyphosphate levels. Blood. 2013;122(8):1478-1486.

[40] Binas English Edition. Handbook for Physics, Chemistry, Biology and Mathematics. Wolters-Noordhoff; 2007, Groningen, the Netherlands.

[41] Donovan AJ, Kalkowski J, Szymusiak M, et al. Artificial dense granules: a procoagulant liposomal formulation modeled after platelet polyphosphate storage pools. Biomacromolecules. 2016;17(8):2572-2581.

[42] de Maat S, Maas C. Factor XII: form determines function. J Thromb Haemost. 2016;14(8): 1498-1506.

[43] Bock PE, Srinivasan KR, Shore JD. Activation of intrinsic blood coagulation by ellagic acid: insoluble ellagic acid-metal ion complexes are the activating species. Biochemistry. 1981;20(25): 7258-7266.

[44] Kunder CA, St John AL, Li G, et al. Mast cellderived particles deliver peripheral signals to remote lymph nodes. J Exp Med. 2009;206(11): 2455-2467.

[45] Cugno M, Marzano AV, Asero R, Tedeschi A. Activation of blood coagulation in chronic urticaria: pathophysiological and clinical implications. Intern Emerg Med. 2010;5(2):97-101.

[46] Sala-Cunill A, Björkqvist J, Senter R, et al. Plasma contact system activation drives anaphylaxis in severe mast cell-mediated allergic reactions. J Allergy Clin Immunol. 2015;135(4):1031-43.e6.

[47] Oschatz C, Maas C, Lecher B, et al. Mast cells increase vascular permeability by heparin-initiated bradykinin formation in vivo. Immunity. 2011; 34(2):258-268.

Supplemental data

S1. Supplemental Materials and Methods

S1.1. Platelet isolation

Platelets were isolated from citrated blood of healthy volunteers under approval of the local Medical Ethical Committee of University Medical Center Utrecht by centrifugation as previously reported. First, platelet-rich plasma (PRP) was prepared from citrated whole blood, supplemented with 8.5 mM tri-sodium citrate, 7.1 mM citric acid, and 11.1 mM D-glucose, by centrifugation at 160 × g for 15 minutes. To obtain washed platelets, PRP was centrifuged a second time at 400 × g for 15 minutes to remove supernatant plasma. The platelet pellet was carefully resuspended in 10 mM (4-(2-hydroxyethyl)-1-piperazineethanesulfonic acid) HEPES, 1 mM $MgSO_4$, 5 mM KCl, 500 nM Na_2HPO_4, 145 mM NaCl and supplemented with 500 nM D-glucose (HEPES Tyrode buffer) pH = 6.5 (Sigma-Aldrich Chemie, Zwijndrecht, the Netherlands), and 10 ng/mL prostacyclin (PGI2; Cayman Chemicals, Michigan, USA) and centrifuged again at 400 × *g* for 15 minutes. Finally, the platelet pellet was carefully resuspended in HEPES Tyrode buffer, pH = 7.4 with 500 nM D-glucose. Platelets counts were diluted to 150,000 platelets/μL.

S1.2. Production of recombinant exopolyphosphatase and a truncated variant

Exopolyphosphatase (PPX) or its polyphosphate binding domains (PPX_Δ12) were expressed in E.coli and purified as previously published with minor modifications [1]. After purification, the PPX and the PPX_Δ12 were dialyzed against phosphate buffer (10 mM Na_2HPO_4, 10 mM NaH_2PO_4, 500 mM NaCl, pH=7.4. Samples were stored at -80 °C prior to use. Alexa488 was coupled to PPX_Δ12 using Alexa Fluor 488 NHS Ester (Succinimidyl Ester) kit (A20000, ThermoFisher) and performed according to manufacturer's instructions. Subsequently Zeba Spin Desalting Columns 7kD (Prod#89892, ThermoScientific) were used to remove unbound Alexa488.

S1.3. Live-cell imaging under flow

Cover glasses were cleaned with chromic acid and coated 90 min at room temperature (RT) with either 10 μg/mL recombinant VWF (Baxter, Vienna, Austria), 100 μg/mL fibrinogen (Enzyme Research Laboratories, South Bend, IN, USA) or 1:10 type I collagen (Horm, Nycomed, Linz, Austria) in HEPES Tyrode buffer pH=7.4. Subsequently, the glasses were blocked with 1% human serum albumin (fraction V; MP Biomedicals, Illkirch, France) for 60 min at RT or overnight at 4°C. Prior to experiments, biotinylated anti-CD63 (Abcam, Cambridge, UK) was mixed with equimolar amounts of streptavidin-Alexa488 to form complexes. Washed platelet suspensions were supplemented with Alexa488-labeled anti-CD63 to visualize dense granule degranulation and 1.5 μM SYTOX Orange (Molecular Probes/Life Technologies, Waltham, MA, USA) or 5 μg/mL Alexa488-conjugated PPX_Δ12 to visualize polyphosphate, and subsequently perfused through a laminar-flow chamber [2] over VWF coated cover glasses at low shear rates (25 -50 s^{-1}). In selected experiments, platelets were preincubated for 30 min at 37°C with 10 μg/mL DAPI (4`,6-diamidino-2- phenylindole; Sigma-Aldrich Chemie, Zwijndrecht, the Netherlands) and centrifuged at 400 × *g*, for 15 min. in the presence of 10 ng/mL prostacyclin to remove unbound dye. Where indicated, the effect of ethylenediaminetetraacetic acid (EDTA; 50 -500 mM), 10 μg/mL RNAse A (Invitrogen,

Bleiswijk, the Netherlands), 10 μg/mL DNAse I (Roche, Mannheim, Germany) or 500 μg/mL PPX was investigated.

Analyses were performed on a Zeiss Z1 microscope with Colibri LEDs and ZEN 2 Blue Edition software. Videos were captured at a magnification of 1,000× for 20-40 min at a frame rate of 2 frames per min. After 20-40 min, snapshots were made outside the previous focus area and cover glasses were fixed with 2% paraformaldehyde (PFA).

Platelet adhesion, spreading and degranulation in plasma, was studied step-wise in the continuous presence of SYTOX. First, PRP was perfused over immobilized fibrinogen at a shear rate of 25 s^{-1} for 10 min. Next, unbound platelets were removed by perfusion with platelet-poor plasma (PPP) for 5 min. Finally, adherent platelets were activated by perfusion with PAR4-activating peptide (Bachem, Bubendorf, Switserland) in PPP for another 10 min. Polyphosphate disposition in thrombus formation was investigated by perfusing citrated whole blood over collagen-coated cover glasses at a high shear rate (1600 s^{-1}).

The captured videos were further analyzed for the behavior of polyphosphate: individual platelets were visually inspected for the development of green (anti-CD63) or orange (SYTOX) fluorescence over time. Time points at which a) a platelet first stably adhered, b) fluorescence set in or c) disappeared, were registered in a blinded manner (i.e. the investigator that scored the videos did not perform the experiments and was kept blinded to the experimental conditions). If the signal persisted, 20 min (end of experiment) was registered. From these data, time to degranulation after stable adhesion ('presentation') and persistence of the presence of fluorescence ('retention') were derived. Co-localization was determined by analyzing single platelets using ImageJ software (National Institutes of Health, Bethesda, USA) and the Coloc 2 plugin.

S1.4. Confocal Microscopy and Scanning Electron Microscopy

After perfusion experiments, cover glasses were removed from the flow chambers and rinsed three times in HEPES Tyrode buffer pH=7.4, blocked with 1% human serum albumin (HSA) and 0.15% glycine (1 hour at room temperature) and rinsed fives more times in HEPES Tyrode buffer pH=7.4. For imaging of single spread platelets, cover glasses were mounted on an object glass with Prolong Gold Antifade Mountant (Molecular Probes/Invitrogen, Waltham, MA, USA) and incubated overnight at room temperature in the dark before storage at 4°C. For imaging of platelet aggregates, cover glasses were subsequently incubated with FITC-conjugated mouse-anti human CD42b (BD Biosciences, Palo Alto, CA) and 1.5 μM SYTOX Orange and 1% HSA in HEPES Tyrode buffer pH=7.4. Cover slides were rinsed five times in HEPES Tyrode buffer and mounted in 10% (m/v) Mowiol 40-88 and 2,5% (m/v) DABCO (1,4-diazabicyclo[2.2.2]octane) (Sigma-Aldrich, Zwijndrecht, the Netherlands) in 20% glycerol (v/v) and 200 mM TRIS-HCl, pH=8.0. Slides were analyzed on a Zeiss LSM700 Confocal Laser Scanning Microscope with ZEN software. Image stacks were acquired at a stack distance of 0.34 μm. 3D reconstructions were made with ZEN 2 Blue Edition software and 3D module. For Scanning Electron Microscopy (SEM), sample glasses were dehydrated in an ethanol series (15 min per step; 10%, 20% in HEPES Tyrode buffer, pH=7.4, 40%, 60%, 80% in distilled water, and finally 100% ethanol). Subsequently, samples were incubated in 50%-50% ethanol-hexamethyldisilazane and 100% hexamethyldisilazane after which the

glasses were dried, resized with a glass cutter, attached to a 0.5" aluminium specimen stub (Agar Scientific, Stansted, Essex, UK) and sputtered with gold. Specimens were analyzed on a Phenom Pro desktop SEM (Phenom World, Eindhoven, the Netherlands).

S1.5. Platelet fractionation by density ultracentrifugation

Washed platelets (2.5×10^6/mL) were resuspended in lysis buffer (25 mM HEPES, 250 mM sucrose, 12 mM sodium citrate, pH=6.5) with 1 mM sodium orthovanadate and 1:100 protease inhibitor cocktail (p8340, Sigma-Aldrich, Zwijndrecht, the Netherlands) and lysed by 3 pulses of mild sonication (5 sec at 3 mV) on a Soniprep 150 (MSE, London, UK). Afterwards, the suspensions were centrifuged at 1,000 × *g* for 15 min at 4°C, supernatants containing polyphosphate nanoparticles were collected on ice. Remaining pellets were resuspended, sonicated and centrifuged in 2-4 additional cycles until no more pellet was observed. Finally, the collected supernatants were combined and centrifuged at 19,000 × *g* for 20 minutes at 4°C. The pellet containing polyphosphate nanoparticles was diluted in 1.4 mL lysis buffer with 250 mM sucrose, and supplemented with 5 μM SYTOX Orange. In select experiments, 250 mM EDTA was added. Samples were loaded on top of a sucrose gradient with 0.7 mL fractions ranging from 0.5 M until 2 M diluted in lysis buffer without protease inhibitors. The gradient was centrifuged at 1,000,000 × *g* for 60 minutes at 4°C using a Beckman SW40 rotor (without brake). Fractions of 350 μL were analyzed for SYTOX fluorescence at 540/570 nm ex/em using a Spectramax340 (Molecular Devices, Sunnyvale, United States) plate reader. The phosphate content in SYTOX-rich fractions was determined by means of acid digestion and subsequent reaction with ammonium molybdate as described by Rouser et al. [3]. Mean particle size of fractions was determined by dynamic light scattering (DLS), using a Malvern ALV CGS-3 multiangle goniometer, equipped with a He–Ne laser source (λ = 632.8 nm, 22 mW output power) under an angle of 90° (Malvern Instruments, Malvern, UK). Size and polydispersity were recorded with an optical fiber-based detector and a digital LV/LSE-5003 correlator at 25 °C.

S1.6. Platelet polyphosphate extraction

Human pheresis platelets (~2-4 × 10^{11} platelets/pheresis unit) were obtained from the Karolinska University Hospital and used for polyphosphate isolation within the expiry date (set for application in human transfusion). Polyphosphate was isolated by two different methods as follows: A) Isolation of soluble polyphosphate from lysed platelets by phenol/chloroform extraction. This was performed as previously described with minor modifications. The pH of the solution after Dowex ion exchanger treatment was neutralized with 40 mM Tris base and the final polyphosphate preparation was dialyzed overnight against 20 mM Tris pH 7.4 and Chelex 100 resin (Bio-Rad) using 1,000 molecular weight cutoff dialysis tubes (GE Healthcare); B) Isolation of total polyphosphate from lysed platelets that includes membrane-associated polyphosphate. A spin column anion exchanger method was performed as described3 with some modifications. Platelets were lysed by 6 freeze-thaw cycles before addition of sulfuric acid (0.3 M) and sodium chloride (3.5 M). Neutralized platelet lysate (pH 7.4) was sonicated (1 × 10 sec) and homogenized using 15 strokes with a tight-fitting dounce. The lysate was diluted (1:4) with 20 mM Tris (pH 7.4) and incubated with 50 μg/mL DNAse I (Sigma-Aldrich) in the presence of 3.5 mM $MgCl_2$ for 30 min at 37°C. The mixture was digested with 750 μg/mL proteinase K (Sigma-Aldrich) for 1 h at 37°C before centrifugation at 14,000 × *g* for 8

min. Subsequently, polyphosphate was isolated by a spin column anion exchanger method as published [4]. The final polyphosphate preparation was eluted in 20 mM Tris (pH 7.4). Polyphosphate concentrations were routinely measured after hydrolysis in 1 M HCl at 95°C for 60 min. The orthophosphate (Pi) released by polyphosphate digestion was estimated using colorimetric phosphate assay kit (Abcam) according to the manufacturer's instructions and absorbance was measured at 650 nm with a MultiskanTMGO Microplate Spectrophotometer (Thermo Scientific).

S1.7. Polyphosphate electrophoresis

Polyphosphate (1 nmol/lane of platelet-purified polyphosphate; expressed as monophosphate units, or 100 ng/lane of synthetic polyphosphate; indicated in figure legends) was separated by electrophoresis on 10% polyacrylamide TBE-urea (7 M) gels and stained by DAPI-negative staining as previously described. Alternatively, calcium-preadsorbed synthetic polyphosphate (70-mers; 40 μg/lane) was separated on 15% Urea-TBE gels [5] and stained with toluidine blue [6]. In some experiments, platelet polyphosphate extracts were incubated with alkaline phosphatase (PSP, 10 U/mL) in presence of 5 mM $MgCl_2$ for 120 min at 37°C prior to separation. In other experiments, calcium-preadsorbed synthetic short polyphosphate (4 mg/mL) and PPX (concentration series) were dissolved in HT buffer containing 5 mM $MgCl_2$ and incubated at 37 °C for 1 hour.

S1.8. Plasma contact system activation

Venous blood was collected from healthy human volunteers into 3.2% trisodium citrate (9:1 blood-to-citrate ratio). The first 10 mL was discarded. Platelet-free plasma was prepared by two consecutive centrifugation steps at 3,000 x g for 10 min. Plasma from individuals with congenital deficiency in FXII was purchased from George King Biomedical (Overland Park, Kansas, USA). Development of kallikrein-like activity was analyzed with 1 mM substrate S-2302 (sensitive to FXIIa and plasma kallikrein; Chromogenix, Mölndal, Sweden) at an absorbance wavelength of 405 nm in a Bio-Kinetics Reader (BioTek Instruments Inc.) at 37°C.

S1.9. Plasma activation with short polyphosphate (70-mers)

Prewarmed citrated plasma was activated by addition of 50 μg/mL polyphosphate. Where indicated, aprotinin (final concentration 100 U/mL) was added prior to plasma activation. Where indicated, polyphosphate was incubated with EDTA, after which it was diluted to a final concentration of 50 μg/mL and 100 mM, respectively. Total kallikrein-like activity was monitored at 37 °C by cleavage of the chromogenic substrate H-D-Pro-Phe-Arg-pNA (0.5 mM final concentration) at 405nm. Alternatively, samples were collected in assay-specific buffer for analysis by ELISA.

S1.10. Ezyme-C1inh complex ELISAs

The C1inh-enzyme complex ELISA was performed as previously described [7] Briefly, nanobody 1B12 (5 μg/mL in HBS) was coated overnight onto a Maxisorp plate at 4 °C. Plasma was activated with 50 μg/mL polyphosphate for 15 minutes after which samples were diluted 32x in 0.5% mHBS (skimmed milk in HBS) containing 200 μM PPACK. Wells were rinsed in PBS, blocked with 2% mHBS, after which the samples were incubated for 2 hours at room

temperature (RT), while shaking. Next the wells were rinsed with PBST (0.1% Tween-20 in PBS) and the wells were incubated with either polyclonal anti-PK or anti-FXI antibody (1:2000 in 0.5% mHBS). Alternatively samples were incubated with a biotinylated polyclonal nanobody mix specifically targeting the catalytic domain. Wells were rinsed with PBST and incubated with a peroxidase-conjugated anti-sheep polyclonal (1:8000 in 0.5% mHBS) or with streptavidin-poly-HRP (1:5000 in 0.5% mHBS) for 1 hour at RT while shaking. Wells were rinsed with PBST, after which they were developed by the addition of 50 µl TMB substrate. Substrate conversion was stopped by the addition of 25 µl H_2SO_4 (0.3 M) and absorbance was measured at 450 nm. An activated plasma standard curve was included on each plate. For FXIIa- and PK-C1inh complexes, plasma was activated with 30 µg/mL DXS-500 for 30 minutes at 37 °C. For the FXIa-C1inh complexes, the plasma standard was activated with 150 µg/mL Kaolin for 30 minutes at 37 °C. Sample concentration was determined by plotting the standard curve in Prism Graphpad 6.0 using a sigmoidal 4PL fit model.

S2. Supplemental Figures

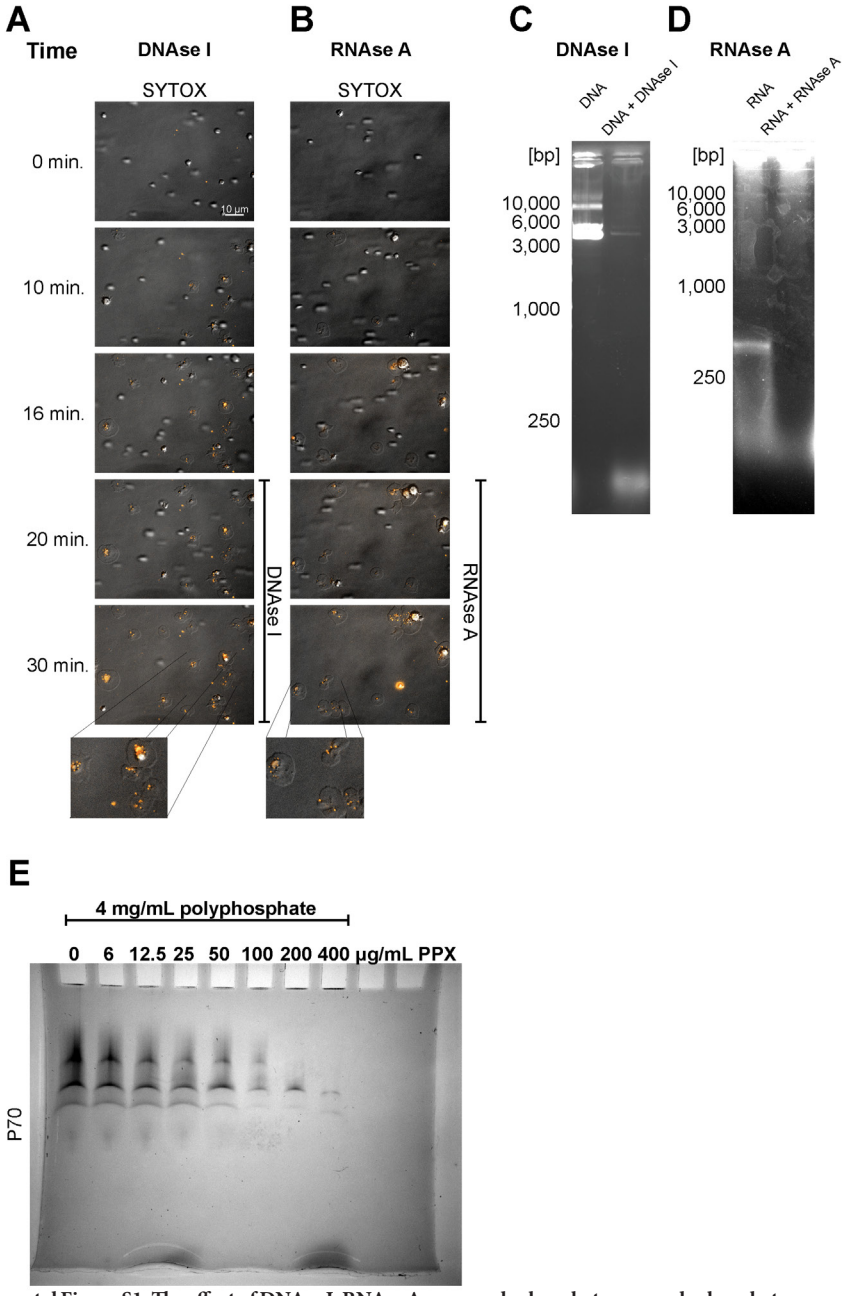

Supplemental Figure S1. The effect of DNAse I, RNAse A or exopolyphosphatase on polyphosphate nanoparticles. (A,B) Platelet adhesion and spreading on immobilized VWF under flow. Polyphosphate was tracked with SYTOX (orange). After 20 minutes, either DNAse I or RNAse A in buffer was perfused over spread platelets. A scale bar is shown in the upper left panel (10 µm). All images are shown at the same magnification. Times (indicated on the left) represent the time course, starting from the first moment of stable platelet adhesion in the image field. Insets shown 2x higher magnification of indicated areas. Images are representative for experiments that were performed >3 times. (C-E) Enzymatic activity of DNase I, RNAse A and exopolyphosphatase (PPX) towards DNA, RNA and calcium-

preadsorbed synthetic short-chain polyphosphate (70-mers), respectively. DNA and RNA were separated on agarose gels and stained with gel red. Calcium-preadsorbed polyphosphate swas separated on 15% Urea-TBE gels[5] and stained with toluidine blue [6].

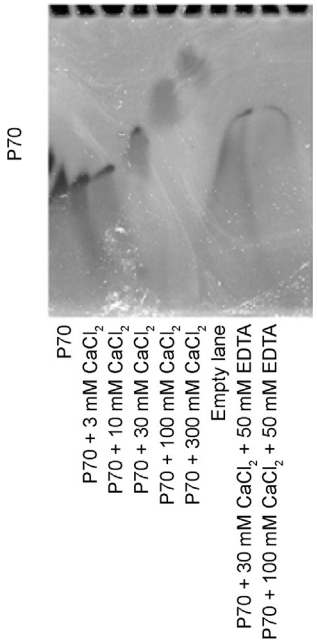

Supplemental Figure S2. Calcium increases the apparent polymer size of polyphosphate. Polyphosphate was incubated with increasing concentrations of CaCl2 and EDTA. 100 ng/lane polyphosphate was separated on 10% polyacrylamide TBE-urea (7 M) gels and visualized by DAPI-negative staining.

S3. Supplemental References

[1] L. Labberton et al., "Neutralizing blood-borne polyphosphate in vivo provides safe thromboprotection," Nat. Commun., vol. 7, p. 12616, 2016.

[2] J. A. Remijn, Y. P. Wu, M. J. Ijsseldijk, J. J. Zwaginga, J. J. Sixma, and P. G. de Groot, "Absence of fibrinogen in afibrinogenemia results in large but loosely packed thrombi under flow conditions," Thromb. Hae most., vol. 85, no. 4, pp. 736–742, Apr. 2001.

[3] G. Rouser, S. Fkeischer, and A. Yamamoto, "Two dimensional then layer chromatographic separation of polar lipids and determination of phospholipids by phosphorus analysis of spots," Lipids, vol. 5, no. 5, pp. 494–496, May 1970.

[4] K. F. Nickel et al., "The polyphosphate-factor XII pathway drives coagulation in prostate cancer-associated thrombosis," Blood, vol. 126, no. 11, pp. 1379–1389, Sep. 2015.

[5] H. Summer, R. Grämer, and P. Dröge, "Denaturing urea polyacrylamide gel electrophoresis (Urea PAGE)," J. Vis. Exp. JoVE, no. 32, Oct. 2009.

[6] S. A. Smith and J. H. Morrissey, "Sensitive fluorescence detection of polyphosphate in polyacrylamide gels using 4',6-diamidino-2-phenylindol," Electrophoresis, vol. 28, no. 19, pp. 3461–3465, Oct. 2007.

[7] S. de Maat et al., "Plasmin is a natural trigger for bradykinin production in patients with hereditary angioedema with factor XII mutations," J. Allergy Clin. Immunol., vol. 138, no. 5, p. 1414–1423.e9, Nov. 2016.

Chapter | 8

Summary and Perspectives

Nanosized delivery systems enable administration of therapeutic compounds, both small molecules and therapeutic proteins, otherwise not suitable due to poor solubility, poor pharmacokinetic properties or toxicity [1–3,4]. Examples of nanosized delivery systems include liposomal formulations, polymeric micelles, iron carbohydrate colloids, conjugates of a therapeutic molecule with a water-soluble polymer, dendrimers and inorganic nanoparticles [5–7]. Despite their clear benefits, nanomedicines pose several challenges due to their interaction with proteins and cells from the innate immune system resulting in a low bioavailability and a relative high risk for hypersensitivity-like reactions [8–13].

This thesis described the interactions of iron nanomedicines with the immune system (chapter 2,3) and proposed a novel, supposedly more safe, formulation for oral iron delivery (chapter 4). To prevent aggregation and to minimize interactions with the immune system, all clinically administered iron nanomedicines are coated with hydrophilic and biodegradable carbohydrate polymers. Another polymer that is widely used to coat nanomedicines is poly(ethylene glycol) (PEG). Although many PEGylated products have been approved, a growing number of scientist claim that PEG can induce anti-PEG antibodies. But validated and well standardized assays to detect anti-PEG have not been characterized resulting in many unanswered questions to proof the existence, and clinical importance of anti-PEG antibodies (chapter 5). We have developed an in-house anti-PEG ELISA and analyzed serum of patients treated with PEG-asparaginase tested positive for anti-drug antibodies in another laboratory (chapter 6). Finally the discovery of nature's own nanoparticles as an important activator of the FXII (contact system)in an attempt to identify the biological mechanisms leading to thrombosis by nanoparticles was described (chapter 7).

1. Iron nanomedicines

Since the 1940's iron nanomedicines have been administered to patients with iron deficiency for whom oral iron supplementation is insufficient or impossible [14]. They can be considered as the first nanomedicines to be clinically used [15,16]. Over time, different iron nanomedicines have been developed with comparable physico-chemical characteristics. They are composed of a polynuclear Fe(III)-oxyhydroxide/oxide core surrounded by carbohydrates which function as a stabilizer preventing direct release of bioactive iron and particle aggregation [17]. They consist of either sucrose, gluconate, dextran, isomaltoside 1,000 or carboxymaltose [15,17].

1.1. Incidence of hypersensitivity-like reactions

Although safe in routine clinical use, administration of intravenous iron is associated with adverse events, such as hypersensitivity-like reactions which can be fatal. An overview of the use of iron nanomedicines (iron sucrose, ferric gluconate, high- and low-molecular weight iron dextran) in Europe and North-America as well as their associated adverse-events were analyzed and described in Chapter 2. Between countries there is a considerable variation in product preference and doses prescribed. Iron sucrose is most widely used, followed by ferric gluconate. The lowest rate of hypersensitivity-like reactions was reported for iron sucrose, followed by ferric gluconate and iron dextran. Odds ratios demonstrate a 37% reduced risk of all adverse events and 69% reduced risk of serious allergic adverse events with iron sucrose compared to sodium ferric gluconate, and 87% and 93% reduced risks, respectively, compared to iron dextran.

1.2. Interaction of iron nanomedicines and the innate immune system

The exact mechanisms leading to these hypersensitivity-like reactions are unknown. The induction of radical oxygen species (ROS) as a result of labile iron release has been suggested as an explanation but does not appear to be the sole driver [18]. In chapter 3 we reported studies investigating the physico-chemical properties of four different iron nanomedicines and their interactions with the innate immune system. We found that those iron nanomedicines with weak bonds between the carbohydrates and their iron core are more prone to aggregate when analyzed by scanning transmission electron microscopy (STEM). They were also actively taken up by HEK293T cells and peripheral blood monocytes through the cholesterol-mediated uptake pathway. These products triggered in vitro activation of intracellular Toll-like receptors (TLR) -3, -7 and -9 which depended on a serum co-factor. Aggregation prone formulations also induced complement activation and induced the production of the pro-inflammatory cytokine IL-1β, but not IL-6. Only those iron nanomedicine with strongly bound carbohydrates induced the release of IL-6.

These observations, confirmed by others, show that carbohydrates in ferric gluconate and iron sucrose dissociate from the iron core more rapid than in ferric carboxymaltose and iron isomaltoside 1,000 [19]. The exposed core is assumed to be cationic and hydrophobic and adsorbs serum proteins with exposed anionic- and hydrophobic domains, such as apolipoproteins, albumin and fibrinogen [20,21]. The formation of a protein corona can consist out of opsonins, proteins that trigger an immune response which either directly bind to the iron core or to proteins which unfolded or were modified upon binding to the core. In this chapter we described studies indicating that opsonization results in phagocytosis mediated by TLR. Due to technical limitations we were unable to characterize the protein-corona on iron nanomedicines. However, activation of the complement system, presumably the mannose-binding lectin pathway, indicates that part of the protein corona consists of complement factors. Hydrodynamic-size, hydrophobicity and charge are well known parameters effecting the formation of a protein-corona [21–23]. Others have shown that smaller sized iron nanoparticles have significantly longer plasma circulation times than larger ones, presumably as a result of larger curvature which has less effect on secondary structure disturbance of opsonized proteins than particles with a smaller curvature [22,24,25],

The findings in this study revealed another mechanism by which iron nanomedicines interact with the immune system. We believe that dissociation of the carbohydrate shell induces opsonization of serum proteins, including complement factors, to the hydrophobic core which subsequently interact with TLR and induce uptake by phagocytic cells. The findings in this chapter may help to explain why iron nanomedicines induce hypersensitivity-like reactions in patients.

1.3. A novel oral iron formulation

Due to the risk of hypersensitivity-like reactions with intravenous administered iron, a safe oral formulation which is able to deliver similar amounts of iron as intravenous iron is desired. In chapter 4 we described a novel oral formulation based on mPEG(5000)-*b*-p(HPMAm-Lac2) block copolymers encapsulating the iron porphyrin hemin. These micelles are stable at pH 5 enabling stomach passage and stability at pH levels in the intestinal tract. Although the loading capacity of these polymeric micelles was only 3.9%, they proved

very effective in delivering iron into Caco-2 cells as measured by ferritin levels, an iron storage protein and a known iron uptake marker [26]. mPEG(5000)-b-p(HPMAm-Lac2) encapsulating Hemin were able to raise ferritin levels to 2500 ng/mg protein, which was found to be 10-fold higher than iron sulfate, the most used oral iron supplement. We also demonstrated that our novel formulation has a much lower cytotoxic profile than iron sulfate and could therefore be an attractive drug candidate for oral iron delivery.

To deliver sufficient quantities of hemin into the epithelium of the intestinal tract, micelles need to remain stable during passage through the gastrointestinal (GI) tract which includes pH shifting from 1-2 in the stomach to 5-7 in the small intestine [27], dilution of the dose, as well as exposure to bile salts and enzymes [28]. We only studied the release of hemin under different pH conditions in saline. We did not study their stability in diluted conditions, and in the presence of both bile salts and enzymes.

Micellar stability needs a certain polymer concentration referred to as the critical micelle concentration (CMC). So the concentration of polymers needs to remain above the CMC when diluted in the GI tract, which may vary between 130 and 740 mL depending on food intake [29]. The CMC of the polymer we studied is 0.015 mg/mL and we formulated our hemin encapsulated micelles at 1.8 mg/mL polymer concentration which is 120 times over CMC. The micelles are subsequently concentrated and may be considered to resist dilution during passage in the GI tract. Bile salts and enzymes can affect the amphiphilic character of the polymer and bile salts also enhance intestinal absorption and improve bioavailability [30]. These effect of these salts and enzymes need further investigation.

The Caco-2 cell-line is a well-known in vitro model to study intestinal adsorption of pharmaceuticals as it expresses a functional microvilli brush border similar to enterocytes in the small-intestine. However, it misses mucous secreting goblet cells as well as brush border peptidases [31]. Endocytosis by epithelium cells, especially M-cells, depend on particle surface properties. Hydrophobic nanoparticles are preferentially taken up compared to hydrophilic and charged nanoparticles [32]. Also cationic nanoparticles are taken up more efficiently, than neutral and anionic particles [33]. Although hydrophobicity is favorable for cellular uptake, it limits the penetration of mucus. Cationic particles are better in penetrating mucus due to their interaction with proteoglycans [32], [33]. Apparently, charge and hydrophobicity are both important parameters determining nanoparticles distribution and uptake and both are influenced by the proteins and dietary content of the GI tract.

2. Immunogenicity of poly(ethyleneglycol)

The second part of this thesis concerns the potential immunological effect of poly(ethyleneglycol) (PEG). Conjugation of PEG to therapeutics has proven to increase serum half-life, solubility and to reduce immunogenicity. However, in the last decade several unexpected immune-mediated side-effects occurred with PEGylated therapeutics claimed to be elicited by anti-PEG antibodies [34].

In chapter 5 we review the studies claiming to have identified anti-PEG antibodies and the different immunoassays applied. We also propose a mechanism for the immunogenicity of PEG based on its haptogenic properties when conjugated to an immunogenic compound.

The extent of the immunogenicity of PEG and its clinical consequences remain uncertain by the lack of standardized and well validated antibody assays [35]. Immunoassays identify binding antibodies and do not give information on neutralizing antibodies which are of clinical concern [36]. PEG can induce activation of the complement system resulting in severe hypersensitivity-like reactions [37]. In chapter 6 we described a study of anti-PEG antibodies in patients treated with PEG-asparaginase, a microbial enzyme. We have studied the immunological response to the product in patients with Acute Lymphatic Leukemia treated who reduced circulating enzyme levels or experienced hypersensitivity-like reactions. We used ELISAs to determine circulating binding antibodies to: asparaginase, PEG or the succinimidyl succinate linker. All patients had antibodies against all three components. However, we have not yet elucidated if these antibodies bind directly to PEG or actually to opsonized serum proteins. A succinimidyl succinate linker is used to attach the PEG to L-asparaginase. This linker is sensitive to hydrolysis splitting of the PEG and leaving a succinic acid conjugate attached to the L-asparaginase molecule. By using succinic acid conjugated to bovine serum albumin as a target in an ELISA assay we identified that patients had anti-linker antibodies [38]. Here, we are the first to report that patients treated with PEG-asparaginase can develop anti-succinate linker antibodies.

We find a high background signal when testing serum from healthy volunteers in our ELISA for antibodies to PEG. This can either mean that there is a high noise-ratio due to serum-matrix formation into the plate or that sera from our healthy volunteers are indeed anti-PEG positive, as reported by others. The latter seems unlikely as patients who were identified as anti-PEG showed high noise-ratio signals as well. We believe that PEGylated surfaces of ELISA microplates can induce the formation of a protein-corona including opsonized proteins IgG and IgM antibodies that are subsequently falsely identified as anti-PEG antibodies. Future experiments should focus on the formation of this protein corona and the specificity of bound IgG and IgM antibodies.

Despite the recognized limitations in current assays, there is a broad perception that anti-PEG antibodies are evoked in a large part of the healthy population due to exposure to PEG in food and cosmetics. A few articles have claimed to have identified anti-PEG antibodies in a large fraction of healthy subjects ranging between 22 and 44% [39], [40]. For instance, Chen et al. showed that 44.3 % of healthy Han Chinese donors residing in Taiwan were positive for anti-PEG antibodies, either IgG, IgM or both [40]. The authors developed a direct ELISA by coating a maxisorp 96-well microplate with 0.5 µg/well NH_2-$PEG_{10.000}$-NH_2 in carbonate buffer pH 9.5 overnight. Binding of diamine-PEG to a polystyrene plate is unlikely. Therefore claims about high percentages of anti-PEG positive donors should be interpreted with care.

3. Nature's nanoparticles and contact system activation

The last part of this thesis focusses on nature's nanoparticles, polyphosphate polymers in blood platelets. This inorganic, negatively charged polymer has been shown to be present in a variety of cell types such as platelets [41], mast cells [42] and tumor cells [43]. It plays a role in a variety of hemostatic and thrombotic mechanisms and is a potential druggable target for interference with thrombosis [44,45]. In chapter 7 we described the mechanism by which polyphosphate is able to activate coagulation factor XII (FXII), which then triggers activation

of the contact system. The contact system connects to the intrinsic pathway and can induce thrombin formation by binding and activation of coagulation factor XII (FXII). Activation of FXII by polyphosphate has always been believed to be restricted to soluble polyphosphate in the extracellular environment. However, in this chapter, we showed that only when polyphosphate is complexed as a nanoparticle with divalent metal ions activation occurs. We showed that human platelets express membrane associated polyphosphate nanoparticles in the core of a thrombus. We believe that polyphosphate nanoparticles function as thrombus stabilizers because when a thrombus 'breaks', these nanoparticles become exposed to the external environment and can induce local activation of FXII to stabilize the thrombus. Polyphosphate nanoparticles act as a cellular 'docking site' for coagulation. Polyphosphate complexation with calcium has been proposed as a drug delivery vehicle to increase circulation times of therapeutics. The findings in this thesis indicate that these nanomedicine will likely be thrombogenic and not be a good drug delivery candidate.

Contact system activation by FXII is believed to occur on hydrophobic and anionic-hydrophilic solid surfaces. However, FXII activation to hydrophobic surfaces in plasma is actually minimized because other more abundant plasma proteins will compete for the hydrophobic binding spots [46]. This is in line with the observation of blood slowly clotting in hydrophobic (silanized-glass) tubes and quickly in anionic-hydrophilic (glass) tubes [47]. FXII is most potently activated on anionic-hydrophilic surfaces due to auto-activation in the protein-coronas covering these materials. As most nanomedicines are covered by hydrophilic polymers, FXII activation on nanomedicines is expected. Indeed, many implants and nanomedicines are known to induce thrombus formation which is partly mediated by FXII activation [46]. Also, FXII can be activated on PEGylated surfaces, depending on PEG density [46]. The findings in this studies imply that the human body has evolved a coagulant response towards nanoparticles which can have broad implications on selecting biomaterials for the development of novel nanomedicines.

References

[1] D. Neuman and J. N. Chandhok, "Patent Watch: Nanomedicine patents highlight importance of production methods," Nat. Rev. Drug Discov., vol. 15, no. 7, pp. 448–449, Jun. 2016.

[2] O. C. Farokhzad and R. Langer, "Impact of Nanotechnology on Drug Delivery," ACS Nano, vol. 3, no. 1, pp. 16–20, Jan. 2009.

[3] R. Duncan and R. Gaspar, "Nanomedicine(s) under the microscope," Mol. Pharm., vol. 8, no. 6, pp. 2101–2141, Dec. 2011.

[4] L. Y. Rizzo, B. Theek, G. Storm, F. Kiessling, and T. Lammers, "Recent progress in nanomedicine: therapeutic, diagnostic and theranostic applications," Curr. Opin. Biotechnol., vol. 24, no. 6, pp. 1159–1166, Dec. 2013.

[5] H. Schellekens et al., "How to regulate nonbiological complex drugs (NBCD) and their follow-on versions: points to consider," AAPS J., vol. 16, no. 1, pp. 15–21, Jan. 2014.

[6] Y. Min, J. M. Caster, M. J. Eblan, and A. Z. Wang, "Clinical Translation of Nanomedicine," Chem. Rev., vol. 115, no. 19, pp. 11147–11190, Oct. 2015.

[7] D. J. A. Crommelin et al., "The similarity question for biologicals and non-biological complex drugs," Eur. J. Pharm. Sci., vol. 76, pp. 10–17, Aug. 2015.

[8] M. Herklotz et al., "Biomaterials trigger endothelial cell activation when co-incubated with human whole blood," Biomaterials, vol. 104, pp. 258–268, Oct. 2016.

[9] O. M. Merkel et al., "In vitro and in vivo complement activation and related anaphylactic effects associated with polyethylenimine and polyethylenimine-graft-poly(ethylene glycol) block copolymers," Biomaterials, vol. 32, no. 21, pp. 4936–4942, Jul. 2011.

[10] J. Szebeni and G. Storm, "Complement activation as a bioequivalence issue relevant to the development of generic liposomes and other nanoparticulate drugs," Biochem. Biophys. Res. Commun., vol. 468, no. 3, pp. 490–497, Dec. 2015.

[11] J. Szebeni, "Complement activation-related pseudoallergy: A stress reaction in blood triggered by nanomedicines and biologicals," Mol. Immunol., vol. 61, no. 2, pp. 163–173, Oct. 2014.

[12] C. M. Dawidczyk et al., "State-of-the-art in design rules for drug delivery platforms: lessons learned from FDA-approved nanomedicines," J. Control. Release Off. J. Control. Release Soc., vol. 187, pp. 133–144, Aug. 2014.

[13] S. Wilhelm et al., "Analysis of nanoparticle delivery to tumours," Nat. Rev. Mater., vol. 1, 2016.

[14] J. Umbreit, "Iron deficiency: a concise review," Am. J. Hematol., vol. 78, no. 3, pp. 225–231, Mar. 2005.

[15] M. Auerbach and H. Ballard, "Clinical use of intravenous iron: administration, efficacy, and safety," Hematol. Educ. Program Am. Soc. Hematol. Am. Soc. Hematol. Educ. Program, vol. 2010, pp. 338–347, 2010.

[16] J. Nissim, "INTRAVENOUS ADMINISTRATION OF IRON," The Lancet, vol. 250, no. 6463, pp. 49–51, Jul. 1947.

[17] P. Geisser and S. Burckhardt, "The pharmacokinetics and pharmacodynamics of iron preparations," Pharmaceutics, vol. 3, no. 1, pp. 12–33, 2011.

[18] A. B. Pai, T. Conner, C. R. McQuade, J. Olp, and P. Hicks, "Non-transferrin bound iron, cytokine activation and intracellular reactive oxygen species generation in hemodialysis patients receiving intravenous iron dextran or iron sucrose," Biometals Int. J. Role Met. Ions Biol. Biochem. Med., vol. 24, no. 4, pp. 603–613, Aug. 2011.

[19] P. Geisser and S. Burckhardt, "The pharmacokinetics and pharmacodynamics of iron preparations," Pharmaceutics, vol. 3, no. 1, pp. 12–33, Jan. 2011.

[20] B. S. Barot, P. B. Parejiya, D. M. Mehta, P. K. Shelat, and G. B. Shah, "Physicochemical and structural characterization of iron–sucrose formulations: a comparative study," Pharm. Dev. Technol., vol. 19, no. 5, pp. 513–520, Aug. 2014.

[21] P. Aggarwal, J. B. Hall, C. B. McLeland, M. A. Dobrovolskaia, and S. E. McNeil, "Nanoparticle interaction with plasma proteins as it relates to particle biodistribution, biocompatibility and therapeutic efficacy," Adv. Drug Deliv. Rev., vol. 61, no. 6, pp. 428–437, Jun. 2009.

[22] M. P. Monopoli et al., "Physical–Chemical Aspects of Protein Corona: Relevance to in Vitro and in Vivo Biological Impacts of Nanoparticles," J. Am. Chem. Soc., vol. 133, no. 8, pp. 2525–2534, Mar. 2011.

[23] J. Huang et al., "Effects of Nanoparticle Size on Cellular Uptake and Liver MRI with Polyvinylpyrrolidone-Coated Iron Oxide Nanoparticles," ACS Nano, vol. 4, no. 12, pp. 7151–7160, Dec. 2010.

[24] M. Lundqvist, I. Sethson, and B.-H. Jonsson, "Protein Adsorption onto Silica Nanoparticles: Conformational Changes Depend on the Particles' Curvature and the Protein Stability," Langmuir, vol. 20, no. 24, pp. 10639–10647, Nov. 2004.

[25] Z. J. Deng, M. Liang, M. Monteiro, I. Toth, and R. F. Minchin, "Nanoparticle-induced unfolding of fibrinogen promotes Mac-1 receptor activation and inflammation," Nat. Nanotechnol., vol. 6, no. 1, pp. 39–44, Jan. 2011.

[26] R. P. Glahn, O. A. Lee, A. Yeung, M. I. Goldman, and D. D. Miller, "Caco-2 Cell Ferritin Formation Predicts Nonradiolabeled Food Iron Availability in an In Vitro Digestion/Caco-2 Cell Culture Model," J. Nutr., vol. 128, no. 9, pp. 1555–1561, Sep. 1998.

[27] A. L. Daugherty and R. J. Mrsny, "Transcellular uptake mechanisms of the intestinal epithelial barrier Part one," Pharm. Sci. Technol. Today, vol. 2, no. 4, pp. 144–151, Apr. 1999.

[28] Y. Lu and K. Park, "Polymeric micelles and alternative nanonized delivery vehicles for poorly soluble drugs," Int. J. Pharm., vol. 453, no. 1, pp. 198–214, Aug. 2013.

[29] C. Schiller et al., "Intestinal fluid volumes and transit of dosage forms as assessed by magnetic resonance imaging," Aliment. Pharmacol. Ther., vol. 22, no. 10, pp. 971–979, Nov. 2005.

[30] A. J. Hoogstraate, S. Senel, C. Cullander, J. Verhoef, H. E. Junginger, and H. E. Boddé, "Effects of bile salts on transport rates and routes of FITC-labelled compounds across porcine buccal epithelium in vitro," J. Controlled Release, vol. 40, no. 3, pp. 211–221, Jul. 1996.

[31] P. Lundquist and P. Artursson, "Oral absorption of peptides and nanoparticles across the human intestine: Opportunities, limitations and studies in human tissues," Adv. Drug Deliv. Rev., vol. 106, Part B, pp. 256–276, Nov. 2016.

[32] I. Behrens, A. I. V. Pena, M. J. Alonso, and T. Kissel, "Comparative uptake studies of bioadhesive and non-bioadhesive nanoparticles in human intestinal cell lines and rats: the effect of mucus on particle adsorption and transport," Pharm. Res., vol. 19, no. 8, pp. 1185–1193, Aug. 2002.

[33] A. des Rieux, E. G. E. Ragnarsson, E. Gullberg, V. Préat, Y.-J. Schneider, and P. Artursson, "Transport of nanoparticles across an in vitro model of the human intestinal follicle associated epithelium," Eur. J. Pharm. Sci., vol. 25, no. 4–5, pp. 455–465, Jul. 2005.

[34] K. Shiraishi et al., "Exploring the relationship between anti-PEG IgM behaviors and PEGylated nanoparticles and its significance for accelerated blood clearance," J. Control. Release Off. J. Control. Release Soc., vol. 234, pp. 59–67, Jul. 2016.

[35] H. Schellekens, W. E. Hennink, and V. Brinks, "The immunogenicity of polyethylene glycol: facts and fiction," Pharm. Res., vol. 30, no. 7, pp. 1729–1734, Jul. 2013.

[36] S. Hermeling, D. J. A. Crommelin, H. Schellekens, and W. Jiskoot, "Structure-Immunogenicity Relationships of Therapeutic Proteins," Pharm. Res., vol. 21, no. 6, pp. 897–903, Jun. 2004.

[37] I. Hamad, A. C. Hunter, J. Szebeni, and S. M. Moghimi, "Poly(ethylene glycol)s generate complement activation products in human serum through increased alternative pathway turnover and a MASP-2-dependent process," Mol. Immunol., vol. 46, no. 2, pp. 225–232, Dec. 2008.

[38] M. J. Roberts, M. D. Bentley, and J. M. Harris, "Chemistry for peptide and protein PEGylation," Adv. Drug Deliv. Rev., vol. 54, no. 4, pp. 459–476, Jun. 2002.

[39] J. K. Armstrong, "The occurrence, induction, specificity and potential effect of antibodies against poly(ethylene glycol)," in PEGylated Protein Drugs: Basic Science and Clinical Applications, F. M. Veronese, Ed. Birkhäuser Basel, 2009, pp. 147–168.

[40] B.-M. Chen et al., "Measurement of Pre-Existing IgG and IgM Antibodies against Polyethylene Glycol in Healthy Individuals," Anal. Chem., vol. 88, no. 21, pp. 10661–10666, Nov. 2016.

[41] F. A. Ruiz, C. R. Lea, E. Oldfield, and R. Docampo, "Human platelet dense granules contain polyphosphate and are similar to acidocalcisomes of bacteria and unicellular eukaryotes," J. Biol. Chem., vol. 279, no. 43, pp. 44250–44257, Oct. 2004.

[42] D. Moreno-Sanchez, L. Hernandez-Ruiz, F. A. Ruiz, and R. Docampo, "Polyphosphate is a novel pro-inflammatory regulator of mast cells and is located in acidocalcisomes," J. Biol. Chem., vol. 287, no. 34, pp. 28435–28444, Aug. 2012.

[43] K. F. Nickel et al., "The polyphosphate-factor XII pathway drives coagulation in prostate cancer-associated thrombosis," Blood, vol. 126, no. 11, pp. 1379–1389, Sep. 2015.

[44] R. J. Travers, R. A. Shenoi, M. T. Kalathottukaren, J. N. Kizhakkedathu, and J. H. Morrissey, "Nontoxic polyphosphate inhibitors reduce thrombosis while sparing hemostasis," Blood, vol. 124, no. 22, pp. 3183–3190, Nov. 2014.

[45] S. Zhu, R. J. Travers, J. H. Morrissey, and S. L. Diamond, "FXIa and platelet polyphosphate as therapeutic targets during human blood clotting on collagen/tissue factor surfaces under flow," Blood, vol. 126, no. 12, pp. 1494–1502, Sep. 2015.

[46] E. A. Vogler and C. A. Siedlecki, "Contact Activation of Blood Plasma Coagulation," Biomaterials, vol. 30, no. 10, pp. 1857–1869, Apr. 2009.

[47] T. Renné, A. H. Schmaier, K. F. Nickel, M. Blombäck, and C. Maas, "In vivo roles of factor XII," Blood, vol. 120, no. 22, pp. 4296–4303, Nov. 2012.

Appendices

De formuleringen van therapeutische stoffen, zowel kleine moleculen als therapeutische eiwitten, in afgifte systemen op nanoschaal maakt het mogelijk deze stoffen toe te dienen die bij zichzelf een ongewenst farmaceutisch profiel hebben vanwege een lage oplosbaarheid, ongewenste farmacokinetiek of toxiciteit. Voorbeelden van deze afgifte system zijn, liposomen, micellen bestaande uit polymeren, dendrimeren en anorganische nanopartiekels. Ondanks hun duidelijke potentie hebben deze systemen toch enkele nadelen die voornamelijk voortkomen uit hun interacties met het 'aangeboren' immuun systeem.

In deze thesis is de interactie van ijzer nanopartiekels beschreven (hoofdstuk 2,3) en tevens de ontwikkeling van een potentieel veiliger, orale formulering. IJzer partiekels zijn bedekt met suikerketens die de ijzerkern beschermen tegen aggregatie en interacties met het immuun systeem dienen te beperken. Een ander, vaak gebruikt polymeer om nanopartiekels te beschermen tegen het immuun systeem is door middel van PEGylering. Poly(ethyleneglycol) (PEG) is een veel gebruikt polymeer en verschillende geregistreerde geneesmiddelen bevatten deze stof. Echter, de laatste decennia een groeiende groep wetenschappers beweren dat dit polymeer antistoffen kan opwekken. Echter, duidelijke bewijzen en gevalideerde testen om deze bewering te onderbouwen ontbreken of missen essentiële informatie (hoofdstuk 5). In deze thesis hebben wij een anti-PEG studie opgezet aan de hand van serum van patiënten die behandeld zijn met PEG-asparaginase en antistoffen hiertegen ontwikkelden (hoofdstuk 6). Het laatste hoofdstuk van deze thesis bestaat uit de ontdekking van nog niet eerder geïdentificeerde lichaamseigen nanopartiekels in bloedplaatjes die de lichaamseigen activator van het contact systeem blijkt te zijn (FXII).

1. IJzer nanopartiekels

Intraveneuze ijzer partiekels worden al sinds de jaren 40 voorgeschreven aan patiënten en kunnen daardoor worden beschouwd als de eerste therapeutische nanopartiekels. In de laatste decennia zijn meerdere verschillende ijzer partiekels ontwikkeld die in eigenschappen sterk op elkaar lijken. Allen bevatten suikerketens die de kern beschermen tegen het direct vrijkomen van vrij ijzer en aggregatie van partiekels met elkaar.

1.1. Voorkomen van overgevoeligheidsreacties

Alhoewel ijzer partiekels veel worden voorgeschreven, is de toediening van deze geneesmiddelen niet geheel veilig. Overgevoeligheidsreacties, waarvan ook van anafylactische aard, kunnen in ernstige implicaties resulteren en zelfs dodelijk zijn. In deze thesis is het gebruik van ijzer sucrose, ijzer gluconaat en ijzer dextraan (zowel laag als hoog molecuulgewicht) in Europa en Noord-Amerika beschreven als zowel het voorkomen van overgevoeligheidsreacties in deze landen. Het gebruik van de ijzerproducten verschilt sterk tussen de verschillende landen. Van de onderzochte producten in deze studie, induceert ijzer sucrose de minste overgevoeligheidsreacties, gevolgd door ijzer gluconaat en ijzer dextraan met respectievelijke odds-ratios vermindering van 37% op alle bijwerkingen en 69% voor ernstige overgevoeligheidsreacties tussen ijzer sucrose en ijzer gluconaat, en 87% en 93% met ijzer dextraan respectievelijk.

1.2. Interacties van ijzer nanopartiekels en het aangeboren immuunsysteem

De exacte mechanismen hoe ijzer partiekels deze overgevoeligheidsreacties induceren is niet bekend. Vooralsnog werd het vrijkomen van vrij ijzer als meest logische verklaring aangedragen. Vrij ijzer produceert radicale zuurstof atomen die schade aan cellen veroorzaken. Echter recent onderzoek laat zien dat deze radicalen niet het gehele klinische beeld verklaren. In hoofdstuk 3 is gekeken naar de karakterisatie van verschillende ijzer partiekels en hoe deze aangrijpen op het immuunsysteem. Partiekels met de minst sterke binding van hun suikerketens aan de ijzerkern lieten meer aggregatie zien. Deze producten werden ook meer door cellen opgenomen (HEK293T) via de cholesterol gemedieerde pathway en tevens meer opgenomen door geïsoleerde immuuncellen (PBMC) van humane donoren. Daarnaast activeerden deze producten ook Toll-like receptoren -3, -7 en 9 en bleek activatie afhankelijk te zijn van plasma eiwitten. Producten met sterk gebonden suikerketens induceerde expressie van IL-6 terwijl deze met de minst stabiele suikerketens vooral IL-1beta induceerden.

De vindingen in dit hoofdstuk laten een nieuw mechanisme zien hoe ijzer partiekels worden herkend door het immuun systeem en kunnen mogelijk dienen als een additionele verklaring voor de overgevoeligheidsreacties die in de kliniek worden gezien. De vindingen ondersteunen de redenering dat de suikerketens van ijzer sucrose en ijzer gluconaat sneller dissociëren van de ijzerkern dan die van ijzer carboxymaltose en ijzer isomaltoside 1,000, de onderzochte producten in deze studie. De resulterende ijzerkern is positief geladen en hydrofoob waardoor het makkelijk plasma eiwitten zoals albumine, fibrinogeen en apoproteïne bindt. Het binden van plasma eiwitten leidt tot de vorming van een eiwit-corona dat ook bestaat uit eiwitten die een immuun respons induceren zoals in het geval van ijzer partiekels complement factoren. In het geval van ijzer partiekels hebben wij laten zien dat de binding van plasma eiwitten essentieel is voor activatie van Toll-like receptoren en mogelijk ook de opname door (immuun) cellen versterkt.

1.3. Een nieuwe ijzer formulering

Vanwege de kans op overgevoeligheidsreacties op intraveneuze ijzer partiekels is een veiligere, liefst orale, formulering gewenst. In hoofdstuk 4 is een nieuwe formulering bestaande uit mPEG-(5000-b-p(HPMAm-Lac2) block co-polymeren beschreven die het molecuul hemin insluit, een porfyrine dat één ijzeratoom bevat. Deze polymeren vormen micellen die stabiel zijn bij pH 5, essentieel voor passage door de maag. Alhoewel de micellen maar een kleine hoeveelheid hemin konden insluiten, zijn deze micellen zeer succesvol om ijzer af te geven aan Caco-2 cellen, een in vitro model om opname in de dunne darm te bestuderen. Deze micellen waren in staat om 10x zoveel meer ferritine, een marker voor intracellulaire ijzer opslag, aan te maken na toediening dan eenzelfde hoeveelheid ijzersulfaat. Daarbij hadden deze micellen een veel lagere toxiciteit dan ijzersulfaat en zijn daardoor een aantrekkelijke kandidaat voor een nieuwe orale ijzerformulering.

2. Immunogeniciteit van poly(ethyleneglycol)

Het tweede deel van deze thesis bestaat uit een review over de mogelijke immunologische implicaties van PEGylering, het coaten van geneesmiddelen met poly(ethyleneglycol) (PEG). Conjugatie van PEG aan eiwitten en nanopartiekels is bewezen de farmacokinetiek en de oplosbaarheid te vergroten en wordt daardoor veel gebruikt in de ontwikkeling van

nieuwe geneesmiddelen. Echter, het laatste decennium hebben een groeiend aantal wetenschappers beschreven dat PEG antistoffen kan opwekken die gePEGyleerde geneesmiddelen snel uit de circulatie klaren. Hierdoor is er momenteel onzekerheid over het gebruik van PEG omdat er enerzijds een groot aantal successen mee zijn gehaald en anderzijds problemen mee zijn gemeld. Het feit dat er maar weinig alternatieven zijn voor PEGylering maakt het noodzakelijk om snel inzicht te verkrijgen of PEG een immuun respons kan induceren. De testen die deze wetenschappers beschrijven missen vaak essentiële controles waardoor het vooralsnog niet mogelijk is om harde conclusies te trekken. In dit hoofdstuk wordt een mogelijke verklaring gegeven voor de immunogeniciteit van gePEGyleerde geneesmiddelen door de activatie van het complement systeem. Binding van PEG aan een niet lichaamseigen eiwit of lichaamsvreemd materiaal versterkt daarbij deze activatie. In hoofdstuk hebben wij de specificiteit van antistoffen in het serum van patiënten behandeld met PEG-asparaginase bestudeerd, een lichaamsvreemd enzym dat gebruikt wordt bij kinderen met acute lymfatische leukemie. Alle bestudeerde patiënten waren positief voor anti-asparaginase, -PEG en de succinimidyl linker dat het PEG polymeer bindt. Echter, waren we niet in staat om te bewijzen of deze antistoffen direct binden aan het PEG polymeer of aan een eiwit reeds gebonden aan het PEG polymeer. Antistoffen tegen de linker is mogelijk doordat wij hebben aangetoond dat de PEG polymeren langzaam hydrolyseren van het enzym waardoor enkel de succinimidyl succinate linker op het enzym achterblijft en zo kan worden blootgesteld aan het immuun systeem.

3. Lichaamseigen partiekels die het contact systeem activeren

Het laatste deel van deze thesis bestaat uit ontdekking van partiekels in bloedplaatjes bestaande uit polyfosfaat gecomplexeerd met divalente atomen. Polyfosfaat is een polymeer dat veel is bestudeerd omdat het een belangrijke rol speelt in de coagulatie cascade. Tot nog toe werd gedacht dat voornamelijk oplosbaar polyfosfaat hiervoor verantwoordelijk was. In dit hoofdstuk hebben wij laten zien dat geactiveerde bloedplaatjes polyfosfaat niet enkel uitscheiden maar juist in een vaste vorm op het celmembraan plaatsen. Het is juist deze vaste vorm dat het contact systeem (factor XII) doet activeren en niet oplosbaar polyfosfaat. Deze partiekels worden in de kern van een trombus op het celmembraan van plaatjes gezet en wij menen dat deze fungeren als een stabilisator van een trombus. In het geval dat een trombus scheurt worden deze partiekels blootgesteld aan plasma waardoor FXII op het celmembraan van deze plaatjes geactiveerd kan worden en middels het initiëren van lokale coagulatie de trombus weer herstelt

Curriculum vitae

After obtaining his Gymnasium diploma in 2007, Jan-Jaap Verhoef (21-12-1988) went to study Innovation Sciences at Utrecht University. He became enthusiastic about pharmaceutical discovery and the organization of the pharmaceutical industry. During his bachelor he performed an internship at Vifor Pharma resulting in the publication of 2 scientific articles. He was also selected to enrol into two interdisciplinary honours programmes, respectively on ethics and entrepreneurship. After a pre-master program Jan-Jaap enrolled into the Graduate School of Life Sciences at Utrecht University following the master Drug Innovation. Under the supervision of Prof. Huub Schellekens he performed an internship on iron nanomedicines and a second internship on anti-PEG antibodies at the University of Colorado under the supervision of Prof. John Carpenter. During his master he followed the honours programme of the Utrecht University masters programme on leadership and entrepreneurship. It was in this period that Jan-Jaap co-founded the Sustainable Healthcare Challenge, a non-profit organization supporting entrepreneurship in healthcare by organizing events and start-up competitions. During his PhD Jan-Jaap was selected to present his work on anti-PEG antibodies during the European Immunogenicity Platform conference and won the abstract price from the *Nederlandse Vereniging voor Trombose en Hemostase* in 2017.

List of publications

Bailie GR, Hörl WH, **Verhoef JJF**. Differences in spontaneously reported hypersensitivity and serious adverse events for intravenous iron preparations: comparison of Europe and North America. Arzneimittelforschung. 2011;61(5):267–75.

Bailie GR, **Verhoef JJF**. Differences in the reporting rates of serious allergic adverse events from intravenous iron by country and population. Clin Adv Hematol Oncol HO. 2012 Feb;10(2):101–8.

Verhoef JJF, Anchordoquy TJ. Questioning the Use of PEGylation for Drug Delivery. Drug Deliv Transl Res. 2013 Dec;3(6):499–503.

Verhoef JJF, Carpenter JF, Anchordoquy TJ, Schellekens H. Potential induction of anti-PEG antibodies and complement activation toward PEGylated therapeutics. Drug Discov Today. 2014 Dec;19(12):1945–52.

Alaarg A, Jordan NY, **Verhoef JJF**, Metselaar JM, Storm G, Kok RJ. Docosahexaenoic acid liposomes for targeting chronic inflammatory diseases and cancer: an in vitro assessment. Int J Nanomedicine. 2016;11:5027–40.

Verhoef JJF*, Span K*, Hunt H, van Nostrum CF, Brinks V, Schellekens H, et al. A Novel Oral Iron- Complex Formulation: Encapsulation of Hemin in Polymeric Micelles and its in-vitro Absorption. Eur J Pharm Biopharm. 2016 Sep 3;

Verhoef JJF, de Groot AM, van Moorsel M, Ritsema J, Beztsinna N, Maas C, et al. Iron nanomedicines induce Toll-like receptor activation, cytokine production and complement activation. Biomaterials. 2017 Mar;119:68–77.

Verhoef JJF*, Barendrecht AD*, Nickel KF,* Dijkxhoorn K, Kenne E, Labberton L, et al. Polyphosphate nanoparticles on the platelet surface trigger contact system activation. Blood. 2017 Jan 3;

**Shared first authorship*

Acknowledgements

The realisation of this thesis and as such completing my PhD has not been one-man show. The ride would have not been as smooth and joyful without the freedom and trust given to me by my promotor Prof. Huub Schellekens and the kindness of my co-promotor Dr. Coen Maas to become part of his research. It's because of them that I appreciate scientific research as one of the few opportunities that truly allows you to invest your most valuable asset (your own time) in trying to answer those questions that excites you most. Being part of the Graduate School of Life Sciences at Utrecht University allowed me to meet many brilliant minds with all kinds of backgrounds that have inspired me to become the person I am today.

I am very grateful to have been part of the Biofarmacie group which does not only exist out of brilliant staff members and PhD-students, but also out of the most kind people from many countries around the world. This diverse environment has not only made me appreciate these different cultures but also enriched me with many friends. The diversity of the Bioformacie group would serve as a great example for modern society.

Huub, thank you for showing me the doors that allowed me to advance my career over the past 10 years. I have been inspired by your passion to challenge certain dogmas in the pharmaceutical industry. Your meetings were always focused on identifying the question you want to answer, rather than going straight into discoveries. The awareness that most challenges are actually relatively easy to solve when the right questions have been formulated changed my perception on problem-solving. It is perhaps this that I am most thankful to have learnt during my PhD.

Coen, thank you for letting me in into the most exciting research group I have ever encountered. You have been one of the few that is able to transform scientific research into teamwork. I experienced your environment as one of passion, ambition and a lot of fun. I cannot be grateful enough that you have allowed me to be part of the polyphosphate research. You allowed me to take credits for the success of this work while also many others have been so important in this research as well. It must be this environment about which my father told many stories how he performed research 45 years ago in the USA which not only resulted in great discoveries but also great friendships for life. I hope you are capable of maintaining this environment when your group is growing. Among others you learnt me how to make comprehensible stories out of research, something that is so often missing in the scientific field. I will do the best I can to keep collaborating with you and your amazing sidekick Steven in the future.

Wim, during the times I encountered several allegations from partners in our consortium you were there to fix it. You let me know I was part of the Biofarmacie group and fought to secure the funding for the rest of my PhD. I cannot be thankful enough for helping me.

Mohammed & Andhyk, it has been great to work together in Huub's Group. You created an environment in which we helped each other and could talk about many different topics. It has been a great time with many great memories and hope we are able to keep working together in the future.

Sarah, Marc and Willem, three completely different personalities who have helped me realizing this thesis. It was a pleasure mentoring you and have many great memories on the fun moment in the lab.

Robin, it has been a great collaboration with you and the Erasmuc MC in our research on anti-PEG antibodies. I am glad you started to enjoy labwork as a physician.

Amr, you are an amazing guy and you have been missed since your departure to the USA. I am very happy for you that you found those great things in New York. I have enjoyed our discussions on science as well as the other things guys our age talk about. Thank you for letting me in into your research. I wish you and your wife all the happiness in the future. Kimberley, thank you for mentoring me during my studies and the collaboration on the micellular work. I wish you all the best in the future.

Lies, Karina, Maria, Kristel, Nataliia, Erik, Maarten and Matthew, I had a great time with you joking around in and outside the lab. I hope our friendships will remain in the future. In particular with my good friend Jeffrey who was always in for fun and drinks. Because of you I rediscovered Utrecht again after moving to Amsterdam. Guli, Michele, Piera and Claudia, grazie mille for letting me into your Italian family. Our trip to Sicily was one of the best, including the discovery of Italian habits such as dinner at midnight and sightseeing at 1 AM. Barbara, Mies, Joep, Roel and Louis, thank you for helping me with any challenges I had along the way. You all created a wonderful atmosphere at Biofarmacie.

Thank you Andhyk and Sebastiaan for being my paranymphs and realzing my PhD defense. Also Lucas and Pieter, thank you for your support and great friendship in the last 10 years as well as your help organizing my PhD party.

Most of all, thank you Mom and Dad for being there to listen to my stories and always supporting me in the decisions I took.